JYVÄSKYLÄ STUDIES IN COMPUTING
55

Janne Kurjenniemi

A Study of TD-CDMA and WCDMA Radio Network Enhancements

JYVÄSKYLÄN YLIOPISTO

JYVÄSKYLÄ STUDIES IN COMPUTING 55

Janne Kurjenniemi

A Study of TD-CDMA and WCDMA Radio Network Enhancements

Esitetään Jyväskylän yliopiston informaatioteknologian tiedekunnan suostumuksella
julkisesti tarkastettavaksi yliopiston vanhassa juhlasalissa (S212)
joulukuun 9. päivänä 2005 kello 12.

Academic dissertation to be publicly discussed, by permission of
the Faculty of Information Technology of the University of Jyväskylä,
in Auditorium S212, on December 9, 2005 at 12 o'clock noon.

UNIVERSITY OF JYVÄSKYLÄ

JYVÄSKYLÄ 2005

A Study of TD-CDMA and WCDMA Radio Network Enhancements

JYVÄSKYLÄ STUDIES IN COMPUTING 55

Janne Kurjenniemi

A Study of TD-CDMA and WCDMA Radio Network Enhancements

UNIVERSITY OF JYVÄSKYLÄ

JYVÄSKYLÄ 2005

Editors
Tommi Kärkkäinen
Department of Mathematical Information Technology, University of Jyväskylä
Pekka Olsbo, Marja-Leena Tynkkynen
Publishing Unit, University Library of Jyväskylä

URN:ISBN:9513922782
ISBN 951-39-2278-2 (PDF)

ISBN 951-39-2296-0 (nid.)
ISSN 1456-5390

Jyväskylä University Printing House, Jyväskylä 2005

ABSTRACT

Kurjenniemi, Janne
A Study of TD-CDMA and WCDMA Radio Network Enhancements
Jyväskylä: University of Jyväskylä, 2005, 144 pages
(Jyväskylä Studies in Computing,
ISSN 1456-5390; 55)
ISBN 951-39-2278-2
Finnish summary
Diss.

The aim of this study is to analyse UMTS terrestrial radio access performance including TDD and FDD modes. 3.84 Mcps TDD Mode of UTRA is based upon a combined time and code division multiple access and it is commonly referred to as TD-CDMA, whereas UTRA FDD mode is based upon a *Wideband Code Division Multiple Access (WCDMA)*.

Analysis of the UTRA TDD mode concentrates on three important radio resource management algorithms, namely power control, handover and dynamic channel allocation. Power control analysis contains both uplink and downlink studies and it is found that careful setting of the main parameters are needed to guarantee a robust system operation.

WCDMA type of handover is considered for the TD-CDMA and the effect of its applicability is evaluated with extensive simulations. The effect of different handover parameters on the system capacity is studied in an indoor environment.

Dynamic Channel Allocation (DCA) is TDD specific algorithm to allocate resources for transmission. It can be divided into *slow DCA (S-DCA)*, which allocates resources to cells and *fast DCA (F-DCA)*, which allocates resources to bearer services. In this thesis different F-DCA algorithms are described and analysed under different S-DCA parameters.

The studied topics for the WCDMA are transmit diversity and advanced receivers. The system performance evaluation with transmit diversity starts from dedicated channels and then the *High Speed Downlink Packet Access (HSDPA)* network performance is analysed. Performance of *Space Time Transmit Diversity (STTD)* and *Closed Loop Mode 1 (CL Mode 1)* are compared to conventional 1Tx transmission.

Further enhancements for the HSDPA are currently an interesting research topic. In this thesis HSDPA system performance with receive diversity and *Linear Minimum Mean Squared Error (LMMSE)* chip level equalizer is compared to conventional Rake receiver with extensive dynamic system level simulations.

Keywords: 3G, WCDMA, TD-CDMA, HSDPA, Radio Resource Management, radio network performance evaluation.

Author's address Janne Kurjenniemi

Department of Mathematical Information Technology
University of Jyväskylä, Finland
P.O. Box 35 (Agora), 40014 University of Jyväskylä
Email: makuja@mit.jyu.fi

Supervisor Professor Tapani Ristaniemi

Institute of Communications Engineering
Tampere University of Technology
Finland

Reviewers Professor Jukka Lempiäinen

Institute of Communications Engineering
Tampere University of Technology
Finland

Professor Sven-Gustav Häggman

Communications Laboratory
Helsinki University of Technology
Finland

Opponent Professor Riku Jäntti

Department of Computer Science
University of Vaasa
Finland

ACKNOWLEDGEMENTS

This study project is done in co-operation with the University of Jyväskylä and Nokia Research Center Helsinki. I wish to express my gratitude to the Nokia Research Center in Helsinki and the Department of Mathematical Information Technology at the University of Jyväskylä for financial support of this study. I would especially like to thank my instructor Tapani Ristaniemi for his continuous guidance and fruitful discussions during this study.

Also I would like to thank the Nokia Foundation, Tekniikan edistämissäätiö, Research foundation of HPY, the Province foundation of Keski-Suomi and the Finnish Foundation for Economic and Technology Sciences - KAUTE for giving financial support during the research work. I am also grateful to my colleagues at Nokia for giving support and guidance. I would like to thank Mika Kolehmainen, Seppo Hämäläinen, Markku Kuusela, Yrjö Kaipainen and Mika Rinne from Nokia Research Center, and Otto Lehtinen and Jorma Kaikkonen from Nokia Technology Platforms and Petri Patronen from Nokia Networks for the help and guidance during this study. I would like to thank my colleagues Timo Nihtilä, Jussi Äijänen and Jari Leino from University of Jyväskylä.

Finally, I would like to thank my wife Katja for her love and patience and for encouraging me forward with this study and to my son Kare for bringing enormous joy to our family.

Jyväskylä, November 16, 2005

Janne Kurjenniemi

LIST OF FIGURES

LIST OF TABLES

CONTENTS

SYMBOLS

α	Weighting parameter in uplink open inner loop power control of UTRA TDD
θ	Synchronisation parameter that describes the timing offset between cell under study and adjacent cell using same or adjacent carrier
δ_D	Vector which have one at the delay D and otherwise zeros
$\hat{\delta}_D$	Square matrix which has ones on the diagonal except the delay D (i.e. row and column D) has zero. Other values are zeros
B	The bandwidth [5 MHz]
b	The total number of correctly transmitted bits by HS-DSCH from all base stations in the simulated system over the whole simulated time
b_n	The number of correctly delivered bits to the UE n
c	Parameter for UTRA TDD uplink power control, which is to be set by the higher layer
c_a	Call arrival rate
C/I	Carrier power to interference ratio
c_s	Packet call size
C_w	Interference matrix, which has other cell interference plus noise on the diagonal and otherwise zeros
d_i	Transmitted QPSK symbols
D	Delay parameter for linear receivers
D_P	Delay between PCCPCH slot and the next uplink slot in UTRA TDD
E_b/N_0	Energy per bit to noise ratio
E_c/I_0	Energy per chip to interference ratio
E_s/N_0	Energy per symbol to noise ratio
F	Filter length for the linear receivers
f	Number of Rake fingers
G	Geometric value i.e. intra-cell interference to inter-cell interference plus noise ratio
$g_{i,j}$	Average path gain of multipath component j from sector i
$\mathbf{H}$	Channel matrix
h	Complex channel coefficient
$\mathbf{h}$	Channel coefficient vector
$h_{1,i,j}$	The complex channel coefficient for sector i and multipath component j from the first transmit antenna
$h_{2,i,j}$	The complex channel coefficient for sector i and multipath component j from the second transmit antenna
$\mathbf{I}$	Covariance matrix of the transmitted signal

I_{BTS}	Measured interference signal power level at cell's receiver in dBm
I_i	Interference from sector i
I_i^n	Interference from sector i towards terminal n
I_i^j	Interference from sector i at the receiver antenna j
$I_{i,j}^n$	Interference from multipath j from sector i to terminal n
$I_{intracell}$	Intra-cell interference without MUD
$I_{intra-cell}^{total}$	Intra-cell interference when MUD is taken into account
I_{tot}	Total downlink interference
I_{tot}^j	Total downlink interference at the receiver antenna j
K	Number of sectors in active set
k	Number of sectors in the simulation area
L	Delay spread of the channel normalized to the chip interval
$L(d)$	Pathloss including distance attenuation, slow fading and fast fading
L_0	Long-term average of L_{PCCPCH} in dB
$L_a(d)$	Distance attenuation
L_F	Fast fading
L_i	Pathloss from sector i including distance attenuation and slow fading
L_{PCCPCH}	Measured path loss in dB
L_S	Slow fading
N_{bad}	Number of bad quality calls
$N_{blocked}$	Number of blocked calls
$N_{dropped}$	Number of dropped calls
N_{good}	Number of good quality calls
N_i	Number of multipath components provided by the simulated environment without transmit diversity in sector i
N_0	Noise power spectral density
N_{Rx}	Number of receiver antennas
n	Terminal number
$\mathbf{n}$	Noise vector
P_i	Total transmit power of the sector i
$P_{i,n}$	Transmit power of the sector i to terminal n
$P_{UE_{dc}}$	Transmit power of the UE for the dedicated channels
R	Average HS-DSCH bit rate [kbps/cell/Mhz]
R_n	User bit rate for the packet session of the UE n
r	Received signal
$\mathbf{r}$	Received chip stream
s	Spreading sequence
$\mathbf{s}$	Transmitted chip stream
S_f	Rate of the satisfied calls

SIR_{TARGET}	Target Signal to Interference Ratio from the outer loop power control
T	The simulated time
T^{n}_{active}	The active time of the UE, which is running whenever the user buffer is not empty
t_{offset}	Timing difference between time slots from different cells
t_{slot}	Length of the time slot
w	Tx-weights i.e. $w = [w1 \;\; w2]^T$
$\mathbf{w}$	Filter coefficients for linear receivers

ABBREVIATIONS

1x	cdma2000, single carrier
1xEV	1x Evolution
1xEV-DO	1xEV - Data Only
1xEV-DV	1xEV - Data and Voice
16QAM	16-point Quadrature Amplitude Modulation
2G	Second Generation mobile communication system
3G	Third Generation mobile communication system
3GPP	Third Generation Partnership Project
3GPP2	Third Generation Partnership Project 2
AC	Admission Control
ACI	Adjacent Channel Interference
ACIR	Adjacent Channel Interference Ratio
ACK	Acknowledgement
ACLR	Adjacent Channel Leakage Ratio
ACS	Adjacent Channel Selectivity
AMC	Adaptive Modulation and Coding
AR	Advanced Receiver
ARQ	Automatic Repeat reQuest
AVI	Actual Value Interface
BCH	Broadcast CHannel
BER	Bit error ratio
BLER	Block error ratio
BPSK	Binary Phase Shift Keying
BS	Base station
C/I	Carrier to Interference ratio
CC	Chase Combining
CCCH	Common Control CHannel
CCPCH	Common Control Physical CHannel
CCTrCH	Common Control Transport CHannel
CDF	Cumulative Density Function
CDMA	Code Division Multiple Access
cdma2000	code division multiple access for the year 2000
CL	Closed Loop
CPICH	Common Paging Indicator CHannel
CQI	Channel Quality Indicator
CRC	Cyclic Redundancy Check
DCA	Dynamic Channel Allocation
DCH	Dedicated CHannel
DL	Downlink i.e. base station to mobile
DPCCH	Dedicated Physical Control CHannel
DPCH	Dedicated Physical CHannel
DPDCH	Dedicated Physical Data CHannel
DS-CDMA	Direct Sequence - CDMA

DSCH	Downlink Shared CHannel
Equ	Equalizer
F-DCA	Fast Dynamic Channel Allocation
FACH	Forward Access CHannel
FCS	Fast Cell Selection
FDD	Frequency Division Duplex
FDMA	Frequency Division Multiple Access
FER	Frame error ratio
GSM	Global System for Mobile Communications
HARQ	Hybrid ARQ
HO	Handover
HSDPA	High Speed Downlink Packet Access
HS-DPCCH	High Speed Dedicated Physical Control CHannel
HS-DSCH	High Speed Downlink Shared CHannel
HS-PDSCH	High Speed Physical Downlink Shared CHannel
HS-SCCH	High Speed Synchronization CHannel
IMT-2000	International Mobile Telecommunication - 2000
IP	Internet Protocol
IR	Incremental Redundancy
IS-95	Interim Standard 95
ISCP	Interference Signal Code Power
ISI	Inter-Symbol Interference
ITU	International Telecommunication Union
L1	Layer 1 i.e physical layer
LC	Load Control
LMMSE	Linear Minimum Mean Square Error
MAC	Medium Access Control
MAI	Multiple Access Interference
Mbps	10^6 bits per second
MC-CDMA	Multi-carrier CDMA
Mcps	10^6 chips per second
MCS	Modulation and Coding Set
MEF	Multi-user Efficiency Factor
MIMO	Multiple Input Multiple Output
MRC	Maximal Ratio Combining
MUD	Multi-User Detection
Node B	Base station in 3GPP vocabulary
NRT	Non-Real Time
OL	Open Loop
OSVF	Orthogonal Variable Spreading Factor
pA	ITU Pedestrian A channel model
PC	Power Control
PCCPCH	Primary Common Control Physical CHannel
PF	Proportional Fair
PICH	Paging Indicator CHannel

PRACH	Physical Random Access CHannel
QoS	Quality of Service
QPSK	Quadrature Phase Shift Keying
RACH	Random Access CHannel
RAN	Radio access network
RLC	Radio Link Control
RNC	Radio Network Controller
RR	Round Robin
RRC	Radio Resource Control
RRM	Radio Resource Management
RSCP	Received Signal Code Power
RSSI	Received Signal Strength Indication
RT	Real Time
Rx	Receiver
S-DCA	Slow Dynamic Channel Allocation
SCCPCH	Secondary Primary Synchronisation CHannel
SCH	Synchronization CHannel
SF	Spreading Factor
SHO	Soft handover
SINR	Signal to Interference plus Noise Ratio
SIR	Signal to Interference Ratio
SNR	Signal to Noise Ratio
SRNC	Serving Radio Network Controller
SSTD	Site Selection Transmit Diversity
STD	Selective Transmit Diversity
TCP	Transmission Control Protocol
TBS	Transport Block Size
TD-CDMA	Time Division CDMA
TD-SCDMA	Time Division Synchronous CDMA
TDD	Time Division Duplex
TDMA	Time Division Multiple Access
TFC	Transport Format Combination
TFCI	Transport Format Combination Indicator
TFRC	Transport Format and Resource Combination
TPC	Transmit Power Control
TSTD	Time Switched Transmit Diversity
Tx	Transmitter
TxP	Transmit power
TTI	Transmission Time Interval
UE	User equipment
UL	Uplink i.e. mobile to base station
UMTS	Universal Mobile Telecommunication System
USCH	Uplink Shared Channel
UTRA	Universal Terrestrial Radio Access (3GPP) or UMTS Terrestrial Radio Access (ETSI)

UTRAN	UMTS Terrestrial Radio Access Network
vA	ITU Vehicular A channel model
VoIP	Voice over Internet Protocol
WCDMA	Wideband Code Division Multiple Access

1 INTRODUCTION

1.1 Background

Wireless telecommunication systems have been under intense research activities in recent years. Second generation mobile communication systems like GSM (Global System for Mobile Communications) and IS-95 have spread around the world and raised the need for more sophisticated mobile devices. Commercial launches of third generation (3G) mobile communication systems started in Japan 2002 and currently 3G systems are available in many cities around Europe and Asia. Although the systems have been available for some time, evolution of standardization for new releases is ongoing in The Third Generation Partnership Project (3GPP) [1].

Initially UMTS air interface was designed to support a wide variety of different services with different Quality of Service requirements (QoS). To reply to the challenges of future applications and services several technical enhancements are being studied to increase an achievable bit rate way over the initial standard of 2 Mbps. The initial targets of the 3G system can be briefly summarized as follows ([127, 118, 49, 73]):

- Sophisticated radio interface to support variable bit rates up to 2 Mbps
- Multiplexing of services with different quality requirements on a single connection, e.g. speech, video and packet data
- Variable bit rate to offer bandwidth on demand
- Delay requirements from delay sensitive real time traffic to flexible best effort packet data
- Quality requirements from 10^{-2} frame error rate to 10^{-6} bit error rate
- Support of asymmetric uplink and downlink traffic, e.g. web browsing causes more loading to downlink than to uplink

- Coexistence of UTRA FDD and TDD modes
- High spectrum efficiency
- Compatible to offer an effective evolutionary path for existing wireless network to support inter-system handovers for coverage enhancements and load balancing

Third generation systems should operate in all radio environments like urban and suburban areas, hilly and mountainous areas, micro cell, pico cell, and indoor environments. High data rate requirements are set up to at least 144 Kbps in vehicular, up to at least 384 Kbps in outdoor to indoor and up to 2 Mbps in indoor and pico cell environments. These requirements are quite well aligned in the different regions of America, Asia, Europa and in the ITU. In addition, global roaming has to be supported in the system design.

UMTS Terrestrial Radio Access (UTRA) is divided to UTRA FDD and TDD modes. UTRA FDD mode is based on wideband CDMA with chip rate of 3.84 Mcps. UTRA TDD mode contains wideband and narrowband schemes, 3.84 Mcps mode of UTRA TDD is based on TD-CDMA where as 1.28 Mcps mode of UTRA TDD is based on TD-SCDMA. In addition to UTRA TDD and FDD modes i.e. TD-CDMA and WCDMA, third mode is the multi-carrier (MC) CDMA mode, based on cdma2000 multi carrier option being standardised by the 3rd Generation Partnership Project 2 (3GPP2)[2]. In the downlink of cdma2000 multiple parallel narrowband CDMA carriers are transmitted from each base station instead of a single wideband carrier. The uplink direction is a direct spread, which is very similar to WCDMA.

1.2 Scope of this study

This study concentrates on the radio network performance analysis of 3G systems and radio resource management algorithms. These studies are based on the dynamic system level simulations. System simulators are important tools for research purposes, but in addition to that these can also be used for network planning, network optimization, training of network engineers and to support decision making e.g. in standardization (3GPP). The ability to test different radio resource management algorithms and for e.g. measurement accuracies effect on the system levels performance is essential to guarantee cost effective network deployment.

Issues covered by this thesis can be divided into three main categories. Firstly, TD-CDMA radio resource management algorithms are analysed including uplink and downlink power control, handover and dynamic channel allocation. Secondly, the radio network performance of WCDMA is analysed and the studies concentrate on the *High Speed Downlink Packet Access (HSDPA)* and transmit diversity. Third topic includes evaluation of HSDPA network performance with advanced UE receivers. Analysis is carried out with dynamic system level simulations.

1.3 Objectives

The main objective of this study is to evaluate the performance of TD-CDMA and WCDMA Radio Network Enhancements. The study can be split into four tasks as presented in the following.

1.3.1 Simulator modeling

Performance evaluation of TD-CDMA and WCDMA radio network is based on the dynamic system simulations. An existing dynamic WCDMA system simulator is used as a platform, to which the studied features are modeled. The first target was to develop the TD-CDMA on top of the existing WCDMA simulator. This task includes modeling of e.g. TD-CDMA frame structure, correlated fast fading for uplink and downlink due to the same carrier frequency and Actual Value Interface (AVI) for mapping system results to link level results. Major modifications are needed for interference calculation methods to take into account TD-CDMA specific interference and interference between TD-CDMA and WCDMA. Several Radio Resource Management algorithms are also needed for detailed studies e.g. uplink and downlink power control; Dynamic Channel Allocation (DCA) and hard handover.

The used simulator already covers WCDMA features and RRM algorithms, thus it should be further extended to support transmit diversity for dedicated channels and High Speed Downlink Shared Channel. Required models include complex channel coefficients, interference modeling for two transmit antennas in the Node B and receiver structure for STTD. CL Mode 1 modeling in the UE side includes transmit weight optimization and signalling of feedback commands to Node B. On the transmitter side filtering of feedback commands are performed and the selected transmit weight is used in the downlink transmission.

Furthermore used models are extended to cover UE advanced receivers, which includes a completely new receiver structure for both the Rake and LMMSE chip level linear equalizer.

1.3.2 TD-CDMA performance evalution

Concerning the TD-CDMA network performance evaluation the following questions are answered in this thesis.

- *Uplink power control in TD-CDMA system in an indoor environment* - Uplink power control in UTRA TDD is based on several UE made measurements, so what is the performance of the uplink power control assuming realistic error modeling? How can the existing power control algorithm be enhanced? How will the frame configuration impact to uplink power control performance?

- *Downlink power control in TD-CDMA system in an indoor environment* - What is the performance of closed loop power control in UTRA TDD

downlink? How well the closed loop power control works in TDD system as the feedback rate is clearly lower as compared to UTRA FDD?

- *Handover in TD-CDMA system in an indoor environment* - Feasibility of WCDMA type of handover to UTRA TDD system? How parameter selection affects UTRA TDD performance?

- *Dynamic Channel Allocation in TD-CDMA system in an indoor environment* - DCA has been widely studied in literature. Now we extend the studies to the TD-CDMA mode. What is the performance of dynamic channel allocation algorithms with realistic modeling including signal delays and measurement errors?

1.3.3 Transmit diversity in WCDMA

For the transmit diversity performance evaluation in WCDMA network the following questions are answered in this thesis.

- *Transmit Diversity on dedicated channels of WCDMA* - What is the system level performance of transmit diversity in the dedicated channels of WCDMA? How do the different methods perform in different environments and UE velocities?

- *Transmit Diversity for HSDPA* - How does the HSDPA specific features i.e scheduling, adaptive modulation and coding and HARQ affect the applicability of transmit diversity for the HSDPA?

1.3.4 Advanced UE receivers

Advanced UE receiver performance evaluation in this thesis answers to the following questions.

- *Advanced UE receivers with HSDPA* - What are the system level effects of the advanced UE receivers? What is the performance gain from advanced UE receivers in SINR distribution and cell throughput? Does the introduction of higher number of channelization codes change the achievable gains? What is the effect of scheduling with advanced receivers?

- *Different advanced UE receiver penetrations* - What is the HSDPA system level performance with different advanced UE receiver penetrations? How the fairness of the system can be guaranteed with different advanced UE receiver penetrations? What is the gain from advanced UE receivers from an end user point of view?

1.4 Original contributions

The main target of this study is to evaluate the performance of TD-CDMA and WCDMA network. This thesis includes the following original contributions.

- *TD-CDMA system simulator modeling* - Existing dynamic WCDMA radio network simulator was used as a platform and it was extended to support TD-CDMA. Simulator modeling includes e.g. TD-CDMA frame structure, correlated fast fading for uplink and downlink due to the same carrier frequency and Actual Value Interface (AVI) to take into account fastly variable conditions in different time slots. Major modifications were needed for interference calculation methods to take into account TD-CDMA specific interference and interference between TD-CDMA and WCDMA. Radio Resource Management algorithms were also modeled in detail including uplink and downlink power control, dynamic channel allocation and hard handover. From the time this simulator model was started and the first simulation results were published we were not aware of any other detailed dynamic TD-CDMA system simulators. These results are published in [P1].

- *Evaluation and enhancements of TD-CDMA uplink power control* - TD-CDMA uplink power control consists of an open inner loop power control and outer loop power control. Open loop power control is based on several UE made measurements, thus detailed studies of the effect of measurement errors on the systems performance was carried out. Based on these studies usage of relative measurements were proposed to 3GPP by Nokia. Effect of two beacon channels to the uplink power control performance was evaluated with different frame configurations. Also performance of the uplink power control was evaluated including the analysis of a required convergence speed for the outer loop power control. These results are published in [P1] and [P6].

- *Evaluation of TD-CDMA downlink power control* - In the downlink of TD-CDMA a closed loop power control is used. Feedback rate of the closed loop signal in the time division duplex system is clearly lower as compared to the WCDMA, thus applicability of the closed loop power control was evaluated for TD-CDMA. Due to a reduced feedback rate variable step size for closed loop power control was proposed in these studies and its applicability was also discussed in 3GPP standardization forum. Power control method where step size selection is based on the received signal quality was developed and it was granted a patent. Usage of variable power control step sizes for the compensation of reduced power control speed was also evaluated. Furthermore multiple level power control command signaling was proposed for the usage of variable power control step sizes (patent pending). These results are published in [P2] and [P3].

- *Evaluation of TD-CDMA handover and effect of parameters* - Applicability of WCDMA type handover for TD-CDMA was evaluated and the effect of different handover parameters for the system performance was studied. These results are published in [P1].

- *Modeling of* Dynamic Channel Allocation (DCA) *for TD-CDMA* - DCA algorithms are widely studied in literature. In theoretical studies very significant quality and capacity improvements have been achieved. However, in real systems DCA performance is limited by several factors so theoretical limits might not be reached. DCA algorithms are affected by unreliable measurements or all necessary information might not be available, since time division multiple access interference and loading conditions can change very rapidly from slot to slot. DCA algorithms can be divided into two parts where *slow DCA (S-DCA)* allocates resources to cells and *fast DCA (F-DCA)* to bearer services [49]. In this study different F-DCA algorithms were evaluated in the presence of measurement errors and signalling delays in an indoor environment. These results are published in [P4], [P5] and [P6].

- *Transmit diversity for dedicated channels of WCDMA* - Transmit diversity methods have been under intense research in recent years, but the performance is mainly analysed in the link level. For this study a detailed system level model of 3GPP release 99 transmit diversity schemes was included to the dynamic WCDMA network simulator. Performance evaluation of transmit diversity in dedicated channels of WCDMA was carried out.

- *Transmit diversity for HSDPA* - HSDPA was included to 3GPP release 5 to support higher data rates. It includes a number of performance enhancing features including Adaptive Modulation and Coding (AMC), fast scheduling at Node B and Hybrid Automatic Repeat Request (HARQ). Comparison of transmit diversity schemes with dynamic system level simulations was carried out and the results from the studies were used to support Nokia's contributions in 3GPP in the discussion of transmit diversity for release 5. Part of these results have been published in [P7] and [P8].

- *Advanced UE receivers with HSDPA* - Further enhancements for the HSDPA are currently an interesting research topic. Different methods have been widely presented in literature, but their effect on the system level performance has not been carefully addressed. In this thesis detailed studies are presented where the performance of receive diversity and Linear Minimum Mean Squared Error chip level linear equalizer are compared to conventional Rake receiver. Studies are also extended to more realistic scenarios where advanced receiver penetration is gradually increased to analyse the system performance with different ad-

vanced receiver penetrations. Simulation results from these studies were also contributed to 3GPP by Nokia in the discussion of 3GPP release 6.

1.5 List of publications

This thesis consists of two journal articles and six conference articles. In addition to previously published results also number of unpublished results are included to this thesis to Chapters 4.2 and 5.

[P1] Janne Kurjenniemi, Seppo Hämäläinen, and Tapani Ristaniemi. Handover and uplink power control performance in the 3.84 Mcps TDD mode of UTRA network. *Wireless Personal Communications*, vol. 27, no. 4, December 2003, pp. 337–351.

[P2] Janne Kurjenniemi, Otto Lehtinen, and Tapani Ristaniemi. Signaled step size for downlink power control of dedicated channels in UTRA TDD. *Wireless Personal Communications*, vol. 31, no. 3-4, December 2004, pp. 161–180.

[P3] Janne Kurjenniemi, Otto Lehtinen and Tapani Ristaniemi, Downlink Power Control of Dedicated Channels in UTRA TDD. In *IEEE Symposium on Personal, Indoor and Mobile Radio Communications (PIMRC'02)*, Lisbon, Portugal, September 2002, pp. 1402–1406.

[P4] Janne Kurjenniemi and Otto Lehtinen. Comparison of dynamic channel allocation schemes in downlink in UTRA TDD. In *IEEE Symposium on Personal, Indoor and Mobile Radio Communications (PIMRC'03)*, volume 1, Beijing, China, September 2003, pp. 901 – 905.

[P5] Otto Lehtinen and Janne Kurjenniemi. UTRA TDD dynamic channel allocation in uplink with slow reallocation. In *IEEE Vehicular Technology Conference (VTC'03-Spring)*, volume 2, Jeju, Korea, April 2003, pp. 1401–1405.

[P6] Jussi Äijänen, Otto Lehtinen, Janne Kurjenniemi and Tapani Ristaniemi. Frame configuration impact to the performance of UTRA TDD system. In *IEEE Symposium on Personal, Indoor and Mobile Radio Communications (PIMRC'03)*, volume 1, Beijing, China, September 2003, pp. 906 – 910.

[P7] Janne Kurjenniemi, Jari Leino, Yrjö Kaipainen, and Tapani Ristaniemi. Closed loop mode 1 transmit diversity with high speed downlink packet access. In *IEEE International Conference on Communication Technology (ICCT'03)*, volume 2, Beijing, China, April 2003, pp. 757–761.

[P8] Jari Leino, Janne Kurjenniemi, and Mika Rinne. Analysis of fast alpha switching for closed loop mode 1 transmit diversity with high speed

downlink packet access. In *IEEE Vehicular Technology Conference (VTC'04 - Fall)*, volume 1, Los Angeles, USA, September 2004, pp. 4466–4470.

1.5.1 Author's contribution to the included articles

The author of this thesis has done the modelling and implementation of the studied features in the articles [P1-P6] for the system simulator. He has conducted the related simulations, analysed the results and has been the main author of the articles [P1-P4]. In [P5] he has run all the simulations and has been co-author of the article. In addition to the modelling and the implementation work of article [P6] the author has participated in the analysis of the simulation results and the writing of the article. The author of this thesis has taken the main responsibility for the modelling and implementation work in articles [P7-P8], but the work has been done together with Jari Leino. The author of this thesis has run several simulations and has done most of the analysis in both [P7-P8]. He has been the main author of [P7] and the co-author of [P8].

1.6 Other publications

During these studies of the 3G radio network performance several other articles have been published which are not included in this thesis. These publications include one US patent, one US patent application and seven conference papers.

1. Janne Kurjenniemi. Method, device and system for power control step size selection based on received signal quality. US Patent, 3760598, 06.07.2004.

2. Janne Kurjenniemi, Otto Lehtinen and Petri Patronen. Multiple Level Power Control Command Signaling. US Patent pending, filed 2002.

3. Janne Kurjenniemi, Seppo Hämäläinen and Tapani Ristaniemi. System simulator for UTRA TDD. In *5th CDMA International Conference & Exhibition*, Seoul, Korea, November 2000, pp. 370-374.

4. Janne Kurjenniemi, Seppo Hämäläinen, Tapani Ristaniemi, Otto Lehtinen and Petri Patronen. Convergence of UTRA TDD uplink power control. In *IEEE Vehicular Technology Conference Spring*, Rhodes, Greece, May 2001, CD-ROM.

5. Janne Kurjenniemi, Seppo Hämäläinen and Tapani Ristaniemi. Uplink power control in UTRA TDD. In *IEEE International Conference on Communications (ICC'01)*, Helsinki, Finland, June 2001, CD-ROM

6. Janne Kurjenniemi, Seppo Hämäläinen and Tapani Ristaniemi. UTRA TDD handover performance. In *IEEE GLOBECOM*, San Antonio, Texas, USA, November 2001, CD-ROM.

7. Janne Kurjenniemi, Otto Lehtinen and Tapani Ristaniemi. Signaled Step Size for Downlink Power Control of Dedicated Channels in UTRA TDD. In *IEEE Conference on Mobile and Wireless Communications Networks*, Stockholm, Sweden, September 2002, CD-ROM.

8. Janne Kurjenniemi, Otto Lehtinen and Tapani Ristaniemi. Improving UTRA TDD Downlink Power Control With Asymmetrical Steps. In *IEEE Vehicular Technology Conference 2003*, Jeju, Korea, April 2003, CD-ROM.

9. Jussi Äijänen, Mika Rinne, Janne Kurjenniemi, Tapani Ristaniemi. UTRA TDD Intra-Frequency Handover Performance. In *Global Mobile Congress 2004*, Shanghai, China, October 2004, CD-ROM.

1.7 Outline

The rest of this thesis is organised as follows. The second chapter gives descriptions of the used dynamic system level simulator that is used for the performance analysis. Then the results of the studies can be divided into three main topics, namely TD-CDMA radio network performance, transmit diversity performance in WCDMA network and HSDPA network performance with advanced UE receivers. The first topic concentrates on the TD-CDMA i.e. 3.84 Mcps TDD mode of UTRA in an indoor environment and the second and third topics to the WCDMA i.e. FDD mode of UTRA in a macro cell environment. The third chapter concentrates mainly on the TD-CDMA uplink and downlink power control, handover and dynamic channel allocation. TD-CDMA related studies are published in [P1-P6]. In the fourth chapter studies of WCDMA are presented, which includes dedicated channel (DCH) and HSDPA simulation results with transmit diversity. Closed Loop Mode 1 related studies have been published in [P7-P8]. In the fifth chapter analysis of performance of advanced UE receivers in HSDPA network are presented. Studies concerning the comparison of transmit diversity schemes and analysis of advanced receiver performance are not previously published. Then in the sixth chapter conclusions of this study have been drawn.

2 MODELLING OF DYNAMIC UMTS SYSTEM SIMULATOR

Third generation mobile networks contain many advanced features and in addition to analytical studies network simulations are very important parts of the analysis. In this chapter the basic principles of the used dynamic system level simulator [38, 70, 69] which includes parametrized models for data traffic, user mobility and radio wave propagation are described in detail. In [46] a very comprehensive study of different network simulation approaches is given and also detailed level results from simulations are presented. UMTS network performance is also studied in [47], which is then extended with a comparison of the simulation data and experimental measurements from the actual network. [41] is also closely related to network simulations and it presents the modelling of WCDMA network through measured propagation data. In [73] simulations and methods for network planning purposes are presented.

2.1 Simulator principle

Realistic cellular networks consists of many base stations and thousands of mobiles, thus modelling everything from transmitted waveforms to tens of base stations would require far too complex simulators. One very commonly used approach is to separate the link and system level simulations to reduce the complexity of the simulators [46, 49]. In the link level simulator connection between one mobile station and one base station is modelled in a very detailed level. Then produced link level data is used through a so called *Actual Value Interface (AVI)* in the system level simulator as presented in [39] for FDD TDMA.

Mostly the system level simulators can be divided into static, quasi-static and dynamic simulators, where the first one is a snapshot type simulator suitable mainly for interference studies and capacity and coverage analysis. To be able to simulate different radio resource management algorithms quasi-static or

dynamic simulators can be used. Also a quasi-static simulator is a snapshot type simulator, but each snapshot contains several time slots to include the effect of fast fading. Mobile stations do not actually move, but fast fading is generated as mobiles move at a certain speed. Detailed modelling of procedures related to call generation and ending and handover are missing from the quasi-static simulators. Due to these included simplifications static and quasi-static simulators are usually clearly lighter than a fully dynamic simulator, which can be used for very detailed level analysis of system performance and RRM algorithm development. A dynamic system simulator is used in these studies and the modelling of the studied features are described in a more detailed level in the following chapters.

Simulation can be divided into three fundamental steps. In the first step all the static objects including a simulation scenario with radio network controllers (RNC), base stations (BS) and mobile units (UE) are generated according to the given parameters. Then the second step contains the actual simulation that starts with a warm up process to generate the initial load for the network. Actual simulation runs in a slot resolution i.e. in every 0.667 ms all relevant actions can be performed. The power levels in the radio propagation model are constant over one slot, so the power changes below the slot level are modelled in link level simulations (for example the *downlink dedicated physical channel (DPCH)* slot format has three different power levels for data, control and pilot bits). In every simulation step interference is calculated between all active radio connections between mobile and base stations. Possible interference scenarios are highlighted in Section 2.5. Simulation control runs through all mobile stations, base stations, radio network controllers and active radio connections and in each case the needed radio resource management algorithms are executed. Before simulation control is stepped to the next time slot statistics variables are updated and then new calls are generated according to the Poisson process. Simulation runs for a given number of slots after which the last statistics are saved and the simulation is finished in the third step.

2.2 Path loss modelling

An understanding of radio propagation is essential to develop a good wireless communication system. There have been many studies made to obtain information about radio channel behaviour in various environments [7]. The total attenuation of the power level when signals propagates through the air to the user can be divided into three components one of which presents a deterministic contribution depending on the distance and two probabilistic contributions: one varying slowly with distance (slow fading) and one varying fast with distance (fast fading). The path loss of the radio channel between a base station antenna and a mobile station antenna separated by d km is expressed in decibels as

$$L(d) = L_a(d) + L_S + L_F, \tag{2.1}$$

where $L_a(d)$ is a distance attenuation, L_S is a random variable modelling the shadow fading and L_F is a random variable modelling fast fading. The random

variables describing the shadow fading and fast fading in one radio link are assumed to be uncorrelated, and independent of the distance d.

2.2.1 Distance attenuation

Macro cell models

The basic path loss model equals to

$$L_a(d) = \max\{L_{min}; A + B\log_{10}(d)\}, \tag{2.2}$$

where L_{min} is the free space loss and d is the distance expressed in km.

The *Okumura-Hata* model is widely used for the calculations of coverage and simulations in a macro-cell environment. It is based on the measurements made by Y. Okumura in Tokyo [86] and it was then fitted to a mathematical model by M. Hata [40]. Due to the fact that original Okumura-Hata model is applicable at frequencies from 150 MHz to 1000 MHz, COST 231 has extended it to the frequency band 1500 ≤ f(MHz) ≤ 2000 by analysing Okumura´s propagation curves in the upper frequency band. This combination is called *COST-Hata-Model* and the coefficients equal to [12]

$$\begin{aligned} A &= 46.3 + 33.9\log_{10}(f(MHz)) - 13.82\log_{10}(h_{bs}) - a(h_{ue}) + C_m, \\ B &= 44.9 - 6.55\log_{10}(h_{bs}), \end{aligned} \tag{2.3}$$

where $f(MHz)$ is the carrier frequency in MHz, h_{bs} is a hight of a base station antenna, h_{ue} is a hight of a mobile antenna, C_m is an empirical correction factor that equals 0 dB for the medium sized cities and 3 dB for the metropolitan centres. $a(h_{ue})$ is defined as

$$a(h_{ue}) = (1.1 \cdot \log_{10}(f(MHz)) - 0.7) \cdot h_{ue} - (1.56 \cdot \log_{10}(f(MHz)) - 0.8). \tag{2.4}$$

The COST-Hata-Model was originally restricted to frequencies below 2000 MHz, but it has been widely applied for the UMTS frequencies. It should be noted that the same path loss is used in the uplink and downlink in our studies, even though path depends on carrier frequency in general. Anyway the duplex distance of 190 MHz is much smaller than the centre carrier frequency used in WCDMA, thus the difference between the uplink and downlink pathlosses are rather small as is presented in Figure 1.

Another used macro cell model is based on [109] and its coefficients equal to

$$\begin{aligned} A &= 128.1, \\ B &= 37.6. \end{aligned} \tag{2.5}$$

Indoor model

The indoor path loss model expressed in dB is in the following form, which is derived from the COST 231 [12] indoor model [108]:

$$L_a(d) = 37 + 20Log_{10}(d) + \sum k_{w_i} L_{w_i} + 18.3n^{\frac{n+2}{n+1}-0.46}, \tag{2.6}$$

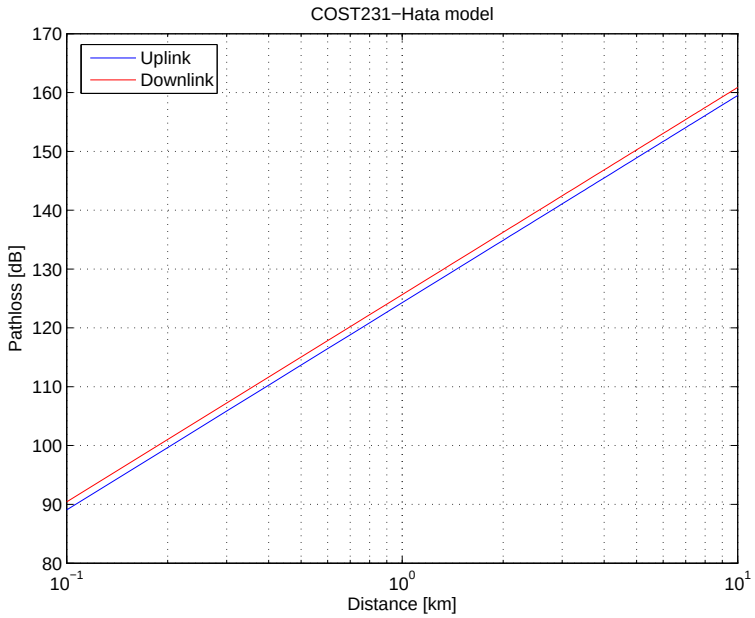

FIGURE 1 The uplink and downlink pathloss as a function of distance with COST-Hata-Model.

where d is transmitter-receiver separation given in metres, k_{w_i} is number of penetrated walls of type i, L_{w_i} is loss of wall type i and n is number of penetrated floors.

2.2.2 Slow fading

In addition to distance attenuation natural obstacles such as hills and buildings create shadowing to the received signal, which is referred to as *slow fading*. The slow fading component varies as the mobile station is moving and with the short distance differences the adjacent slow fading values are correlated. The correlation is modelled with an exponential function according to [22, 128]

$$R(\Delta x) = e^{-\frac{|\Delta x|}{d_{cor}} \ln 2}, \tag{2.7}$$

where d_{cor} is a correlation distance, which depends on the environment. Slow fading process L_S is generated in a logarithmic scale around the mean path loss. It is characterized by a Gaussian distribution with zero mean and standard deviation e.g. 8 dB in macro cells and 6 dB in micro cells.

2.2.3 Fast fading

Radio propagation is characterized with multiple reflections, diffractions and attenuation of the signal energy. The radio signal transmission is obstructed by natural obstacles such as buildings and hills, resulting in multipath propagation like presented in Figure 2. When these multipath signals propagates through

air, the time delay for each multipath component is random. This delay results in a random phase of received signals, so these multipath components can cause a constructive and destructive addition of the arriving plane waves which manifests itself as large variations in the amplitude and phase of the composite received signal.

When phases are adding destructively, the resultant received signal is very small or practically zero and the channel is said to be in a fade. In Figure 3 a typical fading process is presented. The rapidity of amplitude variation and accordingly the distance between two fades in time is influenced by the speed of the mobile receiver/transmitter. Hence, distinctions of slow and fast fading are made, where the former is generally understood as a situation, where the channel remains constant during one symbol duration.

The existence of different paths let the signal interfere with itself, which is known as inter-symbol interference (ISI). The severity of the ISI depends on the time difference of multipath components as compared to a symbol duration. When the time difference of multipath components is short as compared to the symbol duration fading is classified as *flat fading*. In this case all frequencies in the transmitted signal will experience the same random attenuation and phase shift due to the multipath fading, i.e., delays of different paths are very similar. Such a channel introduces very little or no distortion into the received signal. This is modelled as a single path case.

On the other hand when the delay spread of the channel is long as compared to the symbol duration fading is classified as *frequency selective*. As the delays of different paths have more differences, which is modelled as a multipath case, the signal waveform is scaled and reshaped i.e. ISI arises. As the path delays grow, even closely separated frequencies in the transmitted signal can experience significantly different phase shifts.

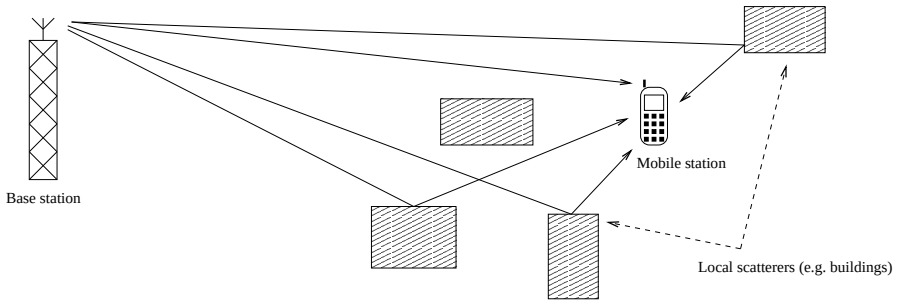

FIGURE 2 Multipath propagation.

Multipath propagation

In spread spectrum systems a receiver can separate different multipath components if the delay between the components is at least one chip duration. With an assumption that multipath components do not fully correlate, independent

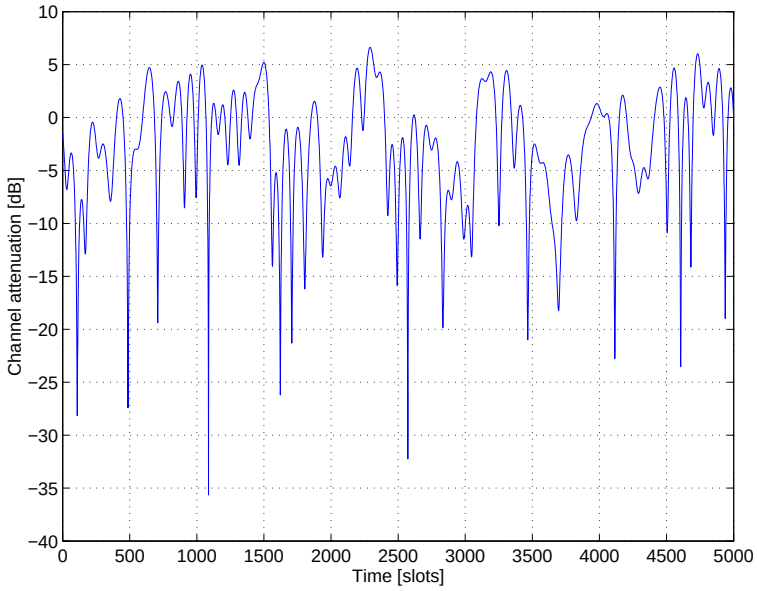

FIGURE 3 An example of a fading process.

signal copies can be received in time domain to take advantage of *multipath diversity*. This diversity can be captured with a Rake receiver or with some other linear detector or channel equalizer [52].

A multipath propagation environment is implemented to the simulator to support radio resource algorithms studies. Each multipath component has its own independent tap gain and fades according to the pre-generated Rayleigh process. The fading process is generated to a file according to Jakes model [57], which includes both power and phase information of the channel state. Complex channel coefficient is then calculated as

$$h = \sqrt{A}(\cos\phi + i\sin\phi), \tag{2.8}$$

where A is power and j is phase. A single fading process is generated even several processes occur during the simulation. For each multipath a path independent starting point to the fading process is generated. The size of the fading vector will be in the order of 500 000 – 1 000 000 samples, one sample per millisecond, when assuming mobile speed 1 m/s.

Fast fading depends on the frequency, and therefore, in FDD systems, fast fading is uncorrelated between uplink and downlink. As the same frequency is used both in uplink and downlink in TDD, fast fading is the same in both transmission directions. Based on the received signal, the TDD transceiver can estimate fast fading, which will affect its transmission. In case of fading between two mobile stations the change in the state of the channel is assumed proportional to the sum of the mobile positions changed. Hence the direction of the movement is discarded as in a conventional base station - mobile station case. Fading is also modelled between TDD-TDD and TDD-FDD base stations due to the changes in surrounding environment.

The combined fast fading component for the radio link, expressed in decibels, equals

$$L_F = 10 \log_{10} \sum_{l=1}^{L} h_l. \tag{2.9}$$

The used power delay profiles are typically selected in coherence with the ITU recommendations i.e. Vehicular-A and Pedestrian-A channel models are commonly used. The power delay profiles are modified from the original ITU power delay profiles so that the delay between paths equals at least one chip-time.

2.3 Traffic modelling

In dynamic system simulations users make calls and transmit data according to the data traffic model. Start of the calls are generated from the Poisson process. For speech calls voice activity and silent periods are taken from exponential distribution and for circuit-switched data calls 100 % activity is assumed. Modelling of data traffic models follows the guidelines given in [128].

Another important traffic model is the web traffic model [128].Start of the packet data sessions are generated according to the Poisson process and each session consists of a number of packet calls. The number of packet calls for each packet session are taken from the geometric distribution. Packet calls are also referred to as documents and these can be considered as web pages. Each of the packet calls contains a number of individual packets, which sizes are taken from geometric distribution. When a user has downloaded one document, the user is said to be in reading time, which models the time when a user can read the document before downloading any new documents. Reading time is also modelled with geometric distribution.

2.4 Mobility modelling

Depending on the simulated scenario users move according to a specific mobility model. [128] presents different mobility models for indoor pico, outdoor micro, and outdoor macro cellular scenarios. In a macro scenario users are uniformly distributed around the simulated area and users start to move in random directions. In each simulation step direction of movement can be changed according to the given probabilities.

The indoor simulation environment consists of office rooms and corridors. Users can be distributed in office rooms and corridors according to the given probabilities. A random destination is selected for each user and users move towards that with certain speed. When they reach their destination, a stationary time is selected for those users. Probability to be stationary is higher in office

rooms than in corridors. When stationary time is expired, user starts to move towards newly destination.

2.5 Interference generation mechanisms

In this section different interference generation mechanisms are introduced, which includes TDD-TDD and TDD-FDD interference scenarios. TD-CDMA specific interference situations are studied in [48].

Interference is a disturbance signal coming to the receiver antenna in some specified frequency band. To calculate the interference at some simulation object, the emitted power and position of all interference sources must be known. For example to calculate the interference perceived by a mobile station all base station positions and the total transmitted power in the direction towards the mobile station must be known.

2.5.1 Interference between uplink and downlink in TDD

The same frequency is used for both uplink and downlink in TDD, which causes additional interference between uplink and downlink if compared to the FDD mode. This kind of interference occurs if base stations are not synchronized or if different asymmetry is used between the uplink and downlink in adjacent cells. Interference between uplink and downlink can also occur between adjacent carriers, thus it can also take place between two operators. According to [37] an intelligent Dynamic Channel Allocation (DCA) algorithm has to be employed to enable co-location of cells in adjacent carriers unless a significant drop of capacity can be tolerated.

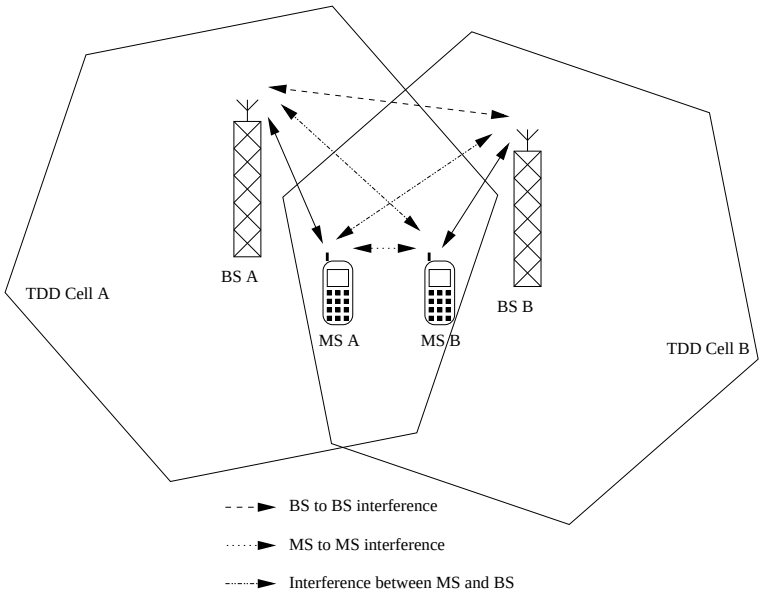

FIGURE 4 TDD - TDD interference generation mechanism.

Mobile station to mobile station interference

The interference between mobiles occurs if mobile station A in Figure 4 is transmitting and mobile station B is receiving simultaneously on the same (or adjacent) frequency in adjacent cells. This type of interference cannot be avoided by network planning because the locations of the mobiles cannot be controlled. Same operators mobiles can interfere with each other especially at the cells borders. Inter-operator interference between mobiles can occur anywhere where two operators' mobiles are close to each other and transmitting on fairly high power. Dynamic channel allocation and power control can be used to control interference between mobiles.

Base station to base station interference

The interference between base stations occurs if base station A in Figure 4 is transmitting and base station B is receiving on the same (or adjacent) frequency in adjacent cells. Interference between base stations can be especially strong if the path loss is low between them. The same also applies for intra-operator interference, thus the best way to avoid base to base interference is by careful planning to provide sufficient coupling loss between base stations.

2.5.2 Interference between TDD and FDD

The lower TDD frequency band is allocated next to the FDD uplink band, which causes interference between FDD and TDD systems [33, 32]. DCA can be used to avoid TDD-TDD interference [33], but DCA is not effective between TDD and FDD due to the continuous transmission and reception of the FDD mode. Interference scenarios between TDD and FDD systems are studied in [119, 32, 34, 36, 31].

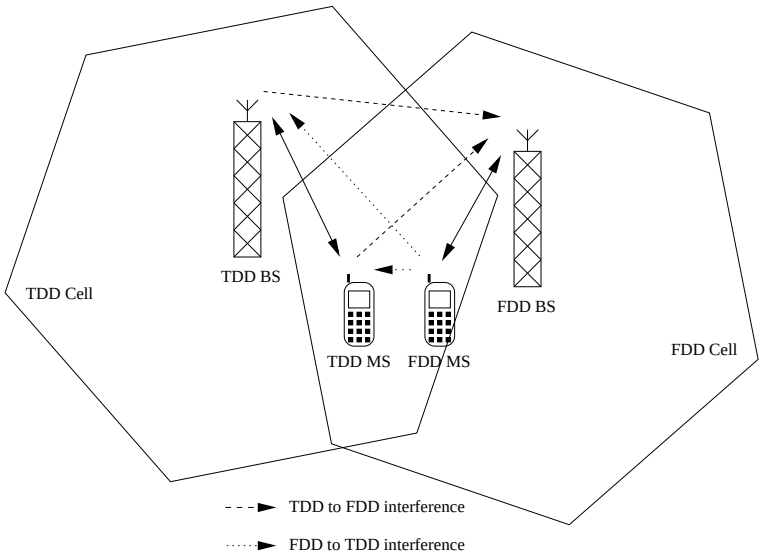

FIGURE 5 Possible interference scenarios between TDD and FDD.

Interference between TDD and FDD may occur in four different situations as is highlighted in Figure 5. First of all, a TDD base stations may interfere with a FDD base station. Secondly, TDD mobiles may interfere with a FDD base stations. This interference is basically the same as that from a FDD mobile to a FDD base station on the adjacent frequency. In pure FDD interference there is always a corresponding downlink interference, while in interference from TDD to FDD there is no downlink interference. Thirdly, a FDD mobile may interfere with the reception of a TDD base station. Uplink reception may experience high interference, which is not possible in TDD only operation. Fourthly, a FDD mobile may interfere with the reception of a TDD mobile. One way to tackle the problem is to use the downlink power control in TDD base stations to compensate for the interference from the FDD mobile.

2.5.3 Adjacent channel interference

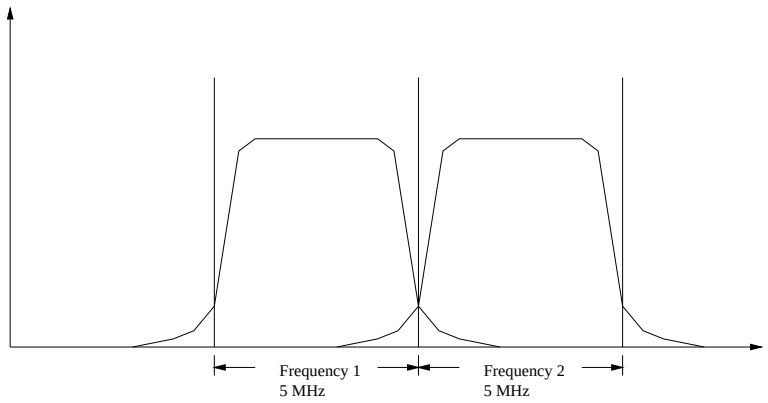

FIGURE 6 Adjacent channel interference.

Power leakage between adjacent carriers cannot be avoided and this property has on impact on adjacent channel interference and thus also on cell capacity. The power leakage results from transmitter mask imperfections and non-ideal receiver filters. *Adjacent Channel Interference Ratio (ACIR)* is a single parameter that sums up the degree of interaction between adjacent channels [105, 106] and it presents both transmitter and receiver performance. *Adjacent Channel Leakage Power Ratio (ACLR)* is the ratio of the transmitted power to the power measured in adjacent channels. *Adjacent Channel Selectivity (ACS)* is a measure of a receiver's ability to receive a wanted signal at its assigned channel frequency in the presence of an adjacent channel signal. ACS is the ratio of the receiver filter attenuation on the assigned channel frequency to the receiver filter attenuation to the adjacent channel(s). The relationship between ACIR, ACLR and ACS was investigated in [98] and was found to be:

$$ACIR \cong \frac{1}{\frac{1}{ACLR} + \frac{1}{ACS}}. \tag{2.10}$$

The ACIR between adjacent carriers in the TDD mode of UTRA must be greater than 30 dB according to [33] unless a significant capacity reduction is tolerable. Simulation results for the impact of ACIR on a systems capacity can also be found from [37].

2.6 Synchronisation and interference calculation

Different degrees of synchronisation is possible to model such that the synchronisation parameter θ describes the timing offset between the cell under study and the adjacent cells using the same or adjacent carrier. It is defined as [48]

$$\theta = \frac{t_{offset}}{t_{slot}}, \tag{2.11}$$

where t_{slot} is length of the time slot and t_{offset} is timing difference between time slots. In [37] a detailed description of synchronisation in the system capacity point of view is shown.

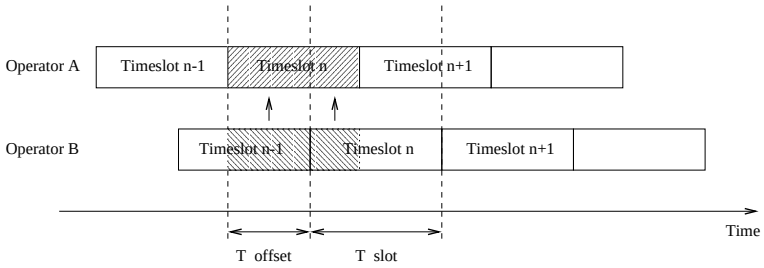

FIGURE 7 T_{offset} describes synchronisation difference between two base stations.

The amount of interference is dependent on t_{offset} presented in Figure 7. Therefore interference power is directly proportional to timing conditions between slots of different users. When this scheme is applied to interference calculations, it may happen that the information from the next slot should be known. This is a contradictory requirement for a normal approach, where calculations are made slot by slot. This can be seen e.g. in Figure 7, where the interference calculation of slot n of base station 2 needs information about power of slot $n+1$ of base station 1 and this data is not yet set. The power of the mobile station or base station is however available because *Primary Common Control Physical Channel (PCCPCH)* for uplink power control and closed loop power control command for downlink is already done or available. Therefore, here this information will be used and thus it is a forecast of the transmit power of the next time slot. If a new call occurs then this will cause a small error in the estimated power.

2.7 Connection to link simulations

The model for the interface between link and system level simulations is similar to the one described in [39] for FDD TDMA called *Actual Value Interface (AVI)*. In

the model for TDD, data is generated in the link level tools so that firstly SIR is measured for a time slot and then it is mapped to a raw BER. Then an average of raw BER values obtained during an interleaving period is calculated and mapped to BLER. By doing so, look-up tables given in Figure 8 are generated. In the system level tool, SIR is correspondingly calculated and mapped to raw BER. Interleaving is modelled by calculating the mean raw BER and mapping it to BLER. TDD specific features are also taken into account, which includes a variable data rate in different time slots of the same frame, multi-user detection and timing difference between time slots.

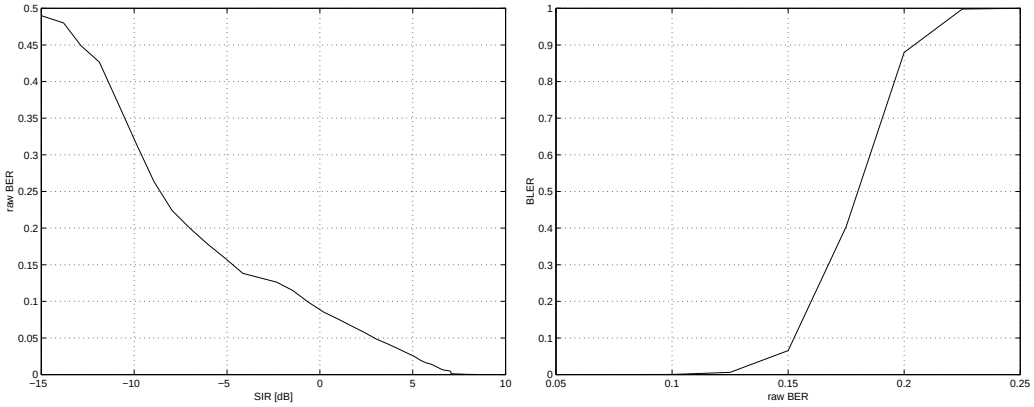

FIGURE 8 Examples of raw bit error rate (BER) as a function of signal-to-interference ratio and block error rate (BLER) as a function of raw BER.

2.7.1 Multi-user detection for TDD mode of UTRA

For the *Multi-User Detection (MUD)* the needed information is got from link level simulations. *Multi-user efficiency factor (MEF)* indicates the amount of interference suppression of intra cell interference. For example, a multi-user efficiency factor equal to 0.9 would mean that the intra cell interference power is suppressed 90 %.

The intra cell users are assumed to be slot-synchronous in TDD. In addition, a base station can control the slot timing alignment, and thus the effect of misalignment for MUD is not considered. All the other interference sources can be slot-asynchronous, and even if they were slot-synchronous timing offsets are expected to occur. Due to this, the interference situation may change rapidly in the middle of the timeslot. At this point, this type of jumping is not considered, but the weighted average of this interference, according to the timing alignment, is taken for the SINR calculation. As a conclusion, the effect of MUD is modelled as

$$I_{intracell}^{total} = (1 - MEF) \cdot I_{intracell}, \tag{2.12}$$

where $I_{intracell}$ is intra-cell interference without MUD and $I_{intra-cell}^{total}$ presents the intra-cell interference when MUD is taken into account.

3 TD-CDMA RADIO RESOURCE MANAGEMENT PERFORMANCE

In this chapter we give an introduction to the 3.84 Mcps time-division duplex (TDD) mode of UTRA (Universal Terrestrial Radio Access) and present the evaluation of its network performance. A detailed description of UTRA TDD mode is presented in 3GPP technical specifications ([100, 101, 102, 103, 104]) and in [24, 49]. In addition a short overview of UTRA TDD mode is given in [17] .

In this study we emphasize three of the radio resource management algorithms, power control, handover and dynamic channel allocation, whose role in the overall system performance is studied extensively. First, the specified uplink power control algorithm is considered. Efficient power control is one of the most important aspects in CDMA, in particular in the uplink. Without it, a single overpowered mobile could block a whole cell. The optimum strategy in the sense of maximising capacity is to equalise the received power per bit of all mobile stations at all times. Since TD-CDMA uplink power control is based on several user-made measurements which may involve both random and systematic errors a careful study of the suitability of the power control scheme is needed. When considering the downlink power control algorithm emphasis is put on the further improvements to compensate for the low power control speed. Secondly, a simple WCDMA handover, tailored to a TDD operation, is considered. This gives rise to a careful setting of different handover parameters, and the evaluation of the effects on the system performance. Thirdly, analysis of dynamic channel allocation (DCA) algorithm is presented. A dynamic system level simulator, where uplink and downlink power control, handover, dynamic channel allocation and admission control are modelled, is used for this purpose. TD-CDMA studies concentrate on indoor environment to reflect the potential use case.

3.1 Overview of TD-CDMA

The TD-CDMA is intended to operate in the unpaired spectrum as shown in Figure 9, whereas the FDD mode of UTRA requires a pair of bands. The TDD mode of UTRA should be usable from low to high data rates concerning symmetrical and especially asymmetrical services. Uplink and downlink are separated in a time domain in TDD operation, which makes it possible to dynamically change the timeslot allocations to move capacity from the uplink to the downlink or vice-versa depending on the capacity requirements.

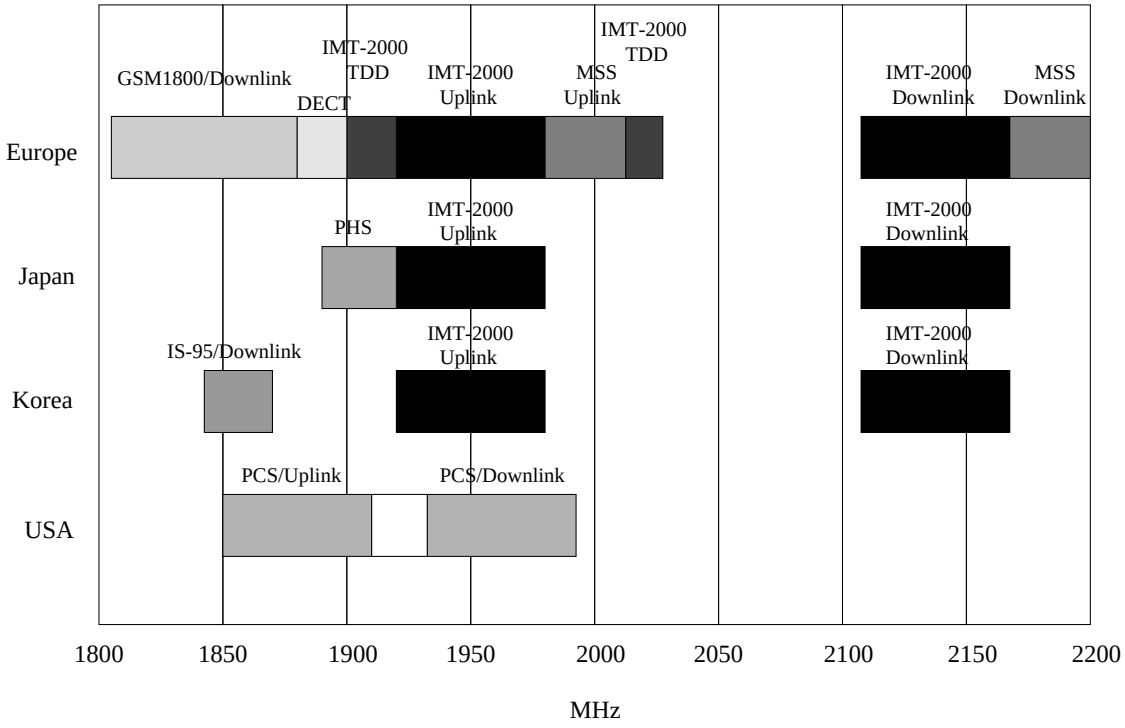

FIGURE 9 Spectrum allocation in Europe, Japan, Korea and USA.

As uplink and downlink share the same frequency band in TDD, additional interference scenarios exist in TDD operation as highlighted in Section 2.5. In FDD interference between uplink and downlink is avoided due to the duplex separation of 190 MHz. Since the mobile station and base station transmission are discontinuous in TDD, a guard period is used in the end of each slot to avoid the overlapping of uplink and downlink transmissions.

TDD can also take advantage of the reciprocal channel. The fast fading depends on the frequency and therefore, in FDD systems fast fading is uncorrelated between the uplink and downlink. As the same frequency is used for uplink and downlink transmissions in TDD, fast fading is the same in both transmission directions. Based on the received signal, the TDD receiver can estimate the fast fading, which will affect its transmission. This can be utilized in power control and also in adaptive antenna techniques in TDD.

3.1.1 Physical layer

The TD-CDMA uses a combined time division and code division multiple access scheme that is well suited for the TDD operation due to its inherent time division component. The different user signals are separated in both time and code domain. Basic system parameters are harmonised within UTRA for TDD and FDD modes, which enables the development of low cost mobile stations supporting dual mode operation [24]. In Table 1 basic system parameters for 3.84 Mcps mode of UTRA TDD and FDD are compared. UTRA TDD also comprises a low chip rate option (1.28 Mcps), which is a part of release 4 in 3GPP.

TABLE 1 Comparison of UTRA TDD and FDD basic system parameters [49].

	UTRA TDD	UTRA FDD
Multiple access method	TDMA, CDMA (inherent FDMA)	CDMA (inherent FDMA)
Duplex method	TDD	FDD
Carrier spacing	5 MHz	
Carrier chip rate	3.84 Mcps	
Timeslot structure	15 slots/frame	
Frame length	10 ms	
Multirate	Multicode, multislot and orthogonal variable spreading factor (OVSF)	Multicode and OVSF
Interleaving	Inter-frame interleaving (10, 20, 40 and 80 ms)	
Modulation	QPSK	
Dedicated channel	Uplink: open loop (Rate: 100 or 200 Hz) Downlink: closed Loop (Rate: $\leq$ 800 Hz)	Fast closed loop, (Rate: 1500 Hz)
Intra-frequency handover	Hard handover	Soft handover
Inter-frequency handover	Hard handover	
Channel allocation	Slow and fast DCA supported	No DCA required
Spreading factors	1 . . . 16	4 . . . 512

3.1.2 Slot and frame format

The frame length of TD-CDMA is 10 ms and it is divided into 15 time slots. The frame structure is presented in Figure 10. The duration of each time slot is 666 μs and length 2560 chips.

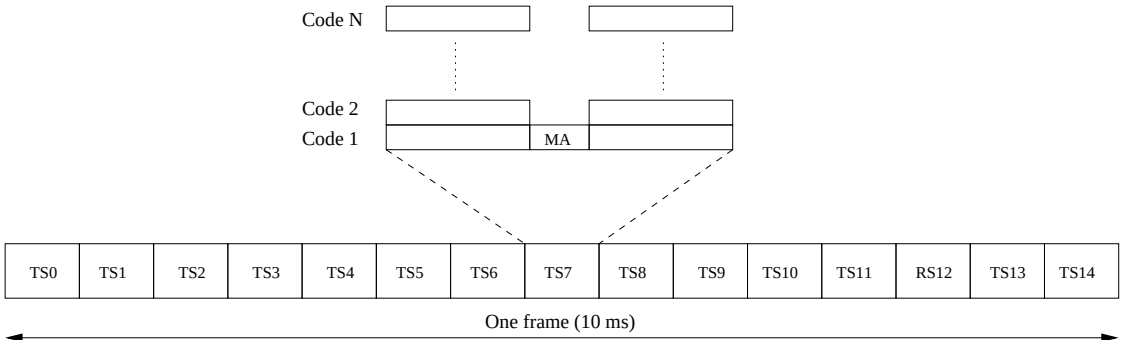

FIGURE 10 TDD frame structure.

Each of the time slots can be allocated either for uplink or downlink. Part of the slots must be fixed for the downlink (*Broadcast Channel (BCH)* and *Synchronisation Channel (SCH)*) and uplink (*Random Access Channel (RACH)*, but other slots could be allocated according to the need. Figure 11 shows examples of multiple slot allocation possibilities available in TDD. It is possible to have multiple switching points per frame, i.e. change of transmission direction. TD-CDMA supports asymmetry well in traffic and that is needed since for instance mobile Internet applications will probably contribute to a significant asymmetry in favour of the downlink. The maximum uplink asymmetry can be served by a slot allocation of 2:13 and maximum downlink asymmetry by a slot allocation of 14:1 [49, 100].

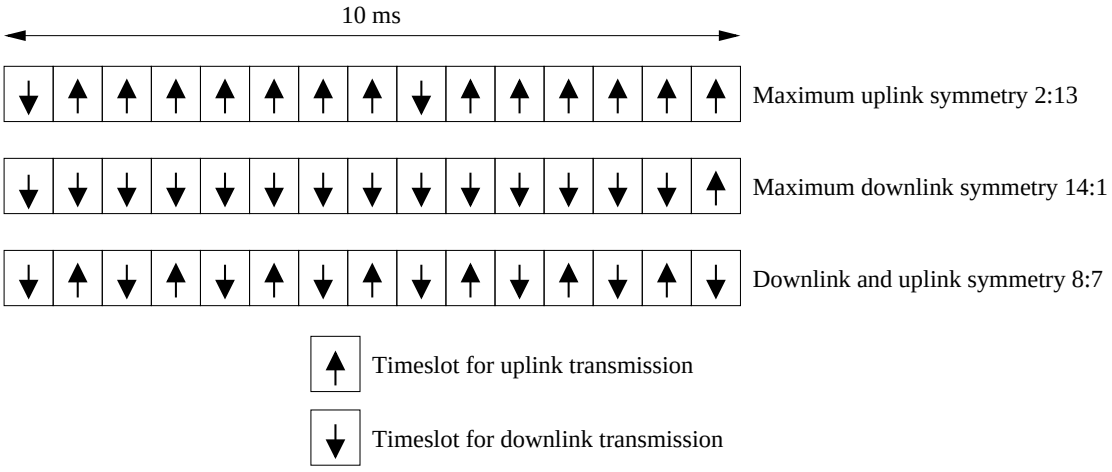

FIGURE 11 Different asymmetries can be used with TDD.

3.1.3 Modulation and spreading

The data modulation scheme in TD-CDMA is *Quadrature Phase Shift Keying (QPSK)*. The spreading codes of UTRA are based on the *Orthogonal Variable Spreading Factor (OVSF)* techniques which allows the spreading factor to be changed and orthogonality between different spreading codes of different lengths to be maintained [49, 102]. The OVSF codes are defined by the same tree structure as in the WCDMA.

Downlink physical channels use only the maximum spreading factor 16 to enable the implementation of low cost mobile stations, but to support higher data rates different channelisation codes may be used in parallel. It is also possible to use a single channelisation code with spreading factor one for the downlink physical channels to transmit high data rates, but it requires that the inter cell interference is low [24].

For the uplink physical channels usage of spreading codes from 1 to 16 with a single channelisation code is supported and it also leads to a smaller peak-to-average transmission power ratio and thereby to lower battery consumption than multi code transmission [24]. For multi code transmission a mobile station can use a maximum of two physical channels per timeslot simultaneously. These two parallel physical channels are transmitted using different channelisation codes.

The modulated and spread data is then scrambled with a cell specific pseudo random sequence length of 16 to reduce inter-cell interference and these scrambling codes are optimized with respect to an efficient use of the wideband spectrum [24].

3.1.4 Transport and physical channels

TD-CDMA mode transport channels can be divided into dedicated and common channels. Common channels can be further divided into *Common Control Channels (CCCH)*, the *Random Access Channel (RACH)*, the *Downlink Shared Channel (DSCH)* in the downlink and the *Uplink Shared Channel (USCH)*. Each of these transport channels is then mapped to the corresponding physical channel [49].

The physical channels of UTRA TDD are *Common Control Physical Channel (CCPCH)*, the *Dedicated Physical Channel (DPCH)*, the *Physical Random access channel (PRACH)*, *Paging Indicator Channel (PICH)*, and *Synchronisation Channel (SCH)*. For the SCH and BCH corresponding transport channels do not exist [49]. A good overview of transport and physical channels of TD-CDMA are given in [49, 24].

3.1.5 Shared channels

The 3GPP specifications also defines the *Downlink Shared Channel (DSCH)* and the *Uplink Shared Channel (USCH)*, which use exactly the same slot structure as do the dedicated channels. The difference is that they are allocated on a temporary basis. In the downlink the signal to indicate which mobile stations need to decode the channel can be done with *Transport Format Combination Indicator (TFCI)*, by

detecting midamble in use or by higher layers. In the uplink the USCH uses higher layer signalling and thus is not shared in practice on a frame by frame basis.

3.1.6 User data rates

The user bit rates with 1/2-rate channel coding and spreading factor 16 are shown in Table 2. These bit rates are time slot and code limited, so the maximum interference limited bit rate can be lower. If the number of needed slots exceed 7, the corresponding data rate can only be provided for either uplink or downlink transmission.

TABLE 2 UTRA TDD air interface user bit rates [49].

	Number of allocated timeslots		
Number of allocated codes with spreading factor 16	1	4	13
1	13.8 kbps	55.2 kbps	179 kbps
8	110 kbps	441 kbps	1.43 Mbps
16 (or spreading factor 1)	220 kbps	883 kbps	2.87 Mbps

3.2 Uplink power control

3.2.1 Algorithm description

Uplink power control is a combination of open inner loop control, where the output power is based on the measured received signal level (path loss) of *Primary Common Control Physical CHannel (PCCPCH)* and outer loop. This directly determines the output power of a user for common physical channels. For dedicated physical channels some additional information is needed, such as the target *Signal-to-Interference-Ratio (SIR)* from the outer loop, and a weighting parameter α, which characterize the effect of different PCCPCH slot locations. Target SIR is set by the network and signalled to the user. The network also sends information about the interference level of each time slot. The outer loop power control algorithm implemented to the simulator is similar as presented in [121].

The transmitter power of a user in a dedicated channel is defined as in [103],

$$P_{UE_{dc}} = \alpha L_{PCCPCH} + (1 - \alpha)L_0 + I_{BTS} + SIR_{TARGET} + c, \tag{3.1}$$

where

- $P_{UE_{dc}}$ transmitter power level in dBm in dedicated channel (DCH),
- L_{PCCPCH} measured path loss in dB (reference transmit power is broadcast on BCH),

- L_0 long-term average of L_{PCCPCH} in dB,
- I_{BTS} measured interference signal power level at cell's receiver in dBm, which is broadcast on BCH,
- α is a weighting parameter,
- SIR_{TARGET} target from the outer loop,
- c is to be set by the higher layer. It is not used in this study.

A weighting parameter α is needed in order to adjust the output power as a function of delay in slots (D_P) between the PCCPCH slot and the next uplink slot. This is because the new power is set at the beginning of the first uplink slot after the PCCPCH slot. Hence, the bigger delay, the more the channel may vary before the power adjustment is done. Therefore the long term average L_0 is stressed more than the bigger delay. Parameter α should also reflect the rate of variation of the fading channel, which depends mainly on the speed of the mobile station. The weighting factor is defined as a function of delay D_P,

$$\alpha = 1 - \frac{(D_P - 1)}{6}. \tag{3.2}$$

If D_P is greater than 6, then α is set to zero.

When the power is adjusted according to Equation 3.1, it requires many measurements, which involve both random and systematic measurement errors. In addition, the power setting also involves error, thus to fully evaluate the quality of the power control scheme, each measurement is accurately modelled.

Systematic errors take place at the beginning of a new call and when performing handover to a new base station. In these occasions absolute power measurements need to be done. The following measurements, after the initial state, can be done as relative measurements with higher accuracy. Error for the initial state is taken care of by the outer loop power control algorithm. This is depicted in Figure 12, where the transient time represents the time needed by the outer loop to track the systematic error.

The time it takes for the outer loop control to cope systematic errors depends, naturally, on the quality of the algorithm. In Figure 12 a solid curve presents the situation in real world, but in the simulator the systematic error is kept constant during the transient time. This is presented with a dashed curve. This is a sort of worst case model, and thus it offers lower bounds for the convergence times.

3.2.2 Network performance evaluation

The performance of the network is measured by the rate of satisfied calls which is defined as

$$S_f = \frac{N_{good}}{N_{good} + N_{bad} + N_{blocked} + N_{dropped}}, \tag{3.3}$$

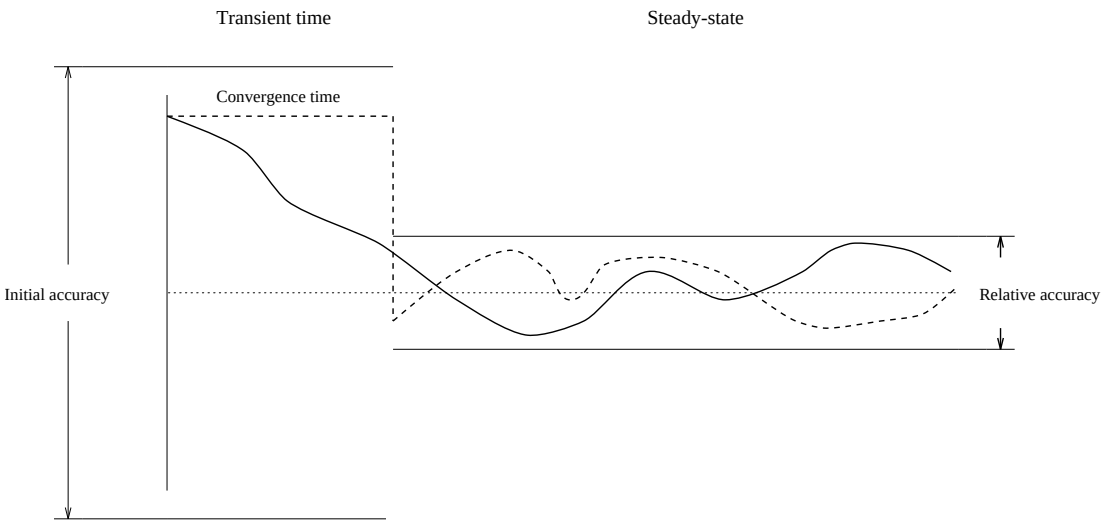

FIGURE 12 Modelling of power control convergence.

where N_{good}, N_{bad}, $N_{blocked}$ and $N_{dropped}$ are the numbers of good, bad, blocked and dropped calls, respectively. In the simulations, only the calls, which start and end during the simulation time horizon, are considered for the number of N_{good} and N_{bad}. Once a call ends it is classified as a good/bad quality call. In these simulations ended call was considered as a bad quality call if more than 2 percent of the transmitted blocks were erroneous. Otherwise it was considered as a good quality call. Dropping of a call is done if 50 consecutive erroneous frames exist.

3.2.3 Achieved results ([P1, P6])

Current TD-CDMA uplink power control is based on the several measurements made by UE, which involve both random and systematic errors. Outer loop power control is used to compensate the systematic error. Since the amount of systematic error is unknown at the beginning of a call and after each handover, the outer loop power control should adapt to the current conditions as fast as possible. The steady state performance of the TD-CDMA uplink power control was a starting point, where it was assumed that the outer loop had already tracked systematic error, and the effect of random errors to the system capacity was studied.

Simulations show clear capacity gain from UTRA TDD uplink power control. As high capacity gain as 500 % was simulated in ideal conditions. With the current specifications path loss measurements are based on absolute power measurements. Such measurements may involve large errors. In fact, in [P1] it was shown that the existing accuracy requirement for path loss measurements is not sufficient but should be tightened by at least 3 dB. In addition to the path loss measurements, accuracy of interference measurements and the setting of PCCPCH power in base stations should be made more stringent. Based on these studies the use of relative measurements was proposed, since they can be implemented with relatively high accuracy.

In [P6] UTRA TDD system performance was analysed with different frame configurations. Based on these simulation results it can be recommend that two beacon channels per frame should be used from system capacity point of view. By using two beacon channels per frame uplink power control can be enhanced by minimizing the delay of a pathloss measurement. Thus the uplink capacity can be increased which more than just compensates the loss of one time slot for DPCH. In addition to that there is also an additional capacity in SCCPCH slot and necessary monitoring can be performed for proper inter-system handover from GSM or UTRA FDD to UTRA TDD.

To cover the whole uplink power control the systematic errors also have to be considered. Since outer loop power control can be used to compensate the systematic error, the effect of its convergence speed on system performance was analysed. This brings the question of how fast the outer loop power control should be not to jeopardize the system capacity too much. The effect of the convergence speed of the outer loop power control to the TD-CDMA system performance was analysed.

Based on the study it can be concluded that the speed of convergence has a clear impact on the rate of satisfied calls in the network. Due to the worst case model, it can be concluded that 200-500 ms is clearly enough to reach the 95 % rate of satisfied calls. It was also noticed that the blocking of calls explain much of the performance degradation. It can be also concluded that the system performance is rather robust against errors in the initial state - even though the quality of the network becomes worse, it do not collapse when more errors are added. Simulations show trade-off between accuracy requirement and required convergence time. Convergence requirements can be relaxed by making measurements more stringent. Convergence times could also be relaxed if measurement tolerance in steady state was tightened. This can be made by e.g. differential measurements.

3.3 Downlink power control

The TD-CDMA downlink inner loop power control was studied using dynamic system simulations. The aim of this study is to evaluate the performance of TDD downlink power control and to gain an understanding of the properties that are important in downlink power control in a stand alone TDD system. To achieve this only limited scenarios were used in the study. This should be mentioned to highlight the fact that limited cases are studied to reflect the potential TDD use cases. The main purpose of the TDD downlink power control is to optimize the used energy in the downlink to maintain the desired *Quality of Service (QoS)*. The downlink power control consists of an inner and outer loop. The focus is on the inner loop techniques and as the behaviour of the outer loop is not considered to be that sensitive as in the uplink direction. The link reciprocity suggests that if the uplink outer loop convergence is analysed in [P1] the downlink direction can achieve similar or better performance due to the fact that the whole downlink

outer loop is located in the UE and the time delay associated with the outer loop is significantly smaller.

In this study three different downlink inner loop power control schemes were studied:

- *3GPP Release 4 solution* - How to choose the optimum step size for the current scheme in the presence of errors and how to interpret TPC command in studied scenarios.
- *UE measured SIR difference* - UE signals the observed DL SIR difference to UTRAN. This is considered to be reference for inner loop despite 1 frame delay in applying the change.
- *Channel prediction* - Utilization of channel reciprocity for adaptive step size selection to counteract the slow 100Hz power control.

The path loss aided closed loop power control for downlink of TD-CDMA is presented in [123], where performance gains are demonstrated by the link level simulations. The largest gains are achieved for slow and moderate fading channels. In [65] an improved outer loop power control algorithm is presented, which is used for the downlink of TD-CDMA. However, the algorithm should also be usable for the uplink of TD-CDMA and also for the uplink and downlink of WCDMA.

3.3.1 Algorithm description

Downlink power control in dedicated channels is based on a closed loop after the initial phase, when the DL power is set by the network. The method is the same as in FDD. Thus a mobile station generates *Transmit Power Control (TPC)* bit based on SIR measurement and sends that bit to BS. The measurement of the received SIR shall be carried out periodically at the mobile station. When the measured value is higher than the target SIR value, TPC bit = "0" and when it is lower than the target SIR value, TPC bit = "1". Transmit power is then adjusted according to the commands. If the TPC bit cannot be received, the transmission power value shall be kept unchanged. Three different power steps can be used: 1, 2, and 3 dB.

The error in the power adjustment is modelled as log-normally distributed random variable, whose deviation is a user-defined parameter, and fulfils the maximum tolerance given by the standard (Table 3).

3.3.2 Achieved results ([P2, P3])

In this thesis TD-CDMA inner loop power control was thoroughly studied in the presence of errors. Simulations showed that the downlink power control gave significant gain over fixed downlink transmission power and when a certain minimum power level is reached, capacity cannot be further increased by allocating more power.

TABLE 3 Downlink transmission power step tolerance and deviation as a function of a power control step.

Step size [dB]	Transmitter power step tolerance [dB]	Maximum deviation [dB]
1	± 0.5	0.15195
2	± 0.75	0.22793
3	± 1	0.30391

Since natural features of TD-CDMA are good support for asymmetrical traffic and flexible channel allocations only *Common Control Transport Channel (CCTrCH)* level power control per frame (100 Hz) is used as compared to FDD fast power control (1500 Hz). The lack of power control speed as compared to FDD mode can be compensated by appropriate step selection as showed in simulations. It should also be noted that the TD-CDMA is mainly intended for the indoor environment, where the UE speeds are low.

Current 3GPP release 4 downlink power control scheme can be improved by controlling the up and down step sizes independently. By setting the step size for the up command higher than the one for down command similar technique that is used in the outer loop power control ([121] can be used to take advantage of bigger step sizes and to decrease performance loss in the presence of errors. The step size selection is a channel dependent process and in the studied scenario the optimized parameters were discovered to be 3 dB for the up command and 2 dB for the down command. Capacity gain of 22 to 42 percent was achieved as compared to 1 dB symmetrical step size when the uplink BER for TPC command is from 0 to 10 percent. Without loosing the generality the independent up and down step size scheme should be adopted.

The system performance with downlink power control can be further improved by signalling the difference between the received downlink SIR and the target SIR from UE to base station and letting the base station apply the difference value at the next frame. The needed number of bits for this signalling were studied. Based on the results it is recommended that 2 bits should be used for this due to back ward compatibility and not being vulnerable to TPC command BER variations. With a two bits signalling a performance gain of 24 to 52 percent can be achieved as compared to symmetrical 1 dB step size when the uplink BER for TPC command is from 0 to 10 percent. It should be noted that power control is most important for real-time services e.g. speech where the operation point for BER remains low and that way introduces the possibility to redefine the usage of two TPC bits. On the other hand non-real-time services e.g. packet traffic usually operates with higher BER levels and without power control.

The UE transmitted TPC command is interpreted in the BS and the change is applied to the downlink transmit power level when within the set limits. The errors in the TPC transmission were studied and it was found that by interpreting the command to be UP had a favourable impact on the system. Under some

conditions the erroneous TPC command could be ignored to reduce the over all interference, but the difference over all in system performance compared to the UP interpretation was fairly small, thus UP interpretation would always be recommended for simplicity.

Also channel reciprocity was utilized in the channel prediction method which uses channel fading information for step size selection. Under ideal conditions it gives a gain in a single cell case, but when several cells form the TDD system the inter-cell interference becomes dominant and thus the channel prediction technique fails. When adding the difficulty of building such an ideal system it seems that the channel prediction / link reciprocity technology would not be beneficial route for TDD downlink improvements.

Power control errors increase the required E_b/N_0 for maintaining the desired BLER. In the studied scenario larger steps are favourable as they counter the channel fading and asymmetrical step sizes are more tolerable to TPC command errors. Asymmetrical step sizes 3 dB up and 2 dB down provides the best performance in the presence of errors in the studied case, but the independent UP and DOWN step size selection as a general rule is a favourable development and the optimum step selection can be done for each individual propagation conditions separately. The performance gain with 2 dB, 3 dB and asymmetrical steps is reduced as compared to a 1 dB step, when the TPC errors are included. Furthermore, symmetrical 1 dB step size should be used when TPC commend BER goes above 20 %. This suggests that asymmetry and step size should be decreased as a function of TPC error [68].

3.4 Handover

Another basic radio resource management algorithm in addition to power control is handover. TD-CDMA supports intra-system handovers and inter-system handovers to UTRA FDD or to GSM. In this study a WCDMA handover (see [49, 96]) tailored to a TDD operation is considered, which is based on UE measurements only. The selected handover algorithm is similar to that used with IS-95 in which pilot signals (for example pilot E_c/I_0 of the received signal code power) of candidate base stations are compared. The base station with the best quality pilot is then selected as active branch. Similar handover procedure of UTRA TDD which is based on downlink SIR is evaluated in [93].

In TD-CDMA the active set size in the handover procedure is always equal to one i.e. only hard handover is supported, while in UTRA FDD soft handover and macro diversity may be utilized. Hence, it is worth careful study in how different handover parameters effect the system performance and whether the selected handover algorithm is suitable at all in the TD-CDMA operation. Extensive dynamic system level simulations are used to analyse the handover algorithm.

3.4.1 Algorithm description

Layer 1 (L1) of TD-CDMA provides the measurement specifications a toolbox of measurement abilities for the mobile station and UTRAN. In the L1 specifications the measurements can be distinguished between the measurements in the mobile station and in the UTRAN. However, it is anticipated that handover algorithms will be based on mobile station measurements only. According to these measurements Radio Network Controller (RNC) makes handover decision. The mobile station measures signals from the base stations, from which it can find out the identification number of the base station and the energy per chip to interference ratio (E_c/I_0) value of the PCCPCH signal of the corresponding base station. In the simulator the E_c/I_0 value is evaluated in following way:

$$\frac{E_c}{I_0} = \frac{PCCPCH\_RSCP}{I_0 + N_0}. \tag{3.4}$$

Measurement accuracy (see [107, 104]) is important for handover performance and filtering is a simple way the improve accuracy. Before the E_c/I_0 is used by the handover algorithm in mobile station or RNC, an arithmetic mean over certain number of latest measured values is taken. This way fast fading can be averaged out. When a longer filtering window is applied, fast fading can be completely removed, but if the filtering window is too long, it leads to long delays in handovers. The optimal filtering window is a trade-off between measurement accuracy and handover delay [49].

3.4.2 Achieved results ([P1])

Considering handover, there is a certain optimum (maximum) value for the hysteresis, after which system performance rapidly deteriorates. High enough hysteresis is needed to avoid unnecessary handovers due to the fading channel. Too high hysteresis, however, makes handover unable to react to the changes in the *Received Signal Code Power (RSCP)* level. On the other hand, high hysteresis is needed to avoid excessive signalling load in the network. In addition, the system performance was noticed to be quite unaffected by the filtering length until it exceeds a certain level. Long filtering is needed to avoid excessive signalling in the network. However, too long filtering leads to late handovers when the system performance degrades.

3.5 Dynamic Channel Allocation

Dynamic Channel Allocation (DCA) has been seen as a promising method for improving the quality and capacity in cellular networks and for TDD systems it has been under intense research activity for a rather long time. In [61] a very comprehensive survey of different DCA approaches are given based on a large number of published papers in the area of fixed, dynamic and hybrid allocation

schemes and a comparison of their trade-offs in terms of complexity and performance. As pointed out also in [124] the best DCA solution depends on the service area characteristics e.g. cordless phones require a fully decentralized algorithm whereas for cellular mobile networks should allow for some coordination between adjacent cells. Locally centralized architecture for resource allocation for UMTS TDD mode is presented in [80, 83, 81, 82] In [30, 29, 35] both decentralised and centralized interference based DCA algorithms are developed which allows different asymmetry for adjacent cells without a significant capacity loss. It has been demonstrated in [28] that the additional interference mechanism of TDD and the flexibility in a TDD system can be exploited constructively in order to minimize interference. Furthermore in [26, 25, 27] new DCA algorithm is presented which exploits interference diversity through randomly opposing uplink and downlink slots in adjacent cells. Interaction between DCA and power control is studied [5, 56].

In theoretical studies very significant quality and capacity improvements have been achieved. However, in real systems DCA performance is limited by several factors so theoretical limits might not be reached. DCA algorithms are affected by unreliable measurements or all necessary information might not be available. Due to time division multiple access interference and loading conditions can change very rapidly from slot to slot. To exploit the full possibilities of the TDD system efficient DCA algorithms are needed to guarantee quality of service in rapidly changing channel conditions and in mixed traffic scenarios. Complexity of DCA in terms of scheduling of measurements and algorithms needed to find optimal allocations needs to be reduced to make it possible to react quickly to the varying conditions.

DCA algorithms can be divided into two parts where *slow DCA (S-DCA)* allocates resources to cells and *fast DCA (F-DCA)* to bearer services [49]. The TDD operation has traditionally exploited the possibility of DCA functions to avoid or minimise the interference and improve system capacity. For UTRA TDD the promise of advanced receivers alleviates the intra cell interference, but this emphasises the importance of minimising the interference between different cells. There are several methods that can be used to aid the channel allocation process, but they all have inherent limitations. A model for the analysis of protocol and measurement impact of errors is proposed. These studies are based on dynamic system simulations that are carried out to find out how the different elements in the DCA process impacts on the UTRA TDD system capacity. In addition to the random allocation effect of interference and transmission power based channel allocation with and without slow DCA information is studied in the presence of signalling delays and measurement errors.

3.5.1 Algorithm description

The requirements for DCA are twofold, limitation of the interference and maximizing the system capacity by allocating intelligently resources for the operation. The TD-CDMA resource allocation can be achieved by either time slot or code

pooling as mentioned in [97] and [49]. Further in [49] the DCA requirements are briefly discussed and some principles outlined. It is proposed that the location of the DCA entities would be based on natural termination points of the DCA processes, i.e. tied to the rate of information exchange and to the bulk sources of information generation, collection and processing used in the resource allocation process. The inherent limitations of the DCA are related to the information collection and communication (protocol) that determines the usability of the DCA algorithm. In order to minimize the user equipment (UE) power consumption and complexity of the measurements the unnecessary monitoring activity should be avoided in the downlink. This requirement on the other hand leads to problems that are related to the validity of the measured information especially from the downlink. Secondly the protocol that is used for communications between the different network entities may be liable to delays and stiff procedures. The channel allocation can be based on two different strategies: avoid interference by separating the potential interfering UE (segregation) totally or use the available information to correct the situation once interference reduces the system capacity. In general the key elements of the resource allocation are information collection (monitoring and identifying the situation) and making an allocation decision based on the available information.

Both the terminal and the base station can perform periodic monitoring and reporting to support DCA functionality. For study purposes the fast DCA will be terminated at the base station, but slow DCA can be terminated at any network entity above the base stations that form the seamless coverage area. In practice an entity split is proposed in [49] and depicted in Figure 13. Also it is assumed in simulations that the coverage area has the same uplink/downlink partitioning in contrast to [97].

The function of S-DCA makes it possible to dynamically allocate resource units based on negotiation and measurements between adjacent cells to fulfil the planned system operation. Also using dynamic allocation interference levels can be minimized and capacity relocation between cells can be achieved. The S-DCA algorithm in this study uses segregation principles when allocating resource units to a cell-related priority and preference lists. These lists are used as input to F-DCA to allocate resources for different bearers.

In addition to time slot priority time slots can be categorised to different preference groups in a cell-related preference list (see Table 4). In the current model three preference groups can be used, which are named as *Own, Shared and Borrowed*. For the *Real-Time (RT)* simulations only Own priority group is used for simplicity. Definition of the different preference groups is explained below in the order of importance. The idea is to classify the slots so that the interference between neighbouring cell time slots is taken into account.

- *Own* These slots are used for terminals who are near cell border and need high transmission powers. Neighbouring base stations can set same slot as "Borrowed". In mixed traffic conditions these slots should be mainly used for RT traffic.

- *Shared* Downlink transmission power in these slots is limited and neighbouring base station can use same slots. In mixed traffic conditions these slots should be mainly used for non-real-time (NRT) traffic. In this study this priority group is omitted.
- *Borrowed* These slots are used for terminals who are near a serving base station and need only low powers. This slot is used as "Own" for at least one of the neighbouring base stations. In mixed traffic conditions these slots should be mainly used for NRT traffic. In this study this priority group is also omitted.

TABLE 4 S-DCA cell priority and preference table for four base station simulation environment.

	Priority	Preference BS 1	Preference BS 2	Preference BS 3	Preference BS 4
0	DL	Own / PCCPCH			
1	UL	Own	Borrowed	Own	Borrowed
2	UL	Own	Borrowed	Own	Borrowed
3	UL	Own	Borrowed	Own	Borrowed
4	DL	Own	Borrowed	Own	Borrowed
5	DL	Own	Borrowed	Own	Borrowed
6	DL	Own	Borrowed	Own	Borrowed
7	DL	Own / SCCPCH			
8	UL	Borrowed	Own	Borrowed	Own
9	UL	Borrowed	Own	Borrowed	Own
10	UL	Borrowed	Own	Borrowed	Own
11	DL	Borrowed	Own	Borrowed	Own
12	DL	Borrowed	Own	Borrowed	Own
13	DL	Borrowed	Own	Borrowed	Own
14	UL	Own / PRACH			

For each preference group particular attributes (e.g. based on PCCPCH RSCP measurement thresholds and maximum downlink transmission power as defined in [104], [107] and [110]) can be set. In this study these preference groups are given in fixed S-DCA table (see Table 4) that is not changed during simulation. With a fully implemented S-DCA algorithm it is possible to control these preference groups according to the current loading conditions and planned service mix to better meet the operation goals.

3.5.2 Uplink DCA algorithm

The F-DCA acquires and releases resource units according to the slow DCA priority and preference list. In this study two separate F-DCA algorithms with slow reallocation are studied in the dynamic system simulator. It is assumed

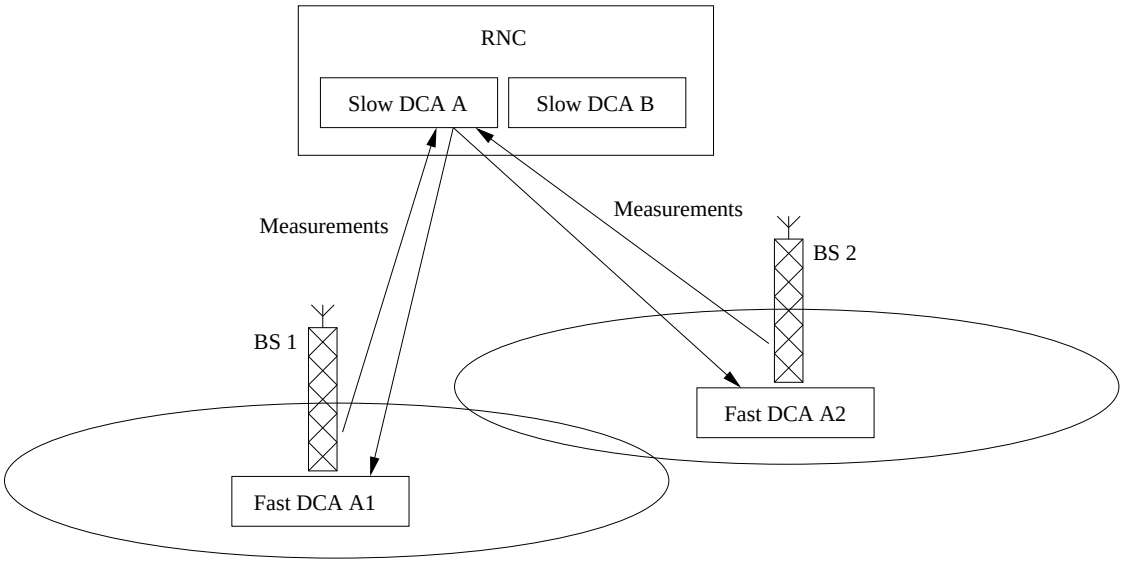

FIGURE 13 Example of DCA partitioning between different network elements.

that the DCA algorithm does not allocate any dedicated channel (DPCH) users to the common channel time slots (e.g. PCCPCH, SCCPCH and PRACH) in Table 4. The reallocation can be done for one user or for all users. The initiation for reallocation can be based on consecutive frame errors or UE moved in cell so that it needs to be allocated to a different preference group. This is called fast reallocation. Slow reallocation on the other hand is done when a user is moving from one cell to another.

Simple F-DCA algorithm is a good reference point for new F-DCA algorithms. It uses the priority list from S-DCA to set the partion between UL and DL slots in the frame. It can operate in the following three strategies:

- Allocate time slots randomly.
- Allocate user to a time slot which has the lowest interference level (e.g. based on *Interference Signal Code Power (ISCP)*[104]).
- Reallocate time slots for one user after consecutive frame errors. Threshold for reallocation can be given as a parameter separately for uplink and downlink. This method is not used in this study.

The intermediate F-DCA algorithm extends the simple F-DCA principle by applying slot preference in the allocation decision making. It uses the priority table from S-DCA to set frame partitioning between the uplink and downlink slots. UE preference allocation algorithm is based on RSCP measurements that UE performs on PCCPCH slot. This is based on the principle to divide users into different preference slots based on RSCP measurements so that the inter-cell interference is minimised. Segregation by maximising the separation between the active users is one way to try to reach good system capacity so that neighbouring base stations can use the same time slots at the same time. The selection with

in the preference slots can again be based on the same three strategies as with simple F-DCA and using the UE and UTRAN measurement information in the decision making.

The intermediate F-DCA will first search for available resources for the uplink. If the RSCP measurement is not available then the highest preference group will be used which in this model is Own slots. It is also possible naturally to delay the beginning of the call, while reliable RSCP measurement is obtained. The delay can be given as a parameter to the simulator. After this delay slot selection is based on a RSCP measurement value. A search will begin from the lowest preference group and it will be used if the RSCP threshold is met. If Borrowed slots (or Shared slots) cannot be used, then allocation is attempted to Own slots. If all resources in Own slots are reserved, then allocation is blocked. After the uplink the same kind of procedure is done for the downlink and if the resources can be found for both uplink and downlink, then time slots will be reserved from the base station and a message is sent from UTRAN to UE to start to use the new time slots at the beginning of next interleaving period. The intermediate F-DCA can easily be adapted to DL by using UE measurements.

Achieved results ([P5])

The UL capacity at 98 % satisfied rate with different F-DCA algorithms in the presence of UTRAN processing delay and ISCP measurement error is collected in Figure 14. The delays in the UTRA TDD system reduce the UL capacity. Introducing interference based allocation to simple F-DCA with slow reallocation increases the UL system capacity from 32 % to 92 % depending on the delay. It is obvious that the information about the interference gives a better situation in this case. Also it makes the UL more tolerant to system delays and the capacity with 200 ms delay is almost identical to 0 ms system delay. The *Interference Signal Code Power (ISCP)* measurement error does not have any impact on the UL capacity.

The S-DCA preference information gives additional tolerance to delay variations and secures the quality of service in UL as the intermediate F-DCA algorithm simulations show. Intermediate F-DCA algorithm gains ranges from 24 % to 147 % depending on the delay. The additional UL capacity provided by other preference classes (e.g. Borrowed and Shared) was not used for simplicity so it is difficult to conclude the UL capacity differences between interference based simple and intermediate F-DCA algorithms in conjunction with slow reallocation. Again the ISCP measurement error did not have any impact to the UL capacity. Most significantly the intermediate F-DCA algorithm gained nothing (< 2%) from the use of ISCP information, so S-DCA can minimise the need for measurements with slow reallocation. The S-DCA reduces the inter-cell interference and thus creating a more stable system as the more gradual capacity reduction shows.

3.5.3 Downlink DCA algorithm

Simple F-DCA algorithm is a good reference point for new F-DCA algorithms. It uses the priority list from S-DCA to set the partition between the uplink and downlink slots in the frame. It can allocate a time slot either randomly or allocate a user to a time slot which has the lowest downlink transmit power.

The intermediate F-DCA algorithm extends the simple F-DCA principle by applying slot priority in allocation decision making. It uses the priority table from S-DCA to set the frame partition between the uplink and downlink slots. UE priority allocation algorithm is based on RSCP measurements that UE performs on PCCPCH slot. This is based on the principle to divide users into different preference slots based on RSCP measurements so that the inter-cell interference is minimised. Segregation by maximising the separation between the active users is one way to try to reach good system capacity so that neighbouring base stations can not use the same time slots at the same time. The selection within the preference slots can be again based on the same strategies as with simple F-DCA and using the UE and UTRAN measurement information in decision making.

Achieved results ([P4])

The downlink capacity at 98 % satisfied rate with different F-DCA algorithms in the presence of UTRAN processing delay is collected in Figure 15. The delays in the UTRA TDD system reduce the downlink capacity. Introducing transmission power based allocation to simple F-DCA with slow reallocation increases downlink system capacity from 7 % to 18 % depending on the delay. The power setting is rather accurate in terms of referential accuracy, thus its error is expected to have only a minor effect on system capacity.

The S-DCA preference information gives additional tolerance to delay variations and secures quality of service in the downlink as the intermediate F-DCA algorithm simulations show. Intermediate F-DCA algorithm gives clear gain from 43 % to 162 % depending on the delay. The additional downlink capacity provided by other preference classes (e.g. Borrowed and Shared) was not used for simplicity so it is difficult to conclude the downlink capacity differences between transmission power based simple and intermediate F-DCA algorithms in conjunction with slow reallocation. The intermediate DCA performance can not be further increased with additional measurements. On the other hand it can be said that measurement requirements can be minimized with intermediate DCA. The S-DCA reduces the inter-cell interference and thus creating a more stable system as the more gradual capacity reduction shows.

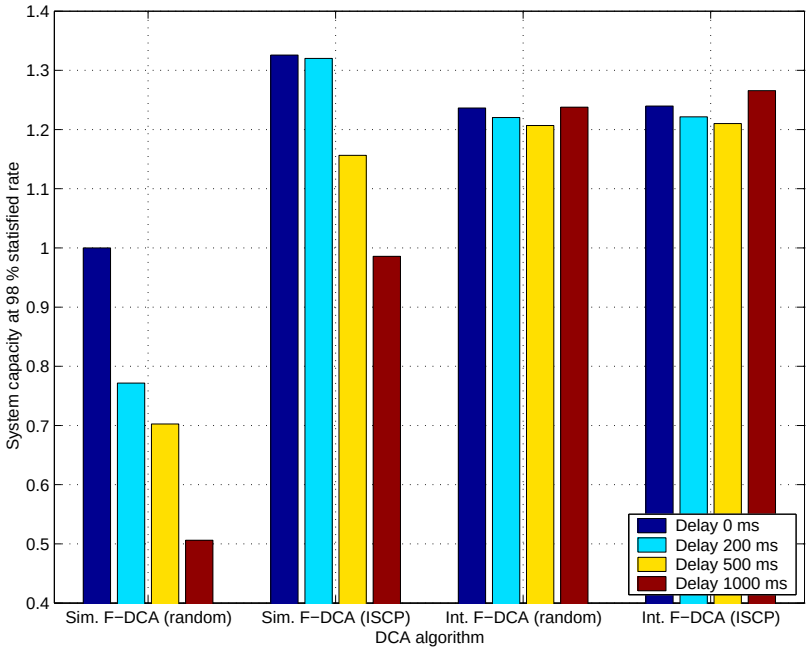

FIGURE 14 Uplink capacity at 98 % satisfied rate with different DCA algorithms.

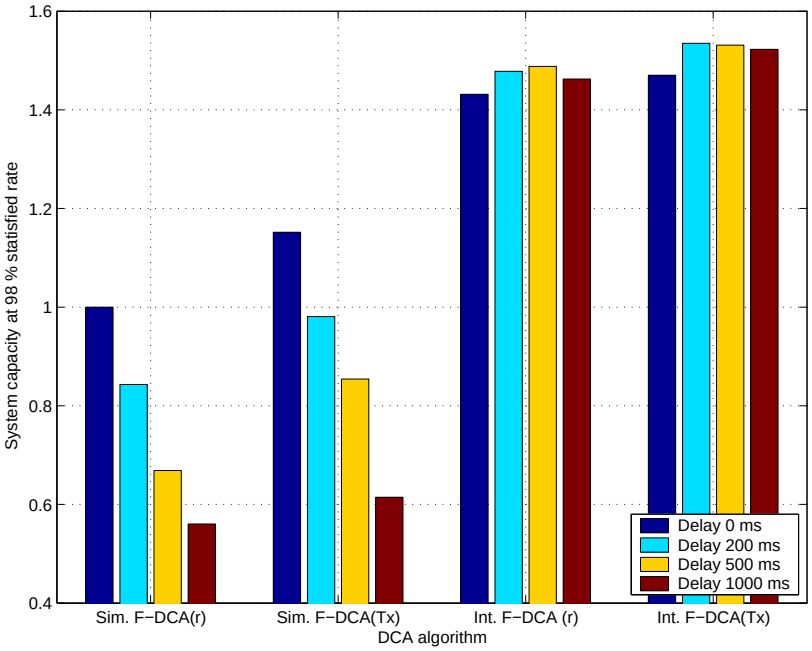

FIGURE 15 Downlink capacity at 98 % satisfied rate with different DCA algorithms.

4 PERFORMANCE OF WCDMA NETWORK WITH TRANSMIT DIVERSITY

WCDMA has emerged as the main air interface solution for 3G networks allowing mobile users to access Internet services. The first release of WCDMA, release 99, supports IMT-2000 specifications allowing data rates up to 2 Mbps and support both packet and circuit-switched traffic. In the evolution of WCDMA standard *High Speed Downlink Packet Access (HSDPA)* was introduced in Release 5 to support higher peak data rates with lower delays and increased spectral efficiency. General descriptions of HSDPA concept are given e.g. in [49, 63, 89] and in 3GPP technical specifications [109]. HSDPA has been an important topic in 3GPP standardization and the most important aspects of HSDPA are covered in the next section.

Already 3GPP release 99 includes specifications to downlink transmit diversity. It has been seen as a cost effective way to improve downlink performance for the new mobile services like web browsing which tends to burden the downlink more heavily than the uplink. The performance of *Closed Loop Mode 1 (CL Mode 1)* and *Space Time Transmit Diversity (STTD)* techniques are first evaluated with speech traffic and then studies are extended to HSDPA.

4.1 High Speed Downlink Packet Access

4.1.1 Introduction

In 3GPP release 99 and release 4 packet data traffic is supported by *Dedicated Channel (DCH)*, *Downlink Shared Channel (DSCH)* and *Forward Access Channel (FACH)*. FACH can carry signalling data on the downlink, but it can also be used for user data. The advantage of common channels is their low set up time, but on the other hand the link performance of a common channel is not as good as a dedicated channel due to the lack of fast power control. DCH is power controlled and also supports soft handover, but it requires a longer set up time than what

it takes to access common channels. DCH can support bit rates up to 2 Mbps, but the downlink orthogonal code must be allocated according to the highest bit rate and therefore a variable bit rate in dedicated channels consume a relative high number of downlink orthogonal codes. To overcome the channelisation code shortage DSCH has been specified for WCDMA systems. It is designed to operate together with DCH and it supports a dynamically varying spreading factor for 10 ms frames, single or multi code transmission and it may be fast power controlled. It is especially targeted to transfer bursty packet data. DCH, DSCH and combined scheme, where DSCH is used for the users close to base station and DCH at the cell borders to take advantage of macro diversity, are compared in [42]. It is found that DSCH is able to provide higher packet data rates than DCH and in addition a combined scheme of DSCH and DCH is able to provide similar bit rates as DSCH but with lower base station transmit powers due to utilised macro diversity.

In the top of the existing DSCH concept advanced schemes known from GSM such as link adaptation and fast physical layer retransmissions and combining are applied [49, 63]. The term *High Speed Downlink Shared Channel (HS-DSCH)* is used to distinguish it from the previous DSCH. The HSDPA concept is a natural extension of the DSCH and it is mainly intended for non-real time traffic, but can also be used for traffic with tighter delay requirements. To support higher peak data rates HSDPA concept has been established for Release 5, which includes *Adaptive Modulation and Coding (AMC)*, fast scheduling at Node B, *Hybrid Automatic Repeat and Request (HARQ)* and short TTI length. *Fast Cell Site Selection (FCS)* and *Multiple Input Multiple Output (MIMO)* are considered for the further releases.

Goals for the HSDPA can be shortly summarized as

- Peak data rates higher than 2Mbps (up to 14 Mbps)
- Reduced (re)transmission delays
- Improved QoS control (Node-B based fast packet scheduling)
- Spectral and code efficient solution for fully loaded sites

Concepts similar to HSDPA are also being introduced into other wireless standards. 3GPP2 has defined 1xEV-DO (1x Evolution Data Only) concept for data only traffic and it includes adaptive modulation and coding and HARQ [2]. Also 1xEV-DV (1x Evolution Data and Voice) has been specified to support simultaneous high speed data and voice services [2]. Adaptive modulation and coding and HARQ are included and the concept is similar to WCDMA/HSDPA but uses a narrower bandwidth.

4.1.2 HSDPA concept

HSDPA concept also requires some changes in the general network architecture, since all the release 99 channels end at RNC. HSDPA *Medium Access Control*

(MAC) is installed to Node B to support fast physical layer retransmissions. RNC still takes care of *Radio Link Control (RLC)*, e.g. RLC retransmissions if HS-DSCH transmission fail after a maximum number of physical layer retransmissions and also RNC still retains all release 99 / 4 functionalities. The key function of a new Node B MAC is to handle HARQ functionality, modulation/coding selection and packet data scheduling.

To allow the system to take advantage of the short term variations the scheduling is done in the Node B based on feedback information from UE and knowledge of the current traffic state. In an optimum scenario the scheduling is able to track the fast fading of the users. Scheduling of users can be conducted as a function of their radio channel conditions, thus one good option is to choose to only schedule users which are experiencing constructive fading (possible due to the shorter TTI length). This is also known as fast selection multi-user diversity transmission. A detailed analysis of Proportional fair scheduler performance in a link and system level is given in [62]. Furthermore, performance of different packet scheduling methods for streaming services are studied in [4], in which proportional fair scheduler is found to be the best choice.

Layer 1 retransmissions are subject to significantly shorter delays than RLC retransmissions, i.e., results in less delay jitter and is very attractive for data services such as TCP, etc. A physical layer packet combining basically means that the UE stores the received data packets in soft memory and if decoding fails, the new transmission is combined with the old one before channel coding. The retransmission can be either identical to the first transmission or contain different bits compared to a channel encoder output that was received during the last transmission. With this incremental redundancy strategy one can achieve a diversity gain as well as improved decoding efficiency. The use of HARQ (using either *Chase Combining (CC)* or *Incremental Redundancy (IR)*) adds increased robustness to the system and a spectral efficiency gain. Performance and modelling of chase combining and incremental redundancy are presented in [18] and it is found that incremental redundancy will provide a small throughput gain compared to chase combining using a simple link adaptation algorithm. Performance of HARQ is also addressed in [19] and in [74] specifically incremental redundancy is considered.

In the HSDPA concept fast power control and variable spreading factor are replaced with adaptive modulation and coding (AMC), extensive multi code operation and a fast and spectrally efficient physical layer retransmission strategy. AMC selects a coding and modulation combination according to varying channel conditions. A user with favourable channel conditions can be assigned a higher order modulation with higher channel coding rate whereas a lower order modulation with a lower channel coding rate when a user has unfavourable channel conditions. AMC performance is studied in [71] in an analytical manner and the results are compared to dynamic system simulations. In [16] performance evaluation of higher order modulation is presented. Studies in [71] are extended in [72] with code multiplexing so that a few code multiplexed users can share the HS-DSCH channel per TTI. To enable large dynamic range for the HSDPA link

adaptation and to maintain good spectral efficiency, a user may simultaneously utilise up to 15 codes in parallel. The use of more robust coding, fast HARQ and multi-code operation removes the need for variable spreading factor [49]. In [6] the theoretical performance of cellular systems with different types of link adaptation is analysed. Among the examined schemes, AMC was found to be the most promising in terms of overall performance. It provided a high system capacity, even when the practical considerations such as limited dynamic range and resolution are imposed. In an [84] outer loop algorithm is presented to fine tune the link adaptation to the desired packet error rate target.

General HSDPA operation can be listed are follows.

- Node B estimates the channel quality of each active HSDPA user based on the HSDPA specific feedback (also power control and ACK/NACK ratio can be used). The *Channel Quality Indicator (CQI)* expresses the data rate that the UE can support, i.e., the recommended modulation scheme, number of HS-PDSCH codes, and transport block size. The CQI definition is given in [111] and the different CQI methods are compared e.g. in [20, 15].
- Scheduling and link adaptation are then conducted in fast pace depending of the selected algorithms.
- Node B identifies HS-DSCH parameters for selected user.
- Node B starts transmitting HS-SCCH two slots before HS-DSCH transmission to inform the UE of necessary parameters.
- UE monitors HS-SCCHs and once part 1 is decoded from an HS-SCCH that is intended for that UE, it starts to decode the rest of that HS-SCCH.
- Based on part 2 of decoded HS-SCCH UE can determine to which ARQ process data belongs to.
- Depending of the *Cyclic Redundancy Check (CRC)* conducted on the HS-DSCH data UE sends ACK/NACK indicator to uplink HS-DPCCH.

4.1.3 HSDPA physical layer structure

Three new channels are introduced for the HSDPA: HS-DSCH for the packet data traffic, HS-SCCH to signal physical layer control information and uplink *High Speed Dedicated Physical Control Channel (HS-DPCCH)* to carry ARQ acknowledgements and channel quality feedback.

HS-DSCH

TTI length of HS-DSCH is 2 ms i.e 3 slots and in addition to QPSK a higher order modulation scheme 16QAM is introduced. A fixed spreading factor of 16 is used, but multi-code transmission and code multiplexing can be used. Depending on

the terminal capabilities the terminal may receive a maximum of 5, 10 or 15 codes. HS-DSCH capable terminal needs to obtain an estimate of the relative amplitude ratio of the HS-DSCH power level compared to the pilot power level and this requires Node B to adjust the HS-DSCH power between the slots if 16QAM is used in the frame. HS-DSCH does not support a soft handover, but transmit diversity (STTD and Closed Loop Mode 1) is supported.

Interleaving of HS-DSCH subframe spans over a single 2 ms period and there is no intra-frame or inter-frame interleaving. Turbo coding is used and the effective coding rate can vary from 1/4 to 3/4 by varying the transport block size, modulation scheme and the number of multi-codes. By varying the code rate the number of bits per code can be increased at the expense of reduced coding gain.

HARQ functionality is basically operated in two different ways: with identical retransmissions it is often referred as chase or soft combining and with different parameters the transmissions will not be identical and then the principle of incremental redundancy is used.

HS-SCCH

HS-SCCH carries information necessary for HS-DSCH demodulation and number of HS-SCCHs equals the number of multiplexed users. The length of the HS-SCCH block is 3 slots and it is divided into two functional parts. First slot i.e. first part carries time critical information that is needed to start the demodulation process (codes to despread and modulation (QPSK or 16QAM)) whereas the next two slots i.e. second part contains less time critical parameters such as a redundancy version, ARQ process number and indication of the first transmission or retransmission. Both parts employ terminal specific masking to find out which terminal HS-SCCH is intended. HS-SCCH uses a fixed spreading factor of 128 and a half rate convolutional coding is used with both parts encoded separately from each other because the time critical information is required immediately after the first slots. Soft handover is not supported for HS-SCCH, but transmit diversity can be used.

The HS-SCCH transmit power is under the control of Node B, so the power level may be constant or time-variant according to a selected power control strategy. Assignment of a constant HS-SCCH transmit power is considered to be an inefficient solution, which will result in a larger power overhead, i.e. loss of capacity. However, the 3GPP specifications do not explicitly specify any closed loop PC modes for the HS-SCCH, where the UE provides feedback information on the recommended transmit power for the HS-SCCH. Node-B must therefore rely on feedback information from the UE related to the reception quality of other channel types, such as: power control commands for the associated DPCH or CQI reports for HS-DSCH. It is typically assumed that the HS-SCCH transmit power should be adjusted so that the residual BLER equals approximately 1 %. In [21] HS-SCCH performance is studied and it is concluded that the control channel design is very robust and meets all the error probabilities under different

scenarios. HS-SCCH performance is also studied in [14] especially with different transmit diversity schemes.

Uplink HS-DPCCH

Uplink HS-DPCCH is used to carry ACK/NACK information and channel quality information (CQI) that presents what terminal can receive in the given channel conditions. Primary modulation is BPSK with a spreading factor of 256. The HS-DPCCH transmit power equals the DPCH transmit power plus an offset. The HS-DPCCH may be received at two sectors on the same Node-B in order to improve the detection probability, but in general soft handover is not supported for this channel. The HS-DPCCH is a power controlled relative to the uplink DPCCH every slot period.

4.1.4 HSDPA performance and UE capabilities

With the introduction of the HSDPA concept into the Release 5 specifications, a new generation of UE capability classes will be introduced. Five main parameters are used to define the physical layer UE capability level ([99]):

- Maximum number of HS-DSCH multi-codes that the UE can simultaneously receive. At least five multi-codes must be supported in order to facilitate efficient multi-code operation.
- Minimum inter-TTI interval, which defines the distance from the beginning of a TTI to the beginning of the next TTI that can be assigned to the same UE. E.g. if the allowed interval is 2 ms, this means that the UE can receive HS-DSCH packets every 2 ms.
- Maximum number of HS-DSCH transport channel bits that can be received within a single TTI.
- The maximum number of soft channel bits over all the HARQ processes.
- Support of 16QAM (e.g. code efficiency limitation).

A UE with a low number of soft channel bits will not be able to support *Incremental Redundancy (IR)* for the highest peak data rates and its performance will thus be slightly lower than for a UE supporting a larger number of soft channel bits. The UE capabilities are sent from *Serving Radio Network Controller (SRNC)* to Node-B, when the HS-DSCH MAC-d flow is established. Depending on the capability class achievable bit rates ranges from 1.2 to 14.4 Mbps.

Naturally the HSDPA performance is affected by the channel conditions, e.g. time dispersion, cell environment, terminal velocity and G value. Terminal capability is one important part of the HSDPA performance, thus improving terminal capability by introducing better detector or increasing the maximum number of supported codes HSDPA performance can be enhanced. Also the nature and accuracy of RRM algorithm affects the HSDPA performance, so that

by increasing the power and code resources allocated to HSDPA channel and improving packet scheduling algorithms performance can be further increased.

In HSDPA network processing is closer to the air interface at Node B for low link adaptation delay. According to [49] HSDPA concept provides 50 % higher cell throughput that release 99 channels in macro-cell and 100 % in micro-cells. 100 % higher peak data rates can be achieved than in release 99 and HSDPA also supports real-time UMTS QoS classes with guaranteed bit rates [49]. Performance of HSDPA concept in the system level is also addressed in [89, 75]. In [91] network performance of mixed traffic on HSDPA and dedicated channels in WCDMA is presented. It is concluded that the available transmit power can be better utilized when introducing HSDPA as no power control headroom is required for HS-DSCH transmission. Also 69 % gain is presented when 5 HS-DSCH codes and 6-7 W is allocated for HSDPA transmission while the remaining resources are used for release 99 channels. In [79] HSDPA network performance is studied with streaming applications in a mixed service scenario. The results shows that the reasonable streaming performance can be achieved without service differentiation if a somewhat fair schedule, like proportional fair scheduler is used. Streaming-aware schedulers can further protect streaming QoS in high load conditions. In [76] HSDPA performance is studied with different service proportions. It is concluded that HSDPA with advanced features like AMC, HARQ with IR, intelligent scheduling and resource allocation can achieve a three times higher sector and user throughputs than the release 99 system.

4.1.5 Further enhancements for HSDPA

HSDPA is currently an important topic in 3GPP standardization. Further enhancements for HSDPA network performance can be achieved by using a multiple receiver and transmitter antennas which is often called *Multiple Input Multiple Output (MIMO)* technique. HSDPA with MIMO has been studied e.g. in [53]. In the scope of this study application of multiple transmit antennas i.e. downlink transmit diversity and multiple downlink receiver antennas i.e. receive diversity is analysed with HSDPA. In addition to that the system level aspects of usage of advanced receivers in the terminal side is thoroughly studied. In 3GPP *Fast Cell Selection (FCS)* technique is also presented, in which the terminal determines which Node B is best for the downlink service through radio propagation measurements. It has been previously studied in [13] and it is a similar concept than the *site selection transmit diversity (SSTD)*, which is already included in release 99 for DCH.

4.2 Transmit Diversity

The application of multiple antennas in the base station transmitter is one way to improve the downlink performance and it is called transmit diversity. The idea of diversity is to supply the receiver with multiple independently faded

components of the transmitted information signal, so that the probability that all the signal components fade simultaneously is reduced.

Two kinds of transmission antenna diversity schemes for two antennas are included in the 3GPP standard release '99 and release 4, namely the open loop (OL) and the closed loop (CL) techniques [111]. In the OL transmit diversity the transmitter does not require any knowledge of the channel state. The signal matrix in single antenna modulation and coding schemes is defined in time, whereas the transmitted signal is defined both in space and in time dimensions in these multiple antenna concepts. The first OL concepts that were proposed to 3GPP were based on Code Division Transmit Diversity (Orthogonal Transmit Diversity) and Time Switched Transmit Diversity [52]. Later more efficient *Space-Time Transmit Diversity (STTD) [3, 11]* was adopted for the WCDMA release '99.

In contrast to the OL diversity, the CL transmit diversity applies channel state information that is provided to the transmitter via closed loop feedback signalling. The channel state information is used to weight the signal phase transmitted from two base station antennas so that these signals arrive in-phase at the terminal receiver. The WCDMA standard release '99 and release 4 include two closed loop transmit diversity solutions, namely Mode 1 and Mode 2. These have been previously studied for dedicated channels in link level simulations (e.g. [43, 44, 9, 87, 114]).

It has not been seen as feasible to use two antennas and receiver chains for small and cheap mobiles, thus therefore WCDMA supports downlink transmit diversity. If Node B is already using receive diversity, a downlink transmission can be duplex to receive antennas, so there is no need for extra antennas. Transmit diversity can provide coherent combining gain and diversity gain against fast fading. Coherent combining gain can be achieved when a signal is combined coherently while interference is combined non-coherently. The gain from ideal coherent combining is 3 dB with two antennas [49]. Coherent combining is not optimal with a closed loop transmit diversity, since feedback signalling involves a certain delay that could change channel conditions. In addition to that there is only a limited number of possible Tx-weights, so the feedback is quantized to the best option from the available Tx-weights.

Both open and closed loop transmit diversity can provide protection against fast fading. This diversity gain depends on the antenna correlation, so that the gain is higher when fast fading is uncorrelated between the transmit antennas. Correlation depends on a distance between antennas and a mobiles direction of movement, thus in practice antenna correlation will vary as well as the achieved diversity gain.

The gain from transmit diversity with uncorrelated antennas is larger when there is less multipath diversity. Multipath diversity reduces the orthogonality of downlink codes, while transmit diversity keeps the downlink codes orthogonal in flat fading channel.

4.2.1 Space-time transmit diversity

The STTD is an open loop transmit diversity concept for two transmit antennas. STTD uses space-time block coding and after transformation, symbol streams for antennas 1 and 2 are spread with the same channelization code. The idea of transmit power control is similar to the non-STTD case. In other words, transmit power of both antennas are equal and the power control adjusts the total power once per slot. The receiver structure is similar to the conventional rake receiver, except that STTD decoding is needed [3]. STTD operation is highlighted in Figure 16.

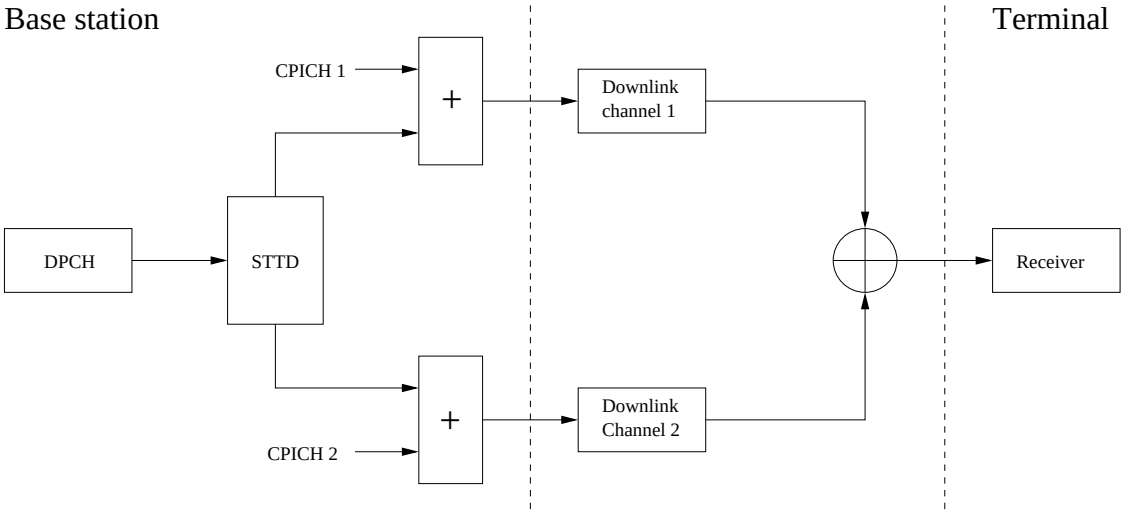

FIGURE 16 Block diagram of STTD operation.

Space-time processing techniques exploit diversity in both the spatial and temporal domains. STTD is an open loop scheme utilizing a space-time block code of length two. STTD is an orthogonal scheme, which means that the encoding for STTD makes the two transmitted signals orthogonal to each other allowing relatively simple detection at the terminal receiver. Two QPSK symbols d_1 and $-d_2^*$ are transmitted simultaneously from antenna 1 and antenna 2, respectively. In the next symbol interval, the symbol d_2 is transmitted from antenna 1 and the symbol d_1^* from antenna 2. In a channel with L paths, the signals received in two consecutive symbol intervals can be expressed as [8, 122]

$$r_1(t) = \sum_{j=1}^{L} \left[d_1 h_{1,j}(t) s(t - \tau_j) - d_2^* h_{2,j}(t) s(t - \tau_j) \right] + n_1(t), \tag{4.1}$$

$$r_2(t) = \sum_{j=1}^{L} \left[d_2 h_{1,j}(t) s(t - \tau_j) + d_1^* h_{2,j}(t) s(t - \tau_j) \right] + n_2(t), \tag{4.2}$$

where $h_{i,j}(t)$ are the complex channel coefficients, $s(t)$ is the spreading sequence

and $n_i(t)$ is noise. The outputs of the jth Rake finger are given by

$$r_{1,j} = \int_0^T r_1(t)s^*(t-\tau_j)dt = d_1 h_{1,j} - d_2^* h_{2,j} + n_{1,j}, \tag{4.3}$$

$$r_{2,j} = \int_0^T r_2(t)s^*(t-\tau_j)dt = d_2 h_{1,j} + d_1^* h_{2,j} + n_{2,j}. \tag{4.4}$$

With perfect knowledge of the channel coefficients, these outputs can be combined to form the following estimates of the transmitted data

$$\hat{d}_i = \sum_{j=1}^{L} \left[h_{1,j}^* r_{1,j} + h_{2,j} r_{2,j}^* \right] = \sum_{j=1}^{L} \left[|h_{1,j}|^2 + |h_{2,j}|^2 \right] d_i + \hat{n}_i, i = 1, 2. \tag{4.5}$$

These estimates are identical to the estimates obtained in a system with a single transmit antenna and dual receive antennas. Hence, both systems have an effective spatial diversity of order $2L$.

Downlink interference from sector i to observed terminal n is calculated as

$$I_i^n = \frac{1}{2} \cdot P_i \cdot L_i^n \cdot \sum_{j=1}^{N_i} \left(g_{i,j}^n \cdot \left(\|h_{1,i,j}^n\|^2 + \|h_{2,i,j}^n\|^2 \right) \right), \tag{4.6}$$

where P_i is the downlink transmission power in sector i and L_i is the slow faded path loss between the terminal and sector i. N_i is the number of multipath components provided by the simulated environment without diversity in sector i, $g_{i,j}$ is the average path gain of the j^{th} component and $h_{1,i,j}$ and $h_{2,i,j}$ are the complex channel coefficients for two Tx antennas for sector i and multipath component j. Orthogonal codes are taken into account in the C/I calculation, see Equation 4.9.

Downlink interference of one path from sector i to terminal n is calculated as

$$I_{i,j}^n = \frac{1}{2} \cdot P_i \cdot L_i^n \cdot g_{i,j}^n \cdot \left(\|h_{1,i,j}^n\|^2 + \|h_{2,i,j}^n\|^2 \right). \tag{4.7}$$

The total interference from all sectors to terminal n, when k is the number of sectors in simulation area, is calculated as

$$I_{tot}^n = \sum_{i=1}^{k} I_i^n. \tag{4.8}$$

The measured C/I in the UE receiver n is

$$(C/I)^n = \sum_{i=1}^{K} \sum_{j=1}^{f_i} \frac{\frac{1}{2} \cdot P_{i,n} \cdot L_i^n \cdot g_i^n \cdot (\|h_{1,i,j}^n\|^2 + \|h_{2,i,j}^n\|^2)}{I_{tot}^n - I_{i,j}^n}. \tag{4.9}$$

Correspondingly the symbol energy to noise ratio E_s/N_0 of HS-DSCH is defined as

$$E_s/N_0 = 10 \cdot log_{10}(16) \cdot (C/I). \tag{4.10}$$

4.2.2 Closed loop Mode 1 transmit diversity

In 3G WCDMA standardisation it was noticed that even crude feedback signalling can be extremely useful for improving downlink performance. The first method was *Selective Transmit Diversity (STD)*, where one feedback bit is used to select the transmit antenna. Then closed loop methods that provide beamforming gain was found to be more efficient than antenna selection techniques [52].

Provided that the transmit antennas share a common delay profile coherent combining or co-phasing in different transmit antennas can be achieved in the terminal receiver. Release 99 and release 4 include two closed loop methods with fast feedback signal of 1500 Hz used to select one of 4 or 16 possible beam weight. The basic principle of CL Mode 1 is highlighted in Figure 17.

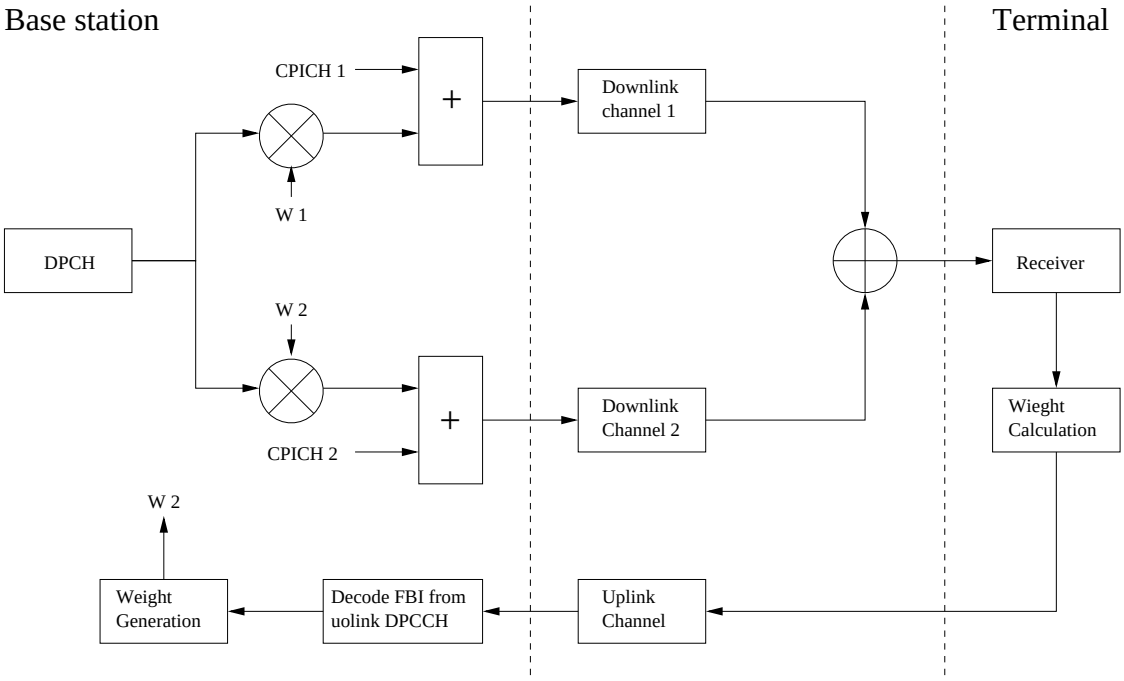

FIGURE 17 Block diagram of CL Mode 1 operation.

Closed loop methods have been widely studied especially in link level. Antenna selection was studied in [54], *Time Switched Transmit Diversity (TSTD)* and STD was studied in [115] and in [55, 45] feedback schemes for closed loop methods was studied. Generalisation to closed loop mode for M-element array was presented in [51].

The effect of channel estimation error for STTD and CL mode was studied in [10] and [85]. Performance of transmit diversity for high data rates in the indoor system was evaluated in [58] with a static simulator. Combining space-time block coding with diversity antenna selection for improved downlink performance was presented in [60]. In [120] 3G transmit diversity schemes are compared in link level. In [88] STTD and CL Mode 1 performance is studied in link level and also comparison of 1Tx and STTD is presented based on the system level simulations.

4.3 Effect of transmit diversity on the system performance in dedicated channels

In this section we consider the performance of CL Mode 1 and STTD in dedicated channels of WCDMA network. Transmit diversity techniques have been around for some time, but traditionally the performance of different methods is analysed at the link level [52]. Here we present a study of the CL Mode 1 and STTD that is based on the dynamic system level simulations. We compare the performance of transmit diversity schemas to single antenna transmission. We pay attention to the effects of terminal speed and CL Mode 1 feedback errors and delays when analysing system performance in a realistic network scenario. We look at the downlink transmit powers and how those maps to the system capacity and the number of satisfied users in the network. Also one important aspect in system level simulations is handover, since it is not usually modelled in link level simulators at all. Detailed modelling of the CL Mode 1 is presented in [P8].

4.3.1 Simulation scenario

Dynamic WCDMA system simulator [38] is used in these studies to evaluate the performance of STTD and CL Mode 1 transmit diversity as compared to single antenna transmission. Mobile terminals move around in the simulation area at the constant speed make voice calls according to the traffic model (see parameters in Table 12). In each simulation step i.e in every slot transmission powers, received interference and *Signal-to-Interference-plus-Noise-Ratio (SINR)* are calculated for each terminal. Then these SIR values are mapped to link level results through so called *Actual Value Interface (AVI)* to obtain the achieved block error ratio. AVI tables are gathered from extensive link level simulations and the same tables are used for a single antenna, STTD and CL Mode 1. Many advanced features such as inner and outer loop power control, soft and hard handover, load control and admission control are modelled in the simulator. Simulations are conducted in a macro cell scenario, which consists of 18 cells. The main simulation parameters are listed in Table 12.

4.3.2 Effect of CL Mode 1 feedback delay

CL Mode 1 tries to optimize Tx-weights so that signals transmitted by different antennas arrive co-phase at the receiver. However, different non idealities, such as feedback errors and delays, soft handover and multipath propagation, reduce the CL Mode 1 performance. In the first simulations the effect of CL Mode 1 feedback delay to the downlink transmit power is analysed. The results are presented in Figure 18 for Pedestrian A and in Figure 19 for Vehicular A channel. These results are compared to the simulation with 3 km/h UE speed and one timeslot feedback delay. For all the cases a 4 % error rate is assumed for the feedback command. As can be seen from the results, up to six slots delay can be used with low terminal speed (3 km/h) without any visible increase in downlink

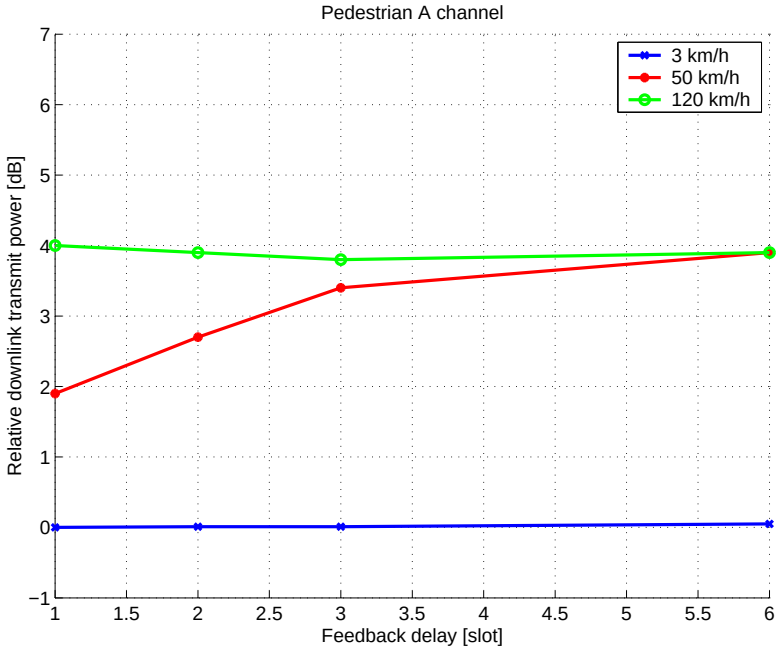

FIGURE 18 Effect of CL Mode 1 feedback delay to downlink transmit power in Pedestrian A channel.

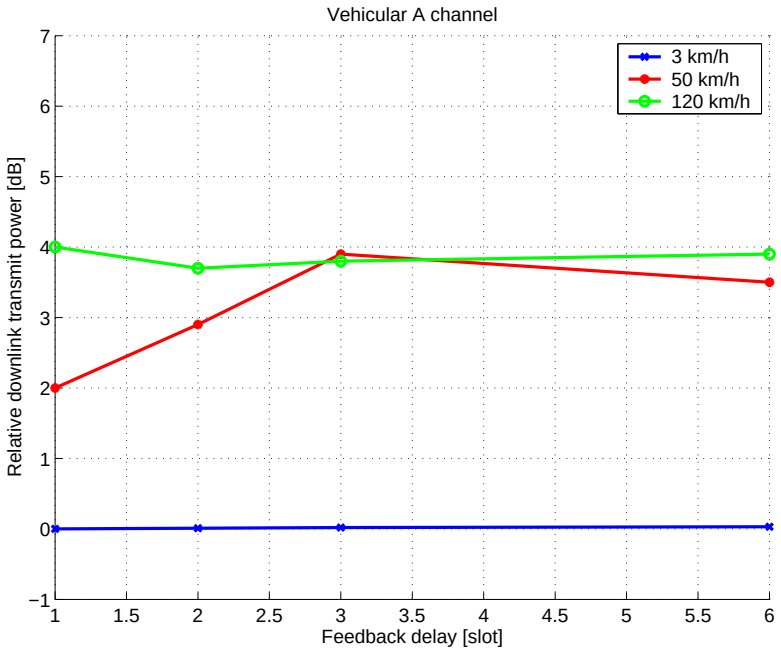

FIGURE 19 Effect of CL Mode 1 feedback delay to downlink transmit power in Vehicular A channels.

transmit power. With moderate terminal speed (50 km/h) about 1.5 dB higher downlink transmit powers can be seen when feedback delay is increased from one slot to three slots. At high terminal speeds the channel is changing too fast for closed loop signalling, thus downlink transmit power is about the same with feedback delays from one to six slots. Based on these results it can be said that 1 or 2 slots delay is tolerable for CL Mode 1.

4.3.3 Effect of downlink transmit diversity to transmit powers

In Figure 20 relative gain in downlink transmit power as compared to single antenna is presented with 3 km/h, 50 km/h and 120 km/h UE speeds in Pedestrian A channel. Corresponding results from Vehicular A channel are presented in Figure 21. With low terminal speed CL Mode 1 gains up to 3.5 dB, but on the other hand it is most sensitive to UE speed. Thus at 50 km/h the gain is about 2 dB and at 120 km/h about 0.6 dB higher transmit power is required than for single antenna. As can be seen, the differences between the 4 % and 10 % feedback errors is quite minor with ideal antenna verification.

STTD provides approximately 2 dB gain in downlink transmit power as compared to single antenna with all investigated velocities. A single antenna is not sensitive to UE speed, thus downlink transmit power is less than half a dB higher with 50 km/h and 120 km/h as with 3 km/h.

In Vehicular A channel a single antenna transmit power increases about 1 dB from 3 km/h to 120 km/h, while STTD gain increases from about 0.7 dB to 2.5 dB. As in Pedestrian A channel CL Mode 1 is most sensitive to UE speed since it uses about 2 dB higher transmit power in 120 km/h than in 3 km/h.

Based on these results it can be said that a single antenna transmission has good performance with different velocities in Vehicular A channel and it is not sensitive to UE speed. With low UE speeds fast power control works well, but when increasing UE speed fast power control is not able to follow the fast channel variations accurately any more. However, with high UE speeds interleaving over two radio frames i.e. 20 ms starts to give gain, thus the performance over the different velocities is rather constant.

Also STTD provides a rather constant performance with different velocities and gives 1-2 dB gain over single antenna transmission. STTD seems most attractive choice for high mobility cases.

Closed Loop Mode 1 is most sensitive to UE speed, but it is superior in low UE speeds. Closed loop signalling works well up to 50 km/h UE speed, but with 120 km/h its capacity drops below STTD and single antenna. Closed Loop Mode 1 seems a natural choice for low mobility scenarios.

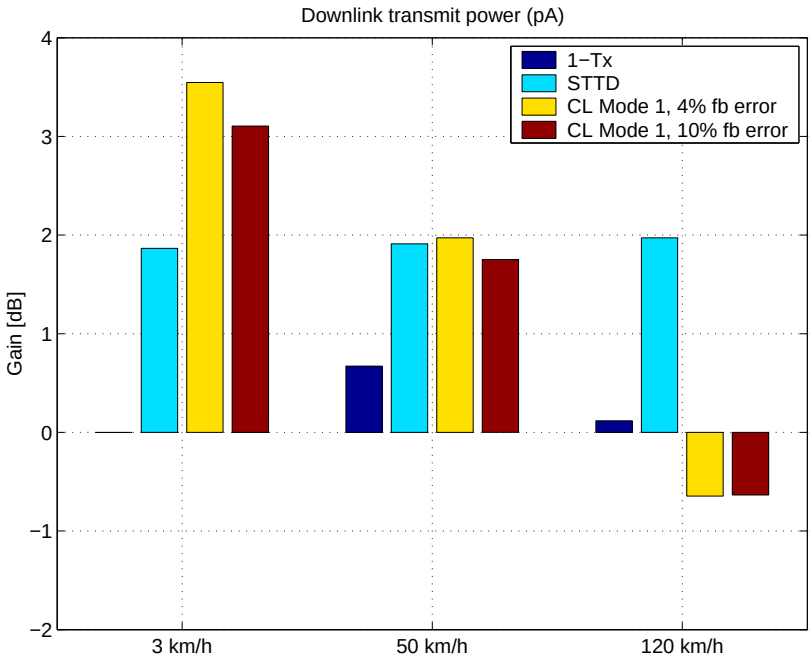

FIGURE 20 Comparison of downlink transmit powers of 1Tx, STTD and CL Mode 1 in Pedestrian A channel.

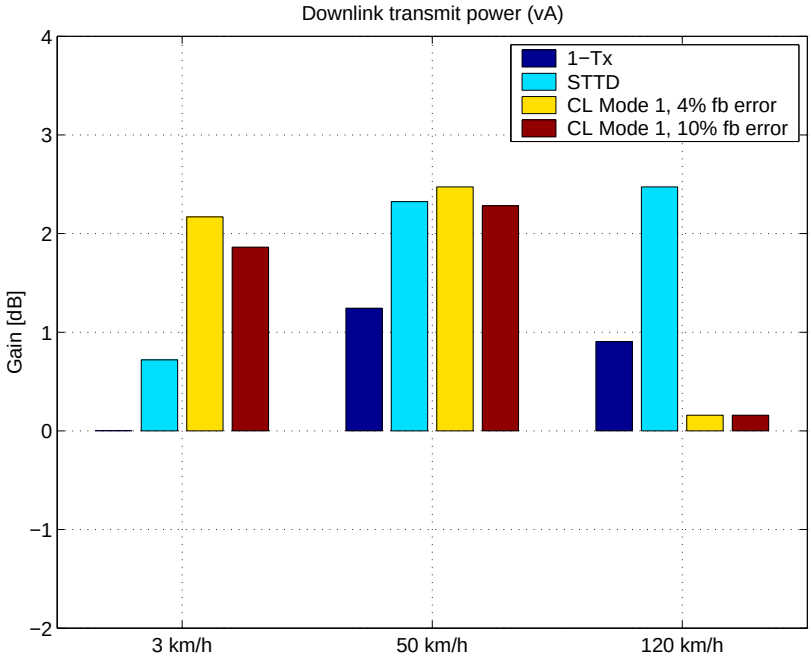

FIGURE 21 Comparison of downlink transmit powers of 1Tx, STTD and CL Mode 1 in Vehicular A channel.

4.3.4 Network performance

The performance of the network is measured by the rate of satisfied calls as defined in Section 3.2.2. Simulation results for the Pedestrian A and Vehicular A channels are presented in Figures 22 and 23, which show the system capacity at the 98 % satisfied rate. As can be seen from the results more than 100 % gain can be achieved with CL Mode 1 in 3 km/h UE speed as compared to 1Tx transmission in Pedestrian A channel. The results also highlight very clearly the sensitivity of CL Mode 1 to UE speed as the gain decreases to around 60 % with 50 km/h and in 120 km/h 1Tx outperforms CL Mode 1. 1Tx and STTD are not sensitive to UE speed and STTD provides about 25 % to 35 % gain over 1Tx with simulated UE speeds.

In Vehicular A channel gains from transmit diversity schemes decreases as multipath diversity increases. Again CL Mode 1 provides around 70 % gain in 3 km/h, but already at 50 km/h its performance is similar as with 1Tx. In 120 km/h again both 1Tx and STTD outperform CL Mode 1. In Vehicular A channel 1Tx and STTD have very similar performance.

4.3.5 Achieved results

In this section the performance of a WCDMA network was analysed when a CL Mode 1 and STTD techniques were applied in downlink dedicated channels with speech service and with ideal mobile receiver modelling. These results indicate that CL concepts have no major problems with low mobile speeds despite feedback errors and delays assuming ideal antenna verification, but with higher UE speeds the performance decreases. On the other hand STTD outperforms a single antenna in a studied scenario with all simulated terminal speeds and also CL Mode 1 in 120 km/h terminal speed.

4.4 HSDPA network performance

Transmit diversity schemes were already included to 3GPP Release 99 and Release 4 and their performance was studied in Section 4.3 on dedicated channels. However, HSDPA concept was added to 3GPP Release 5 to increase spectral efficiency and provide higher data rates. Applicability of the transmit diversity schemes, namely STTD and CL Mode 1, needed to be analysed for HSDPA. This section presents the system level comparison of 1Tx, CL Mode 1 and STTD when HSDPA is used. For the CL Mode 1 effect of feedback errors, feedback delay, UE speed and soft handover are studied with Max C/I and Round robin schedulers. In [117] different transmit diversity schemes and also receive diversity with HSDPA are studied with quasi-static simulator. As discussed in Chapter 2.1 quasi-static simulator lacks some of the detailed modelling in the fully dynamic simulator.

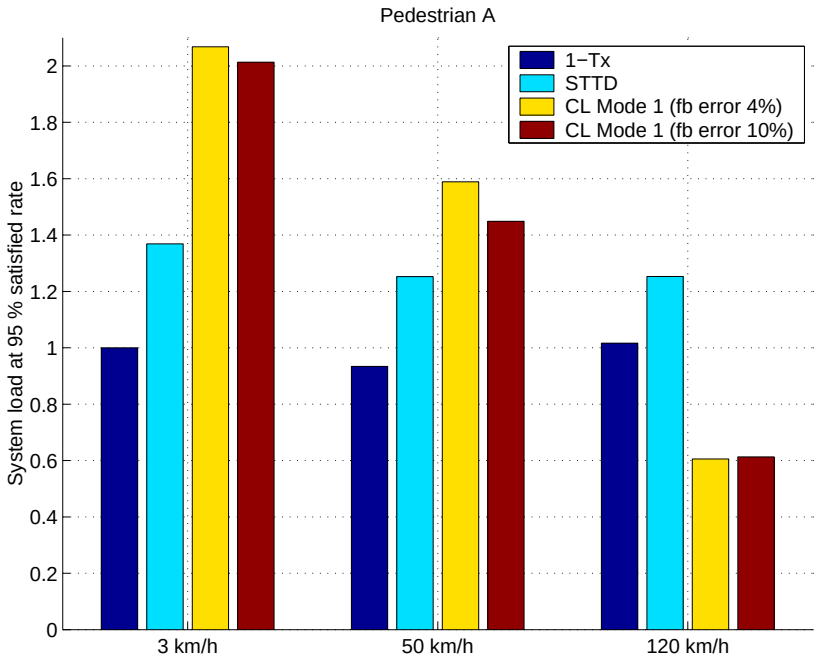

FIGURE 22 Comparison of STTD and CL Mode 1 network performance in Pedestrian A channel.

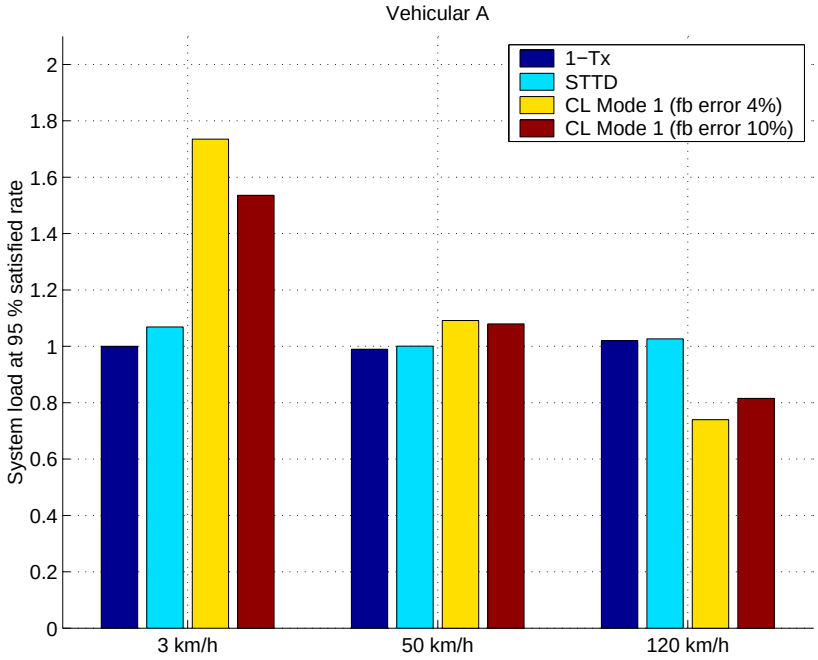

FIGURE 23 Comparison of STTD and CL Mode 1 network performance in Vehicular A channel.

4.4.1 Simulation scenario

In the following simulations CL Mode 1 and STTD performance with HSDPA is analysed and compared to a single antenna transmission in the macro cell scenario, which consist of 18 hexagonal cells of radius of 933 meters with 3 sector directional antennas. Used antenna pattern is similar as in [113]. In this study focus is on CL Mode 1 and STTD performance thus HSDPA parameters are mainly kept constant in these simulations.

A radio frame that corresponds to the Transmission Time Interval (TTI) is 3 slots i.e. 2 ms. The *Carrier to Interference (C/I)* ratio measurements from the *Common Paging Indicator Channel (CPICH)* are used for the determination of the CQI. C/I measurement is assumed ideal, but 0 and 3 TTI delays are applied for the signalling of the CQI from UE to Node B. Max C/I scheduling is based on the reported CQIs. As a comparison point to Max C/I also Round Robin scheduler is used. Available *Modulation and Coding Sets (MCS)* for *Adaptive Modulation and Coding (AMC)* were QPSK $\frac{1}{2}$, QPSK $\frac{3}{4}$, 16QAM $\frac{1}{2}$ and 16QAM $\frac{3}{4}$ and the number of utilized channelisation codes may vary from 1 to 15.

Code multiplexing of HS-DSCH is not used, thus the maximum number of HS-DSCH users per sector is 1 and for DPCH that is 15. These studies concentrate on HS-DSCH performance and therefore the effect of DPCH transmission is minimized by setting its bit rate to 1 kbps. HS-DSCH transmission power is 14 W, which is 70 % percent of the total base station transmission power and can be considered as reasonable for the HSDPA only scenario.

Mobility and traffic models are based on UMTS 30.03 [128] and used UE speeds are 3 km/h, 50 km/h and 120 km/h. High UE speeds do not present realistic usage scenarios for CL Mode 1, but those are included in these studies for the complete analysis. Users make calls and transmit data according to a packet data traffic model, which presents a typical web browsing session [128] including reading time.

A COST231-Hata propagation model is used to model path losses [128, 12] and minimum coupling loss between different transmitters and receivers was assumed to be 70 dB. Slow fading was modelled with log-normally distributed random variable with deviation of 8 dB. Correlation of 0.5 was assumed for the adjacent slow fading values up to 50 meters distance.

The effect of UE speed and CL Mode 1 feedback errors and feedback delays are analysed in Pedestrian A and Vehicular A channel. Network throughput is evaluated by the average HS-DSCH bit rate [kbps/cell/MHz] and it is measured as

$$R = \frac{b}{k \cdot T \cdot B}, \tag{4.11}$$

where b is the total number of correctly transmitted bits by HS-DSCH from all base stations in the simulated system over the whole simulated time, k is the number of cells in the simulation, T is the simulated time and B is the bandwidth [5 MHz].

4.4.2 Effect of CL Mode 1 feedback command delay

As presented in [P7] and also in DPCH simulations in Section 4.3.2 feedback command delay has a minor effect on system performance when the UE speed is low. However, with moderate and high UE speeds feedback delay has a crucial effect on system performance, thus it is proposed that feedback command delay should be one or two slots. Based on these findings feedback delay is set to one slot for these HSDPA simulations.

4.4.3 Network throughput

The CL Mode 1 and STTD transmit diversity are compared to single antenna transmission by the means of dynamic system simulations. Average cell throughput gains with CL Mode 1 and STTD as compared to 1Tx are presented in Figures 24 and 25 when the Round robin scheduler is used. Simulations are carried out with 3 TTIs delay in CQI reporting. As can be seen from Figure 24 STTD provides gains from 8.5 % to 11.5 % as velocity is increased from 3 to 120 km/h. CL Mode 1 provides gains of 34.9 % and 19.5 % with 3 and 50 km/h UE speed, but with 120 km/h 1Tx provides slightly better throughput. When CL Mode 1 feedback delay is increased to 10 % then CL Mode 1 gain decreases to 29.7 % at 3 km/h UE speed.

In Vehicular A channel gains from transmit diversity clearly decreases as multipath diversity increases as seen in 25. STTD gives about 6 % gain in 3 km/h and with other speeds the performance is about the same as 1Tx. CL Mode 1 provides gains of 17.1 % and 15.8 % with feedback error rates of 4 and 10 % and in 50 km/h gains reduces to 4.7 % and 3.5 %, respectively. In 120 km/h CL Mode provides around 10 % lower throughput than 1Tx and STTD.

Average cell throughput gains with CL Mode 1 and STTD as compared to 1Tx are shown in Figures 26 and 27 when Max C/I scheduler is used. Simulations are carried out with 3 TTIs delay in CQI reporting, that affects to AMC and scheduling. Now 1Tx outperforms STTD in 3 km/h as can be seen from Figure 26. STTD reduces the C/I variance (see e.g 32) thus the possible gain from Max C/I type of scheduling disappears. However STTD still provides gains of 7.9 % and 14.6 % with higher velocities, when CQI delay is too long for the AMC and scheduling to track fast channel variations. CL Mode 1 provides lower gains with Max C/I than with Round robin and the gains are 5.7 %, 10.5 % and 5.3 % with 3, 50 and 120 km/h UE speeds. When CL Mode 1 feedback delay is increased to 10 % the gains are only slightly reduced.

In Vehicular A channel gains from transmit diversity decreases some what as multipath diversity increases as seen in Figure 27. Similarly as in Pedestrian A channel 1Tx outperforms STTD with 3 km/h UE speed, but now with high UE speeds STTD provides only similar performance as 1Tx. Whereas CL Mode 1 is able provide slightly higher gains in Vehicular A channel than in Pedestrian A channel with 3 km/h UE speed. But again CL Mode 1 gains reduces as the velocity is increased and in 50 km/h 1Tx and CL Mode 1 have about equal performance and in 120 km/h CL Mode 1 throughputs are about 8 % lower than 1Tx.

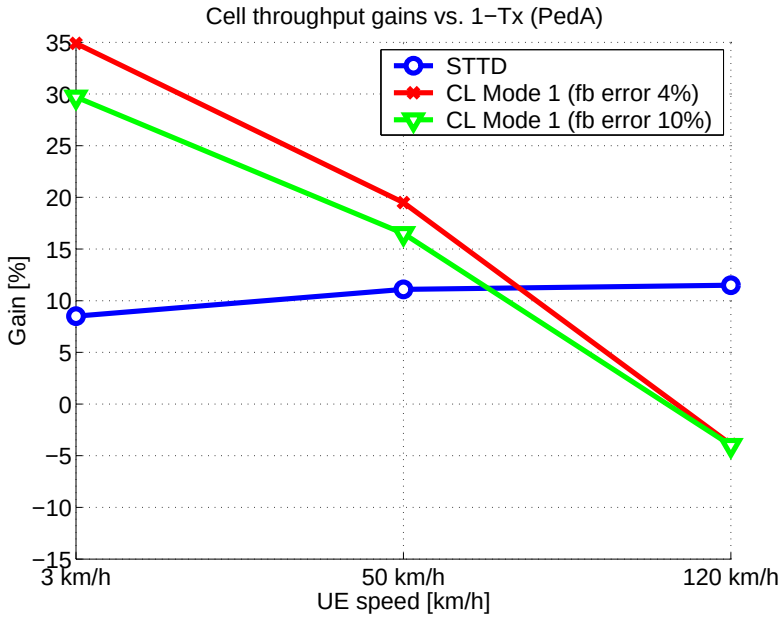

FIGURE 24 Cell throughput gain of STTD and CL Mode 1 as compared to 1Tx in Pedestrian A channel with Round robin scheduler.

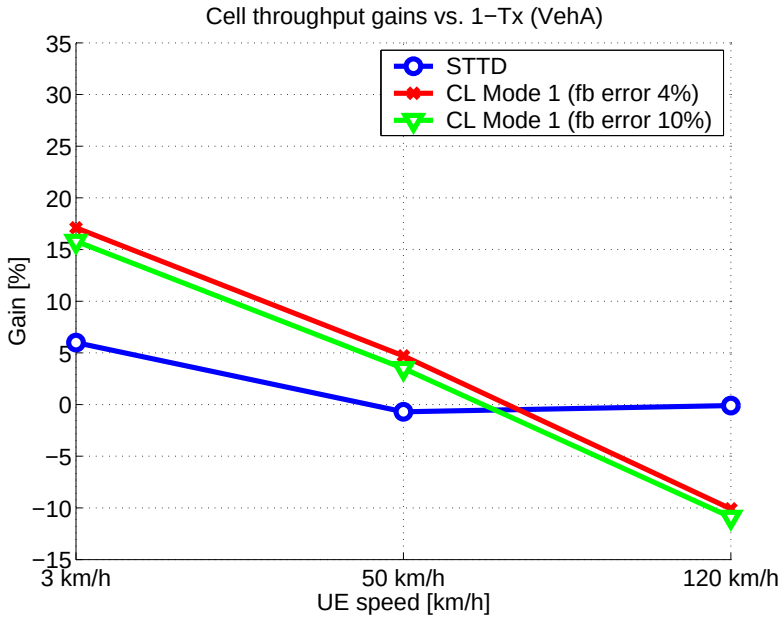

FIGURE 25 Cell throughput gain of STTD and CL Mode 1 as compared to 1Tx in Vehicular A channel with Round robin scheduler.

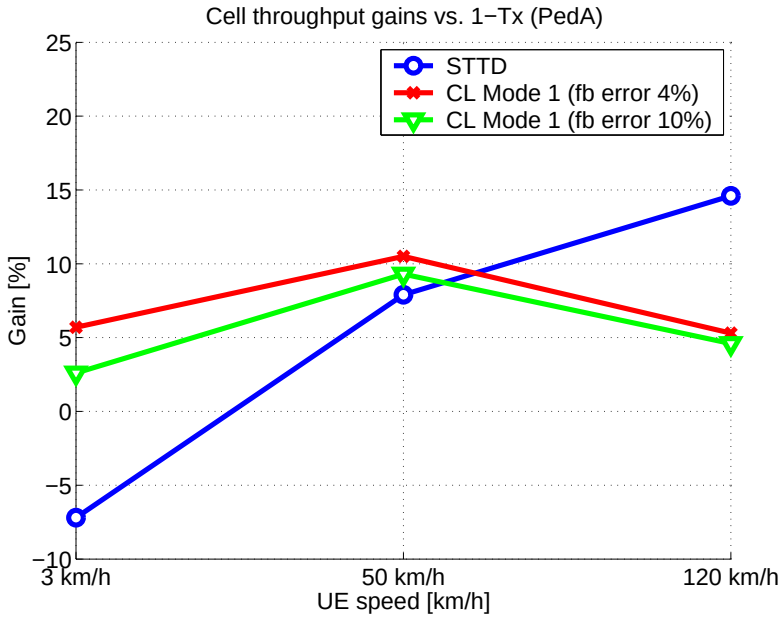

FIGURE 26 Cell throughput gain of STTD and CL Mode 1 as compared to 1Tx in Pedestrian A channel with Max C/I scheduler.

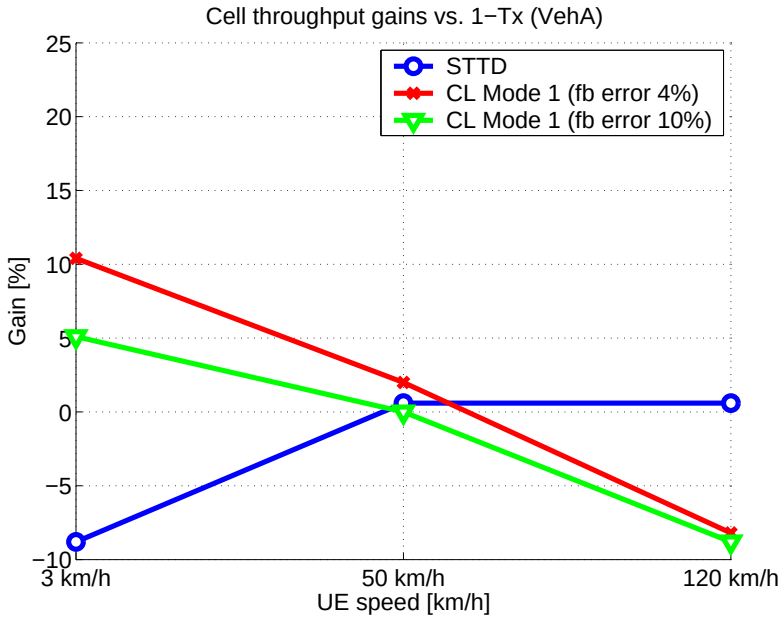

FIGURE 27 Cell throughput gain of STTD and CL Mode 1 as compared to 1Tx in Vehicular A channel with Max C/I scheduler.

These studies are carried out with a fully loaded network i.e. almost 100 % utilisation of HS-DSCH to find out maximal achievable gains from the transmit diversity schemes. The packet scheduler consists of two parts. Firstly every 200 ms 15 users are selected with Round robin fashion from all users that are admitted to the system. Then during the 200 ms period either Round robin or Max C/I scheduler is used for HS-DSCH allocation. Due to the web traffic model [128] there is a different amount of data for different users and it might happen that all the data will be transmitted to the certain users during this 200 ms allocation period, thus the number of available users for the HS-DSCH scheduling could be lower than initial value that is 15. This will limit the achievable multi-user diversity gain from Max C/I scheduler, but on the other hand it will provide service to the cell borders also.

The Max C/I scheduler gains as compared to Round robin are presented in Figures 28 and 29. Max C/I provides highest gains with 1Tx (about 76 %) with 3 km/h UE speed and lowest gains with CL Mode 1 (about 38 %). The Max C/I gains reduce clearly when UE speed is increased from 3 km/h to 50 km/h as the channel variations are too fast to be tracked by the CQI reports. However, still 20 to 30 % gain is seen from Max C/I with 50 km/h and 120 km/h UE speeds in Pedestrian A channel and 40 to 50 % gains in Vehicular A channel.

4.4.4 Effect of HSDPA transmit power

In these simulations HSDPA transmit power is varied with values of 8 watts and 14 watts, which correspond to 40 % and 70 % of total downlink transmit power. In Figures 30 and 31 relative gain in throughput of diversity schemes with Round robin and Max C/I as compared to single antenna are presented. As can be seen transmit diversity schemes provide slightly higher gains with lower transmit power allocation when a Round robin scheduler is used as the coverage starts to limit the achievable throughput of 1Tx in Pedestrian A channel with lower power allocation.

4.4.5 Effect of Soft handover parameters

In the following simulations two different soft handover parameter values are compared with Max C/I scheduler in Pedestrian A channel. For the first case window add and drop have values 4 and 7 dB and for the second case 1 and 3 dB. In the second case the HS-DSCH average bit rate is more than 15 % higher than in the first case.

The serving HS-DSCH sector is only updated when it is dropped from the active set. When window drop parameter is decreased from 7 to 3 dB, the old HS-DSCH sector is removed earlier from the active set i.e. the HS-DSCH connection is switched to a new sector. Thus with decreased soft handover region the variance between different sectors in an active set in terms of path loss is smaller and there is a higher probability that users have HS-DSCH connection to the best sector in active set.

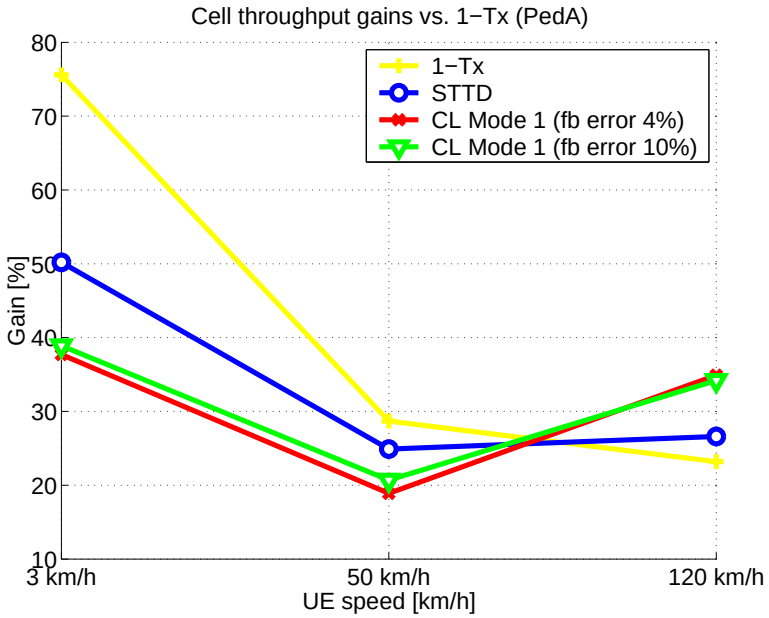

FIGURE 28 Cell throughput gain of STTD and CL Mode 1 with Max C/I scheduler as compared to 1Tx with Round robin in Pedestrian A channel.

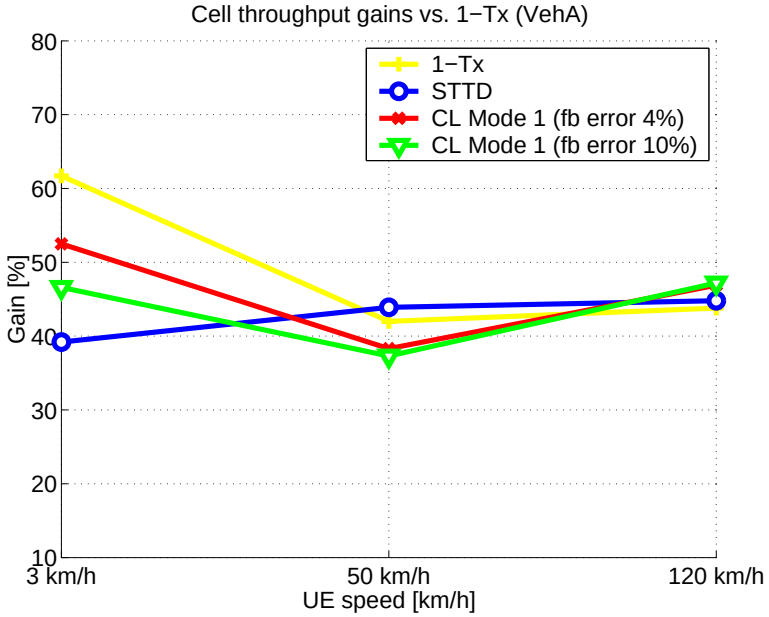

FIGURE 29 Cell throughput gain of STTD and CL Mode 1 with Max C/I scheduler as compared to 1Tx with Round robin in Vehicular A channel.

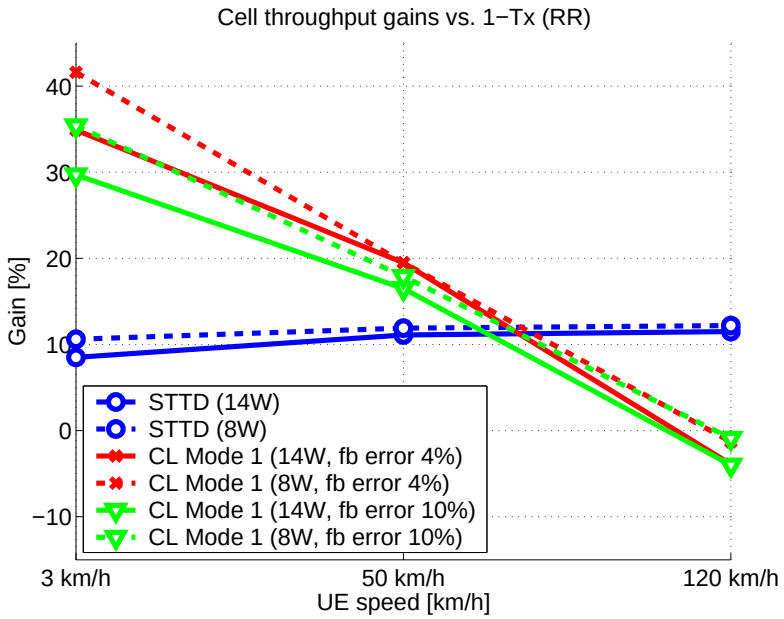

FIGURE 30 Cell throughput gain of STTD and CL Mode 1 as compared to 1Tx in Pedestrian A channel with Round robin when HS-DSCH power is set to 14 watts and 8 watts.

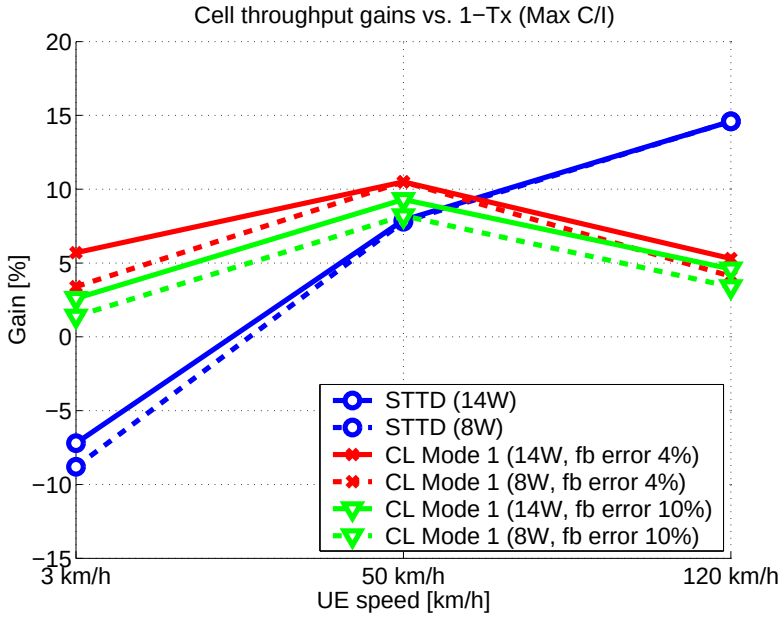

FIGURE 31 Cell throughput gain of STTD and CL Mode 1 as compared to 1Tx in Pedestrian A channel with Max C/I schedulers when HS-DSCH power is set to 14 watts and 8 watts.

In [92] two different methods are presented for the HSDPA handover. The preferred method is the same as is used here i.e. hard handover is made on HS-DSCH. In another option HS-DSCH is released during soft handover and traffic is carried on dedicated channel. HS-DSCH channel is set up when an active set becomes one again. This second option requires that soft handover windows are rather small.

4.4.6 HS-DSCH E_s/N_0 distributions

Distribution of HS-DSCH E_s/N_0 values with Max C/I and Round robin schedulers are presented in the Figures 32, 34 and 36 for Pedestrian A channel and in the Figures 33, 35 and 37 for Vehicular A channel.

From these distributions the differences between single antenna, STTD and CL Mode 1 can be seen. In the case of the Round robin scheduler the shape of the distributions of a single antenna and CL Mode 1 are similar but the average of E_s/N_0 with CL Mode 1 is higher. This E_s/N_0 gain from CL Mode 1 is visible in 3 and 50 km/h, but it decreases as a function of UE speed and it is disappeared at 120 km/h speed, since CL Mode 1 feedback command delay is too long to follow fast channel variations. With STTD shape of the E_s/N_0 distribution is different from single antenna and CL Mode 1. STTD provides more stable channel thus E_s/N_0 distribution is sharper i.e variance is smaller than that of single antenna or CL Mode 1. Also as compared to a single antenna and CL Mode 1 STTD works better with high UE speeds.

With Max C/I scheduler single antenna and CL Mode 1 have very similar E_s/N_0 distributions. Max C/I scheduler decreases CL Mode 1 gain over single antenna, thus also with low UE speed E_s/N_0 averages are about the same. STTD works as in case of Round robin i.e. E_s/N_0 variance is smaller than with single antenna or CL Mode 1. Since STTD averages channel it causes small decrease to E_s/N_0 distribution in low UE speeds with Max C/I as compared to single antenna or CL Mode 1.

The shape of the E_s/N_0 distributions from simulations in Vehicular A channel is quite different from the distributions from Pedestrian A channel simulations, since multipath interference limits the performance in Vehicular A channel. Due to multipath diversity variation in E_s/N_0 values is smaller in Vehicular A channel than in the Pedestrian A channel.

4.4.7 User bit rate

In the Figures 38, 40 and 42 user bit rates are presented with both Max C/I and Round robin schedulers in Pedestrian A channel and in the Figures 39, 41 and 43 for Vehicular A channel. User bit rate [kbps] for the packet session of the UE n is defined as

$$R_n = \frac{b_n}{T^n_{active}}, \tag{4.12}$$

where b_n is the number of correctly delivered bits to the UE n and T^n_{active} is the users active time, which is running whenever the user buffer is not empty. Thus,

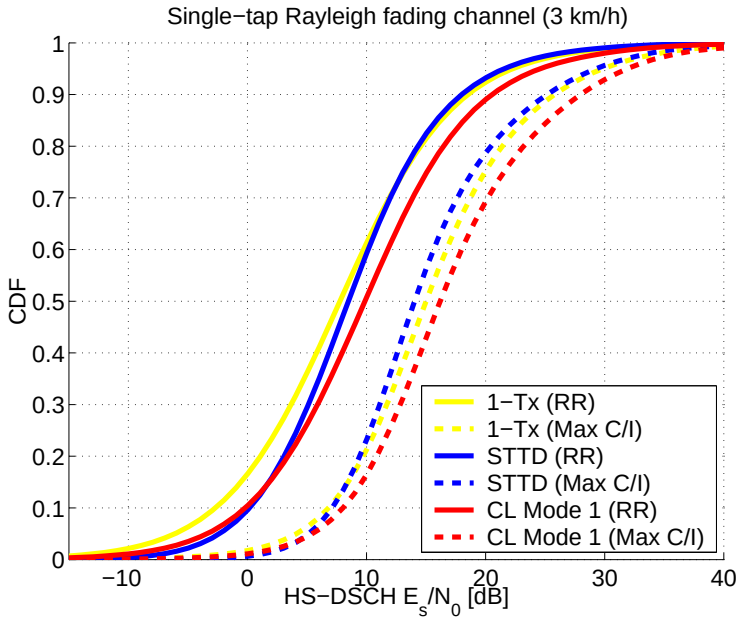

FIGURE 32 HS-DSCH E_s/N_0 comparison of 1Tx, STTD and CL Mode 1 with Round robin and Max C/I schedulers in Pedestrian A channel with 3 km/h UE speed.

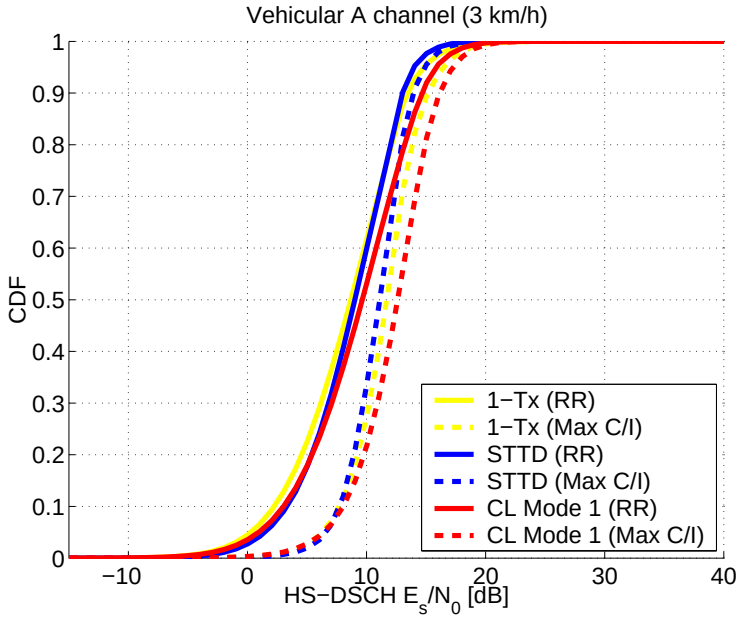

FIGURE 33 HS-DSCH E_s/N_0 comparison of 1Tx, STTD and CL Mode 1 with Round robin and Max C/I schedulers in Vehicular A channel with 3 km/h UE speed.

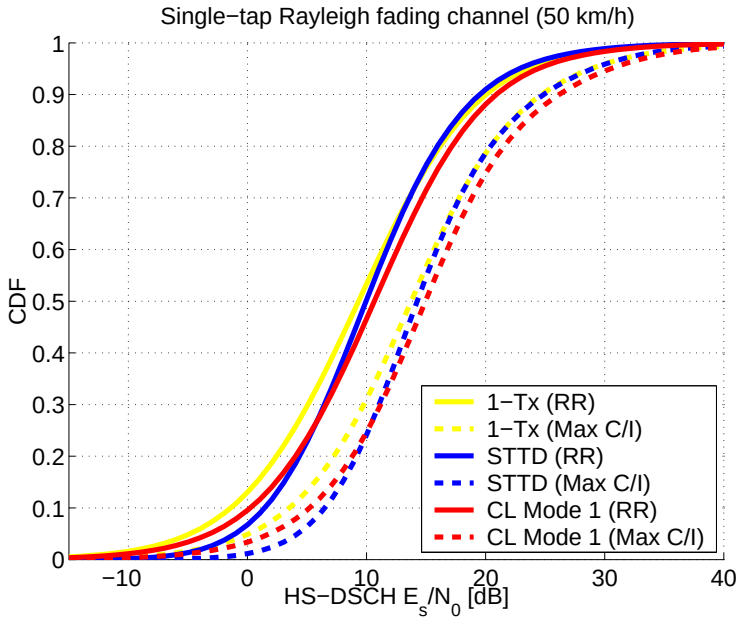

FIGURE 34 HS-DSCH E_s/N_0 comparison of 1Tx, STTD and CL Mode 1 with Round robin and Max C/I schedulers in Pedestrian A channel with 50 km/h UE speed.

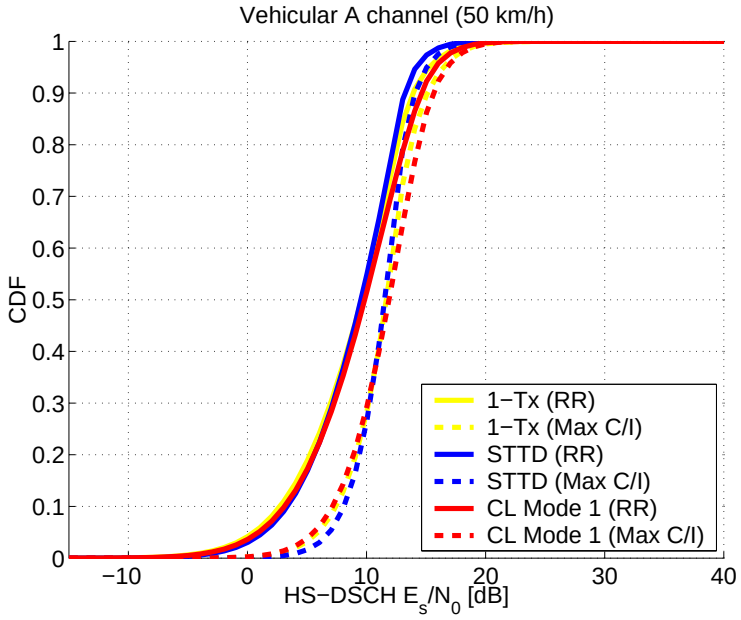

FIGURE 35 HS-DSCH E_s/N_0 comparison of 1Tx, STTD and CL Mode 1 with Round robin and Max C/I schedulers in Vehicular A channel with 50 km/h UE speed.

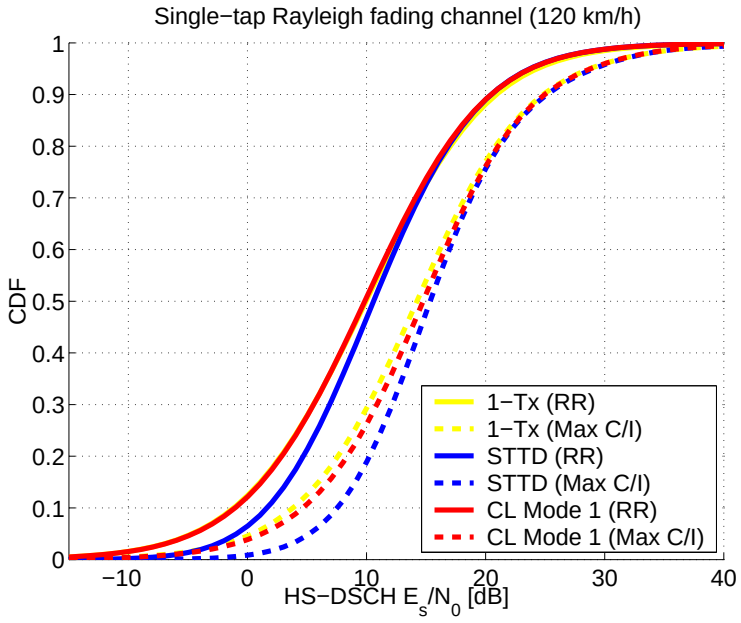

FIGURE 36 HS-DSCH E_s/N_0 comparison of 1Tx, STTD and CL Mode 1 with Round robin and Max C/I schedulers in Pedestrian A channel with 120 km/h UE speed.

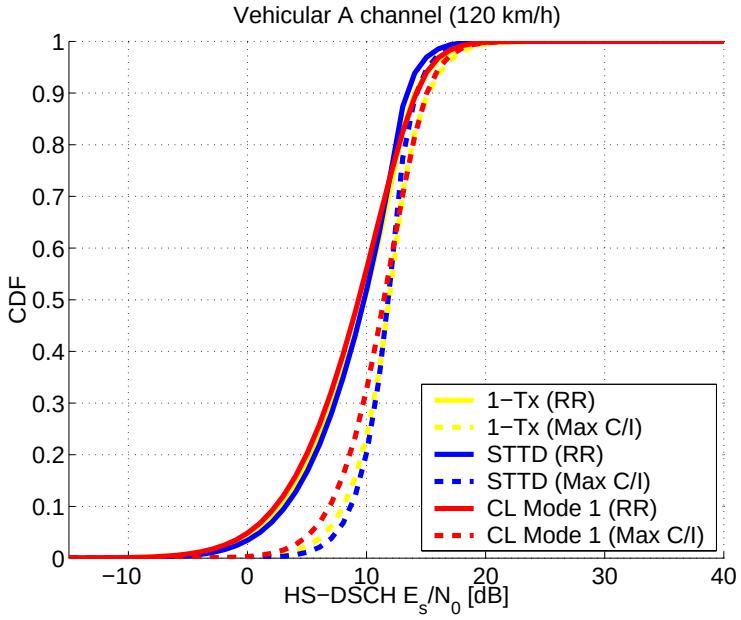

FIGURE 37 HS-DSCH E_s/N_0 comparison of 1Tx, STTD and CL Mode 1 with Round robin and Max C/I schedulers in Vehicular A channel with 120 km/h UE speed.

in this output value the time on DCH and HS-DSCH as well as the queuing time are taken into account.

In general user bit rate results are aligned with HS-DSCH throughput results (see Figures 24, 25, 26 and 27). However the differences between single antenna, STTD and CL Mode 1 are rather small and mainly the effect of the used scheduler is visible i.e. bit rates with Max C/I scheduler are higher than those with Round robin.

4.4.8 Achieved results

In this section simulation results with CL Mode 1, STTD and single antenna transmission are presented. Motivation for the use of multiple antennas arise from the expected gains in performance of a wireless link. These simulation results clearly indicate that CL Mode 1 has good performance especially in low mobility environments as compared to STTD and single antenna. With low mobile speed Mode 1 is not sensitive to the feedback command delay and also feedback error rate of 10 % has only a small impact on the overall system performance.

Relative throughput gain of about 30 % was achieved with CL Mode 1 in Pedestrian A channel with Round robin scheduler as compared to a single antenna, while the relative throughput gain is reduced to 26 % when UE speed is increased to 50 km/h. In a multipath environment (Vehicular A) the relative throughput gain is reduced to 18 % and 4 % with 3 and 50 km/h UE speed. Naturally CL Mode 1 performance decreases with moderate and high UE speeds due to fast channel variations.

With Max C/I scheduler CL Mode 1 provides smaller gain than with Round robin, since Max C/I scheduler selects users with good channel conditions so diversity schemes can only provide small gains over single antenna transmission. However in Vehicular A channel CL Mode 1 provides 13 % gain with 3 km/h UE speed as compared to single antenna.

4.5 Fast Alpha Switching for Closed Loop Mode 1 ([P8])

In this section, we present an analysis of *the Fast Alpha Switching (FAS)* technique in the WCDMA using the Closed Loop (CL) Mode 1 transmit diversity [111] and utilizing the High Speed Physical Downlink Shared Channel (HS-PDSCH) [112] for a data service based on [P8]. When applied to the HS-PDSCH channel, CL Mode 1 utilizes the antenna weights used on the associated Dedicated Physical Channel (DPCH). Therefore when the terminal is in soft handover (SHO) in the DPCH i.e. connected to more than one sector, the antenna weight, which is optimized for all sectors in the SHO, is hardly optimal for the HS-PDSCH, which is always received from a single sector. In the FAS technique, the antenna weight calculation is based on the received pilot from the HS-PDSCH sector when the HS-PDSCH is in use and otherwise the calculation is based on the pilots of all sectors in SHO. At first sight, this seems to be a desirable feature, but several

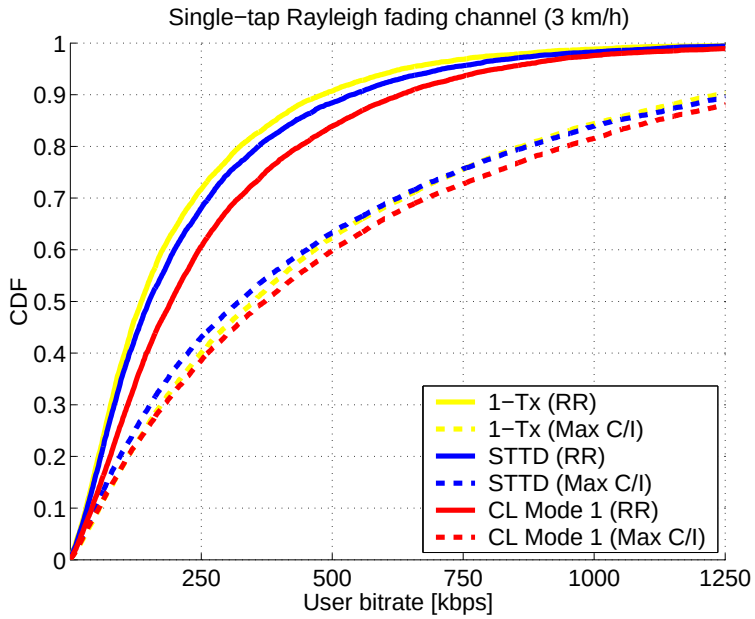

FIGURE 38 User throughput comparison of 1Tx, STTD and CL Mode 1 with Round robin and Max C/I schedulers in Pedestrian A channel with 3 km/h UE speed.

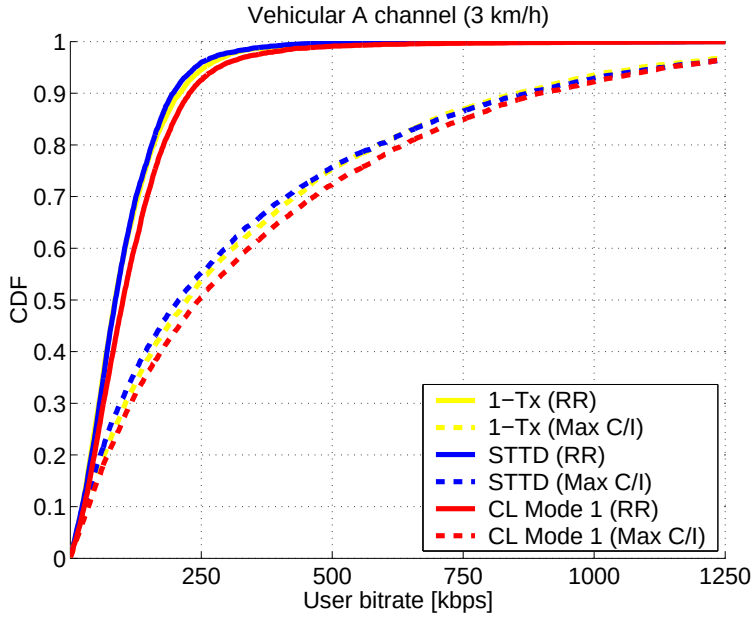

FIGURE 39 User throughput comparison of 1Tx, STTD and CL Mode 1 with Round robin and Max C/I schedulers in Vehicular A channel with 3 km/h UE speed.

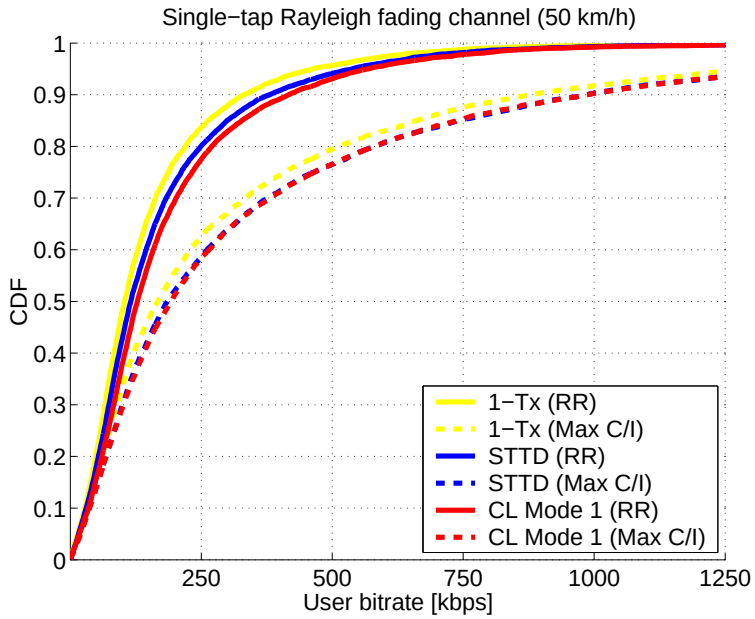

FIGURE 40 User throughput comparison of 1Tx, STTD and CL Mode 1 with Round robin and Max C/I schedulers in Pedestrian A channel with 50 km/h UE speed.

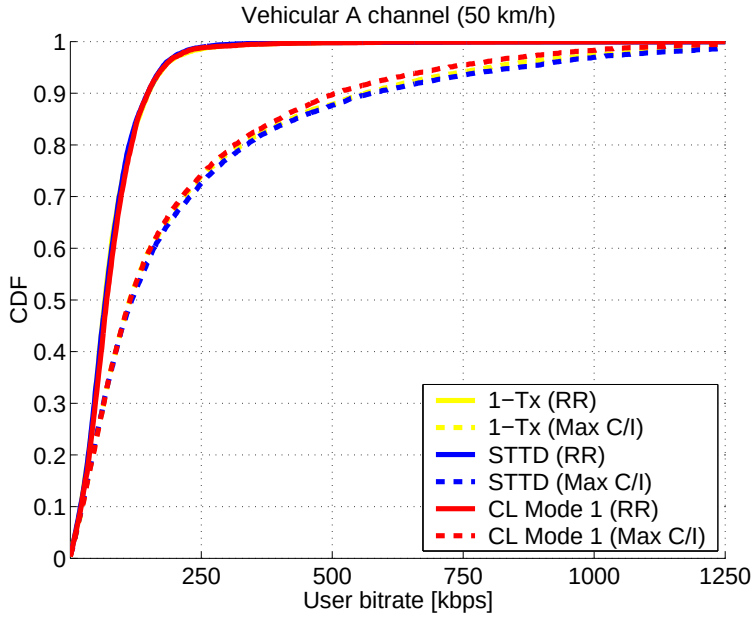

FIGURE 41 User throughput comparison of 1Tx, STTD and CL Mode 1 with Round robin and Max C/I schedulers in Vehicular A channel with 50 km/h UE speed.

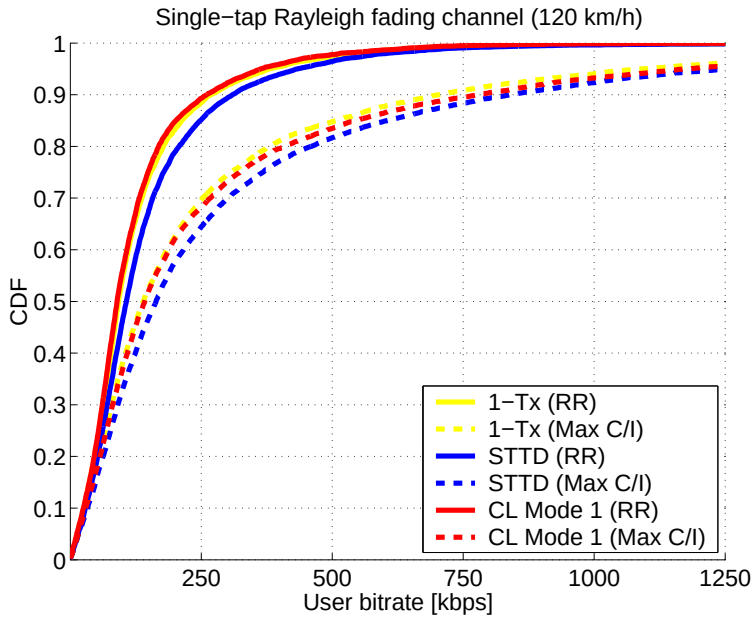

FIGURE 42 User throughput comparison of 1Tx, STTD and CL Mode 1 with Round robin and Max C/I schedulers in Pedestrian A channel with 120 km/h UE speed.

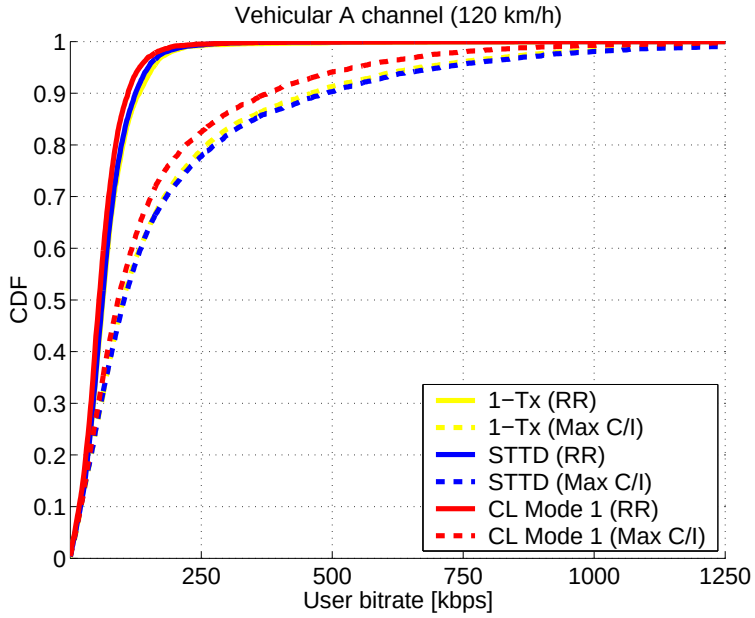

FIGURE 43 User throughput comparison of 1Tx, STTD and CL Mode 1 with Round robin and Max C/I schedulers in Vehicular A channel with 120 km/h UE speed.

factors more have to be considered before any conclusions. The FAS technique is affected by the feedback delay, thus the applied weight is not always optimal for the HS-PDSCH. Moreover the SHO probability is important for the analysis, since the gain can only be achieved, when the terminals are in SHO. Therefore, dynamic system simulations are necessary to study, what are the expected gains from the FAS technique in realistic scenarios.

The system performance was studied with the max C/I and Round robin schedulers in Pedestrian A and Vehicular A channels. With the Round robin scheduler, all active terminals are scheduled alternately thus it is also very probable that terminals, which are in soft handover, are scheduled. Where as with the max C/I scheduler it is typical that primarily terminals, which are close to the serving base station are scheduled. In such a situation the throughput of the network is high, but there might be several terminals near the edge of the cell, which are not frequently served.

In the FAS technique, the antenna weight calculation is based solely on the HS-PDSCH sector, when it is allocated for the given terminal and otherwise the weight calculation is based on all sectors in SHO. The results, anyway, show that with this technique a very minor performance gain can be achieved. With the Round robin scheduler its performance is limited due to the feedback signalling delay of a minimum one slot and due to the short HSDPA sub-frame length of three slots. These will actually cause a situation, where only the last feedback bit is optimized as received by the base station during the HSDPA sub-frame. With the Max C/I scheduler, the reason for small gains of the FAS was that the terminals are primarily scheduled when they are not in SHO and they are thus served entirely by one sector.

5 PERFORMANCE OF HSDPA NETWORK WITH ADVANCED UE RECEIVERS

HSDPA is currently an important topic in 3GPP standardization and further enhancements for HSDPA network performance are evaluated. One interesting enhancement is advanced UE receivers and in this chapter system level aspects of usage of advanced receivers in the terminal side is thoroughly studied.

5.1 Introduction

In the WCDMA downlink the main interference sources are intra-cell interference caused by multiple access and inter-cell interference caused by neighbouring base stations. The latter is characterized by different scrambling codes, channel states and angles-of-arrivals than the signal from the desired base station. In a synchronous WCDMA downlink employing orthogonal spreading codes the intra-cell interference is caused by multipath propagation. This is due to the high cross-correlation values between the spreading sequences with arbitrary time shifts, which results in significant MAI. The level of this intra-cell interference depends strongly on the channel response. In nearly flat fading channel the physical channels remain almost orthogonal and intra-cell interference does not have a significant impact on the receiver performance. On the other hand, the performance of the Rake receiver can be severely deteriorated by intra-cell interference in frequency selective channels. Frequency selectivity is common for the channels in WCDMA networks. Advanced detectors are one option in an effort to mitigate the effect of MAI. In this thesis, the effect of the suppression of intra-cell interference with channel equalizers for the HSDPA system performance is studied by the means of dynamic system simulations.

5.2 Detector algorithms

CDMA detector algorithms can be divided into two main categories, which are single-user and multi-user detection (MUD). In the latter class the knowledge of the spreading sequences are utilized non-blindly or blindly in order to mitigate the effects of MAI. In [130] and [59] a comprehensive study on MUD is presented. Even though MAI is present in WCDMA downlink when the channel is frequency selectively fading, the effect of MAI can be mitigated without the knowledge of MAI by using chip-level equalization.

In this thesis we only focus on single-user detection algorithms, namely Rake and LMMSE chip-level linear equalizer, which are implemented in an advanced system level simulator and their performance is studied with extensive simulations. With the single-user detectors each user or code channel is detected separately without taking into account other users, thus the single-user detector does not take explicitly consider the existence of MAI. The Rake is a good example of a detection algorithm belonging to this category.

5.2.1 Rake

The Rake receiver is the most commonly used receiver in CDMA systems and third generation networks are designed so that it can be used [49]. It was first proposed to spread spectrum systems for mitigating fading [94, 125, 126, 95]. This ability of the spread spectrum signal is utilized in a Rake receiver by first separating multipath propagated signals and then combining these signals coherently, so multipath diversity is achieved and utilised to combat fading. The received multipath signals can be combined in several ways, but the maximal ratio combining (MRC) is preferred in a coherent receiver. The major benefit of the Rake is its simplicity and also its reasonable performance. However the complexity depends linearly on the number of Rake fingers and also from the number of used codes. The drawback of the Rake is that its performance is degraded by multiple access interference (MAI) which arises from simultaneous transmission of different data channels through a multipath channel. Any means to suppress or to avoid MAI increases the capacity of CDMA networks. For this reason it is of great interest to develop enhanced receiver techniques.

5.2.2 LMMSE chip-level equalizer

Chip-level linear equalization is another kind of single-user detector, which utilizes the channel information and equalizes the channel to be flat again prior to despreading. As a by-product, the orthogonality between the channels which was lost due to a dispersive channel is restored, and hence, MAI is mitigated. A link-level analysis of chip-equalization is presented in [50]. One of the major benefits of the detection algorithm based on the use of a linear chip-equalizer is its good performance and simplicity in frequency selective channels. These benefits however are only valid if the delay spread of the channel is relatively short. The

larger the delay spread is the longer and thus a more complex equalizer is required. The delay spread is the limiting factor for the practical use of the linear chip-equalizer [50].

5.3 Earlier work

Employing dual antennas at the receiver is a straight-forward solution in combating against channel fading and intra-cell interference. [116] shows a recent study of the WCDMA system performance for dedicate channels when a certain penetration of dual antenna terminals is assumed. This analysis is extended in [129] where in addition to dual antennas chip equalizers are also considered. It shows clear capacity gains over the conventional Rake-based dual antenna reception given that dual antenna terminal penetration is high enough. In that study no code resource limitations were considered. In [131] and [77] the study was extended to HSDPA network, where the Rake receiver and LMMSE equalizer performance with/without receive diversity was analysed. However, a quasi-static system level tool was used and hence handover or call generation and termination procedures can not be modelled in detail. We extend the above mentioned studies in HSDPA network where both code resource limitation and all the radio resource management algorithm are modelled in detail.

Spatial equalization is the most straightforward way to suppress inter-cell interference [132, 90], but efficient spatial equalization requires a relatively large number of receiver antennas due to the multiple neighbouring base station signals arriving to the terminal. However some suppression can be already achieved with two receiver antennas, but the number of required antennas limits the feasibility of inter-cell interference suppression in WCDMA terminals [50].

5.4 Modelling of advanced receivers and UE receive diversity

In this section modelling of advanced receivers and UE receive diversity are presented, which is based on the [66, 67].

5.4.1 Signal model

It is assumed that there exists one Tx-antenna at Node B and N_{Rx} Rx-antennas at UE. The received chip sequence equals

$$\mathbf{r}(m) = \mathbf{H}^T \mathbf{s}(m) + \mathbf{n}(m), \tag{5.1}$$

where transmitted chip stream is

$$\mathbf{s}(m) = [s(m + F + L - D) \cdots s(m) \cdots s(m - D)]^T \tag{5.2}$$

and $\mathbf{n}(m)$ is the noise vector. Here D is the delay parameter satisfying $(0 \leq D \leq F)$, L is the delay spread of the channel normalized to the chip interval and F is filter

length. Multiplication by the $(F + L) \times (F \times N_{Rx})$ channel coefficient matrix $\mathbf{H}$ in Equation 5.1 models the convolution between the transmitted chips and the impulse response of the channel. Thus,

$$\mathbf{H} = \begin{bmatrix} \mathbf{h}_{N_{Rx}\times(L+1)} & \mathbf{0}_{N_{Rx}\times 1} & \cdots & \mathbf{0}_{N_{Rx}\times 1} \\ \mathbf{0}_{N_{Rx}\times 1} & \mathbf{h}_{N_{Rx}\times(L+1)} & \cdots & \vdots \\ \vdots & \vdots & \ddots & \mathbf{0}_{N_{Rx}\times 1} \\ \mathbf{0}_{N_{Rx}\times 1} & \mathbf{0}_{N_{Rx}\times 1} & \mathbf{0}_{N_{Rx}\times 1} & \mathbf{h}_{N_{Rx}\times(L+1)} \end{bmatrix}^T, \tag{5.3}$$

where $\mathbf{h}$ is the $N_{Rx} \times (L + 1)$ channel impulse response matrix defined by

$$\mathbf{h} = \begin{bmatrix} h_1(0) & h_1(1) & \cdots & h_1(L) \\ h_2(0) & h_2(1) & \cdots & h_2(L) \\ \vdots & \vdots & \ddots & \vdots \\ h_{N_{Rx}}(0) & h_{N_{Rx}}(1) & \cdots & h_{N_{Rx}}(L) \end{bmatrix}. \tag{5.4}$$

In Equation 5.4 $h_i(l)$ is the channel impulse of i^{th} Rx-antenna at delay l.

The $F \times N_{Rx}$ chip long linear filter $\mathbf{w}$ is used at the receiver to obtain the chip estimate $\tilde{\mathbf{s}}$ for the transmitted chip sequence $\mathbf{s}$. i.e.

$$\tilde{\mathbf{s}}(m) = \mathbf{w}^{\mathbf{T}}\mathbf{r}(m). \tag{5.5}$$

5.4.2 Calculation of filter coefficients

In this section, calculation of filter w (see Equation 5.5) coefficients is presented for Rake and LMMSE.

Rake

For the Rake receiver the linear filter coefficient vector w for N_{rx} receiver antennas consists of channel coefficients (which are ideal on the system level) and it can be written as

$$\mathbf{w} = \mathbf{H}^H \delta_D, \tag{5.6}$$

where

$$\delta_D = \begin{bmatrix} 0 & \cdots & 0 & 1 & 0 & \cdots & 0 \end{bmatrix}^T. \tag{5.7}$$

LMMSE

When a channel is frequency selective, orthogonality of different code channels disappears. However, it is still possible to de-orthogonalize the channel before despreading by equalizing the channel at chip (or fractional chip) level. After the chip-level equalizer, the overall channel (convolution of the channel $h(t)$ and the equalizer filter w) is frequency non-selective again with 1 tap only.

If the LMMSE solution in [66, 67] is applied, the equalizer coefficient vector

$$\mathbf{w} = \mathbf{C}_w^{-1}\mathbf{H}^H(P_i\mathbf{H}\mathbf{C}_w^{-1}\mathbf{H}^H + \frac{\mathbf{I}}{L_i})^{-1}\delta_D, \tag{5.8}$$

where P_i is total transmit power of sector i, $\mathbf{I}$ is signal covariance matrix, L_i is pathloss containing distance attenuation and slow fading and δ_D is a column vector of length $(L+F)$, which defines the delay of the equalizer. Note that delay can be optimized for LMMSE as in [66].

The $(F+N_{Rx}) \times (F+N_{Rx})$ interference matrix

$$\mathbf{C}_w = \begin{bmatrix} \sigma_1^2 & 0 & 0 & 0 & 0 & 0 \\ 0 & \ddots & 0 & 0 & 0 & 0 \\ 0 & 0 & \sigma_{N_{Rx}}^2 & 0 & 0 & 0 \\ 0 & 0 & 0 & \sigma_1^2 & 0 & 0 \\ 0 & 0 & 0 & 0 & \ddots & 0 \\ 0 & 0 & 0 & 0 & 0 & \sigma_{N_{Rx}}^2 \end{bmatrix}, \tag{5.9}$$

where

$$\sigma_j^2 = I_{tot}^j - I_i^j. \tag{5.10}$$

The antenna wise total downlink interference from all sectors to UE is calculated as

$$I_{tot}^j = \sum_{i=1}^{k} I_i^j + N_0, \tag{5.11}$$

where k is the number of sectors in simulation area and N_0 is system noise. Then downlink interference from one sector to observed UE is calculated as

$$I_i^j = P_i L_i \sum_{l=1}^{N_i} (g_{i,l} \| h_{i,l}^j \|^2), \tag{5.12}$$

where P_i is the downlink transmission power in the sector i and L_i is the slow faded path loss between the UE and sector i. N_i is the number of multipath components provided by the simulated environment in sector i, g_i, l is the average path gain of the l^{th} component and $h_{i,j}$ is complex channel coefficient for sector i, multipath component l and receiver antenna j.

5.4.3 Calculation of (C/I) for linear receivers

In general, the signal-to-interference and noise ratio at the output of a linear filter may be calculated by evaluating the power of the specific signal and noise terms after filtering as in [64, 78]. These methods can be directly applied in calculating the (C/I) at the output of the linear receiver. Thus,

$$(C/I) = \frac{P_{HS-DSCH} |\mathbf{w}^T \mathbf{H}^T \delta_D|^2}{P_i \mathbf{w}^T \mathbf{H}^T \hat{\delta}_D \hat{\delta}_D^T \mathbf{H}^* \mathbf{w}^* + \frac{1}{L_i} \mathbf{w}^T \mathbf{C}_w \mathbf{w}^*}, \tag{5.13}$$

where the left-most term in the divisor models the intra-cell interference (i.e. inter-path interference) and right-most term models the inter-cell interference and background noise. (C/I) is calculated according to Equation 5.13 for all

linear receivers and it is the definition of **w**, which varies according to the linear receiver type used. Moreover, in Equation 5.13 $\hat{\delta_D}$ is a $(F \times F)$ matrix defined by

$$\hat{\delta}_D = diag(\begin{bmatrix} 1 & \cdots & 1 & 0 & 1 & \cdots & 1 \end{bmatrix}), \tag{5.14}$$

and it is used in the matrix product $\mathbf{H}^T \hat{\delta}_D \hat{\delta}_D^T \mathbf{H}^H$ to extract the elements from the channel matrix that are used in the inter-path interference calculation.

Correspondingly the symbol energy to noise ratio E_s/N_0 of HS-DSCH is defined as

$$E_s/N_0 = 10 \cdot log_{10}(16) \cdot (C/I). \tag{5.15}$$

Any spatial interference cancellation is not taken into account in the current model, but it should be noted that with multiple receiver antennas i.e. with receive diversity the signals received by the antennas can be weighted and combined to maximize the output SINR. Thus with co-channel interference, space diversity is used not only to combat Rayleigh fading of the desired signal (as with maximal ratio) but also to reduce the power of interfering signals at the receiver [132].

5.4.4 Simulation scenario

The performance of HSDPA network with Rake and LMMSE chip-level equalizer with/without receive diversity is studied in macro cell scenario which consists of 7 Node B's and 21 hexagonal cells (sectors) of radius of 933 meters. BS-to-BS distance is 2800 meters. Propagation model is based on [109] and the log-normally distributed slow fading has a 8 dB standard deviation. A correlation coefficient of 0.5 is used for adjacent slow fading values up to 50 meter distances. Used channel profiles are modified Pedestrian A and Vehicular A.

MAC-hs packet scheduling is based on Round Robin and Proportional Fair scheduling algorithms and code-multiplexing is not used thus only one UE is scheduled per TTI. The maximum numbers of HS-DSCH codes are 5 and 10 with a spreading factor of 16. HS-DSCH power is 14 W, which is 70 % of the total base station transmission power. One code is allocated for HS-SCCH with a spreading factor of 128 and it is ideally decoded. HS-DSCH link adaptation is based on the UE reported channel quality indicators (CQIs) (inner loop) and UE's reported Ack/Nacks from past retransmissions (outer loop). Aimed BLER target for the first transmission is 30 % and link adaptation outer loop is used to control the BLER target with the same principle as in [84]. CQI tables are throughput optimized with BLER target of 30 %. Six parallel stop-and-wait (SAW) channels are used for the Hybrid ARQ and maximum of 4 retransmissions are allowed per transport block. Chase Combining is used with retransmissions. Signalling on the HS-DPCCH is modelled with a fixed delay and a fixed decoding error probability.

Mobility and traffic models are based on UMTS 30.03 [128] and used UE velocity is 3 km/h. A traffic model is modified so that the users do not have a reading time during a download session. Simulation time is 6 minutes. The call

arrival rate in the network is 140 calls per second and the average packet call size is 112 kilobytes. Thus, the total average offered load per cell can be calculated as

$$O = c_a \cdot c_s / k, \tag{5.16}$$

where c_a is the call arrival rate, c_s is the average packet call size and k is the number of cells in the network. In our simulations the average offered load per cell is approximately 6 Mbps. New calls are generated according to homogeneous Poisson process and the offered traffic is sufficiently high to have 100 % utilization of the HS-DSCH. Admission control allows up to 16 HSDPA users per cell.

5.5 Simulation results analysis

In this section the system simulation results of Rake and LMMSE chip-level linear equalizer with/without UE receive (Rx) diversity are presented when High Speed Downlink Packet Access (HSDPA) is used. The aim of these simulations is to identify the effect of receive diversity and advanced receivers with different schedulers (Round robin and Proportional fair) on HSDPA system performance.

Throughout these simulations it is assumed that the radio resource management algorithms do not know which kind of receivers are employed in the network i.e. similar RMM algorithms are used for all the receiver structures. However, advanced receivers provide improvement in E_s/N_0 distribution, thus the RRM algorithms are able to automatically capture the gain of advanced receivers. By taking the UE receivers into account in RRM algorithms, the throughput gain can be distributed for e.g. users of the advanced receiver or to all users in the network. This type of RRM algorithms can be based on the quality of service provisioning for different user classes [23], but analysis of these are out of the scope of this thesis.

Evaluation is started from the E_s/N_0 distributions and then cell throughputs and user throughputs are presented. Finally simulations are conducted with different advanced receiver penetrations.

5.5.1 E_s/N_0 improvement with advanced receivers

In Figure 44 E_s/N_0 distributions of Rake 1Rx, Rake 2Rx, Equalizer 1Rx and Equalizer 2Rx are presented from Pedestrian A channel and in the Figure 45 from Vehicular A channel simulations. As can be seen from the figures an equalizer provides clear improvement especially in the high end in the E_s/N_0's in Vehicular A as compared to Rake with the same diversity order. If Vehicular A and Pedestrian A channel results are compared the gain of the equalizer towards Rake with the same diversity order diminishes along the reduced amount of multipath interference, thus only minor gains from the equalizer in terms of throughput could be expected in Pedestrian A channel. In Pedestrian A channel E_s/N_0's have higher variance as compared to Vehicular A channel due to lower multipath diversity. Receive diversity reduces the variance of E_s/N_0 in both channel models

and also receive diversity provides almost constant improvement in E_s/N_0 for both Rake and equalizer. Due to the higher E_s/N_0's bigger transport blocks can be allocated to the UE with advanced receivers, thus the throughput can be increased.

5.5.2 Throughput improvement with advanced receivers

As the analysis of the E_s/N_0 distribution in the Section 5.5.1 suggested significant improvement in the cell throughput is visible with advanced receivers as can be seen in Figures 48 and 49, which shows the cell throughput gain of advanced receivers as compared to Rake 1Rx. Simulations are done with Round robin (RR) and Proportional fair (PF) schedulers and maximum number of HS-DSCH codes is 5 or 10.

As can be seen from the Figures 48 and 49 the receive diversity provides the largest gains with all the used scheduler or code resource combinations in both channel models. In Vehicular A channel 2Rx Rake provides from 50 % to 90 % gain as compared to 1Rx Rake, which is then doubled by the 2Rx equalizer. 1Rx equalizer provides 25-30 % gain compared to 1Rx Rake in system level throughput regardless of the used scheduler and number of codes. In Pedestrian A channel the gain of 1Rx equalizer towards Rake 1Rx diminishes along the reduced amount of multipath interference with all schedulers and used code resources. Similarly 2Rx equalizer gains over the 2Rx Rake are halved compared to the gains in Vehicular A channel.

Average cell throughputs in Vehicular A channel are collected to Table 5 and in Pedestrian A channel to Table 6, from which it can be seen that the absolute cell throughputs in Pedesrian A Channel are higher than in Vehicular A channel. This is due to an improved average E_s/N_0's in Pedestrian A channel as compared to Vehicular A channel, as seen in Figures 44 and 45. Due to the increased E_s/N_0's higher *Transport Block Sizes (TBS)* can be allocated, which leads to improved throughput.

TABLE 5 Average cell throughput with different receivers in Vehicular A.

Throughput [kbps] and gain [%]	Round robin		Proportional fair	
	5 codes	10 codes	5 codes	10 codes
Rake 1Rx	1004.3	1196.4	1239.7	1600.5
Rake 2Rx	1657.9	2245.6	1784.3	2512.5
Equ 1Rx	1252.1	1511.4	1544.3	2085.1
Equ 2Rx	2240.3	3161.7	2327.7	3443.9

Rake 2Rx provides bit lower gains in Pedestrian A channel than in Vehicular A, which indicates that cell throughputs in Pedestrian A channel are limited due to the code limitation when receive diversity is used, as can be seen from Figure 46. When the maximum TBS is reached, the higher available CQI's will be transmitted using the same TBS as can be seen from Figure 50, but the transmit

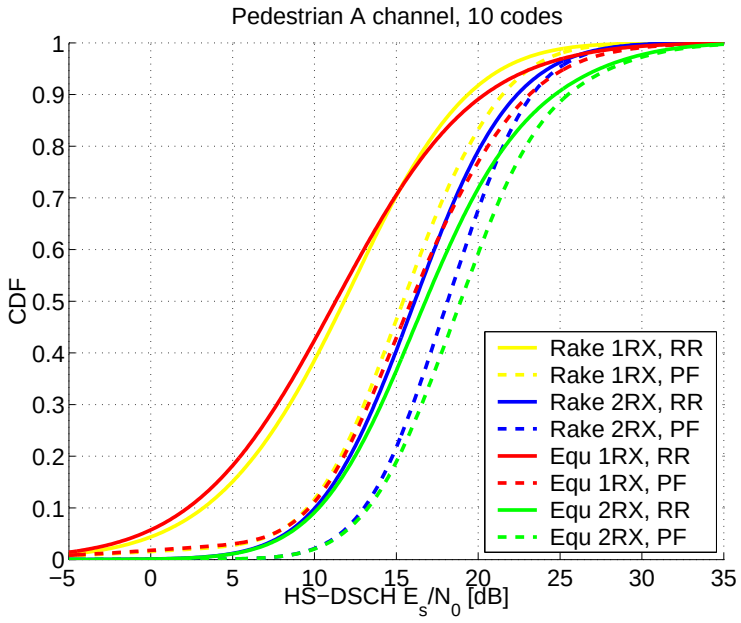

FIGURE 44 HS-DSCH E_s/N_0 of advanced receivers with Round robin and Proportional fair scheduler in Pedestrian A channel when maximum number of HS-DSCH codes is 10.

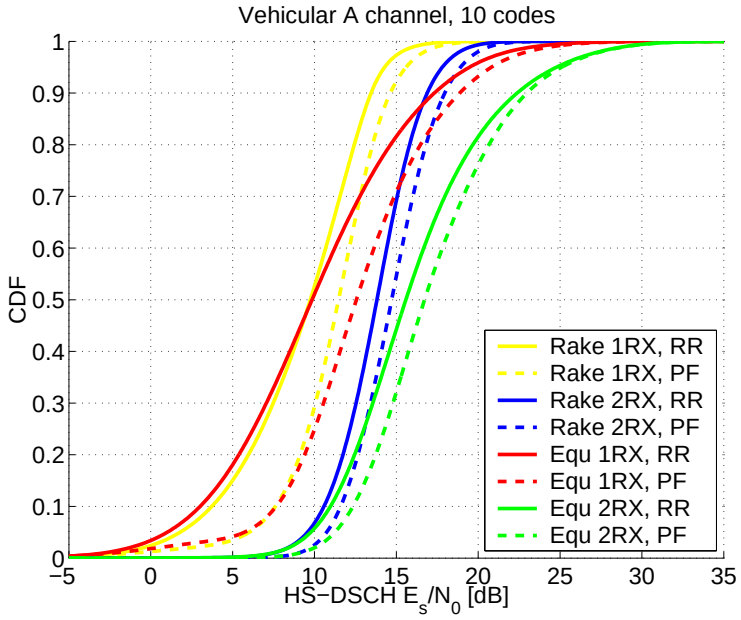

FIGURE 45 HS-DSCH E_s/N_0 of advanced receivers with Round robin and Proportional fair scheduler in Vehicular A channel when maximum number of HS-DSCH codes is 10.

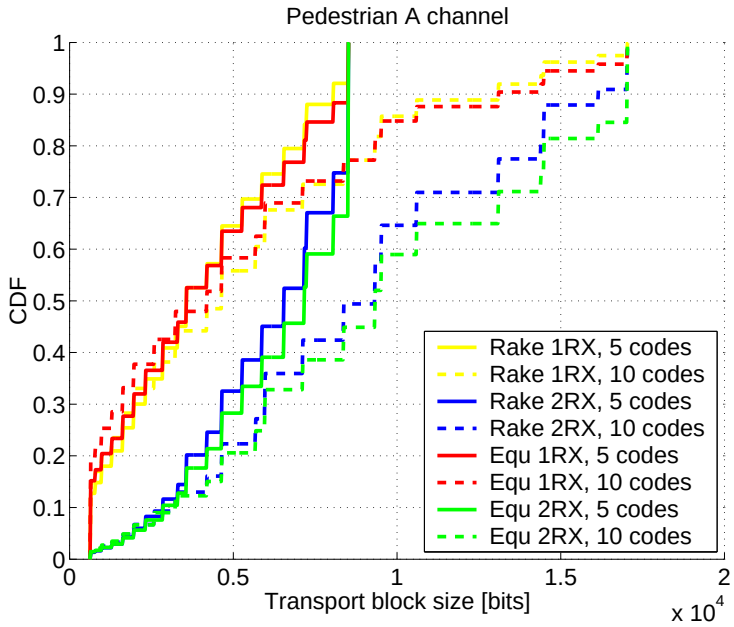

FIGURE 46 Transport block sizes with different receivers with Round robin scheduler in Pedestrian A channel.

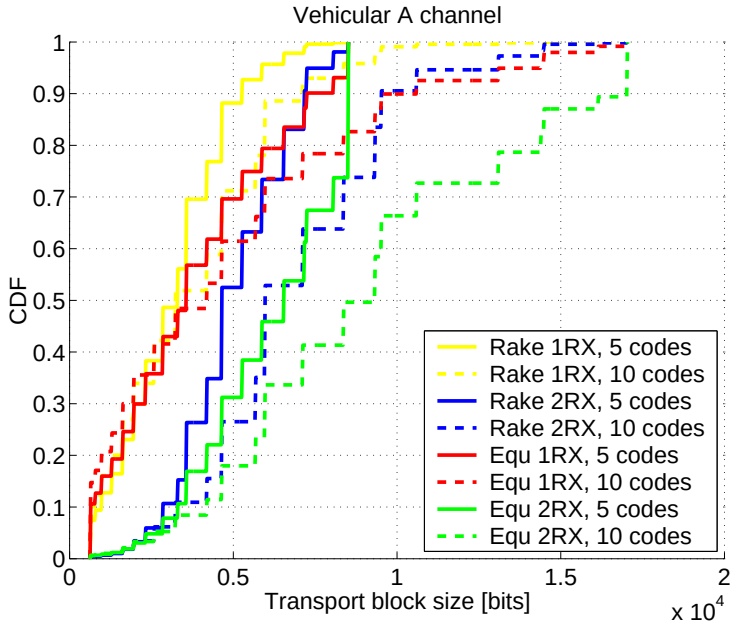

FIGURE 47 Transport block sizes with different receivers with Round robin scheduler in Vehicular A channel.

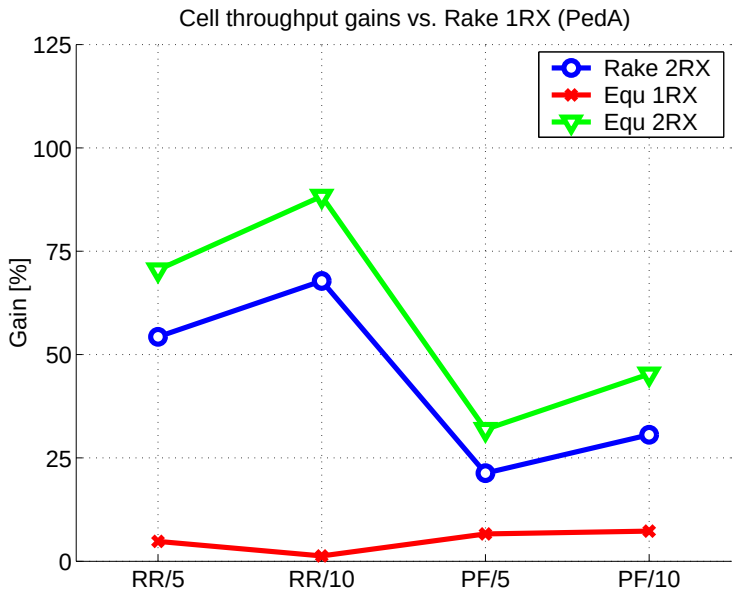

FIGURE 48 Cell throughput gain of advanced receivers in Pedestrian A channel when Round robin (RR) and Proportional fair (PF) schedulers are used with 5 or 10 HS-DSCH codes.

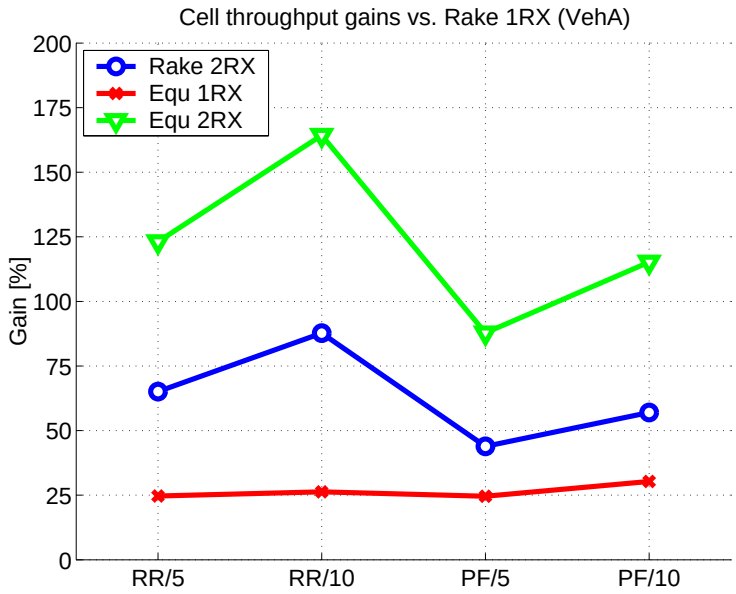

FIGURE 49 Cell throughput gain of advanced receivers in Vehicular A channel when Round robin (RR) and Proportional fair (PF) schedulers are used with 5 or 10 HS-DSCH codes.

TABLE 6 Average cell throughput with different receivers in Pedestrian A.

Throughput [kbps] and gain [%]	Round robin		Proportional fair	
	5 codes	10 codes	5 codes	10 codes
Rake 1Rx	1463.4	1914.6	2044.5	2903.2
Rake 2Rx	2258	3213.3	2480.8	3792.1
Equ 1Rx	1533.7	1938.8	2178.6	3114.9
Equ 2Rx	2495.4	3605.8	2695.8	4217.2

power is reduced causing lower interference to the system. The reduction of transmission power is defined by power offset parameter of the used *Transport Format and Resource Combination (TFRC)*, which are presented in Tables 14 and 15 at the end of this thesis. It should be noted that rather high transmit power is allocated for HSDPA (see appendix 6), thus by allocating lower transmit power for HSDPA operation point in CQI table would be lower and that way bit higher gains could be achievable with receive diversity schemes. Anyhow high transmit power allocation would be realistic for the HSDPA only scenario.

As shown in Figures 52 and 53, the instantaneous bit rate of HS-DSCH versus distance is the highest with an equalizer near the base station where the own cell multipath interference dominates. As the equalizer is able to effectively suppress the own cell interference near the base station, its bit rates are clearly higher than bit rates of Rake which suffers from the multipath interference. As the distance from the base station increases, it is more beneficial to use receiver diversity, which gives protection against fading and the power gain. Closer to the cell borders the throughputs achieved with equalizer and Rake approach to each others, being practically equal with 1Rx schemes. This is expected as the other cell interference starts to dominate over own cell (multipath) interference, reducing the gains attainable from equalization. This leads to a very high difference in equalizer performance in the middle of the cell and at the cell borders.

5.5.3 Effect of the scheduler and code resources

This section considers the effect of a number of HS-DSCH codes and packet scheduling algorithms to cell throughput. Cell throughput gains of 10 codes as compared to 5 codes and gains of PF scheduler as compared to RR scheduler in Vehicular A channel are presented in Table 7 and in Table 8 for Pedestrian A channel.

As the PF scheduler tries to allocate the HS-DSCH to the users with favourable channel quality conditions, the resulted HS-DSCH E_s/N_0 distribution of scheduled users with PF is higher than with RR (see Figure 45) and consequently it allocates on average a higher TBS as can be seen from Figure 47. By replacing the blind RR scheduling with PF gives in each scheme gain varying from 4 % to 23 % with 5 codes. The 1Rx schemes benefit more than 2Rx schemes as their E_s/N_0 (CQI) distribution is wider and similarly the benefit from

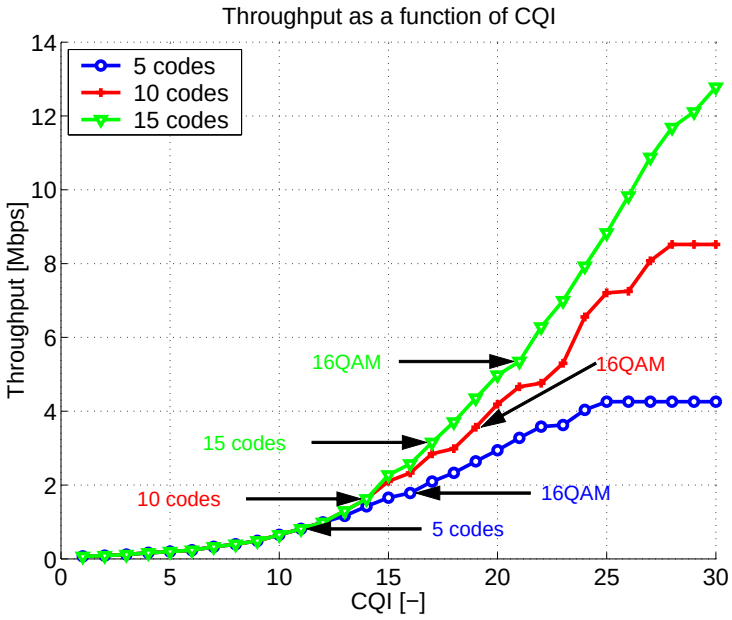

FIGURE 50 Throughput as a function of CQI with 5, 10 and 15 codes.

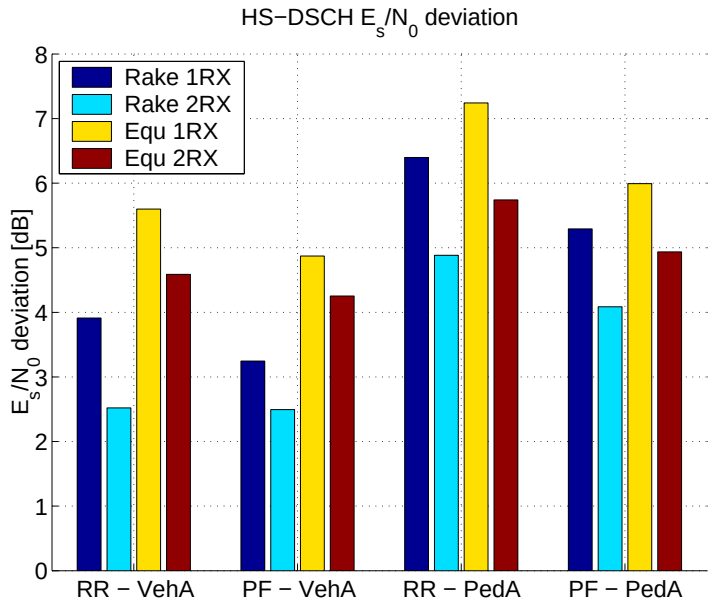

FIGURE 51 Standard deviation of HS-DSCH E_s/N_0 in Pedestrian A and Vehicular A channels.

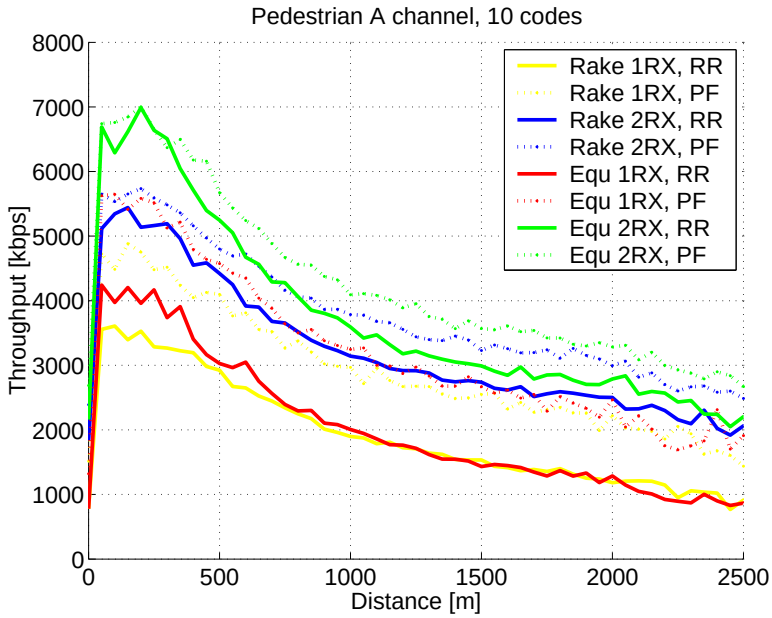

FIGURE 52 Instantaneous bit rate of HS-DSCH as a function of distance in Pedestrian A channel.

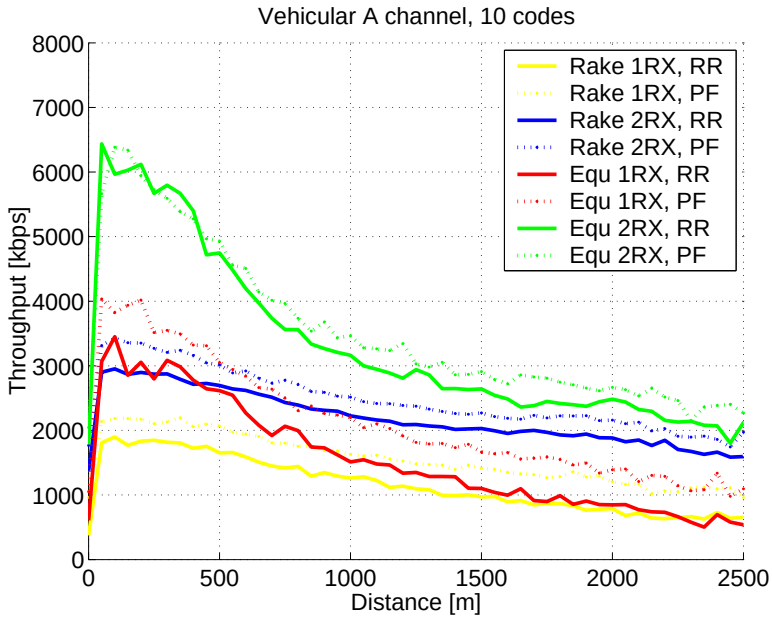

FIGURE 53 Instantaneous bit rate of HS-DSCH as a function of distance in Vehicular A channel.

TABLE 7 Average cell throughput gains of 10 codes and Proportional fair scheduler in Vehicular A.

Throughput gain [%]	Throughput gain of 10 codes		Throughput gain of PF	
	RR	PF	5 codes	10 codes
	5 ⇒ 10	5 ⇒ 10	RR ⇒ PF	RR ⇒ PF
Rake 1Rx	19.1%	29.1%	23.4%	33.8%
Rake 2Rx	35.4%	40.8%	7.6%	11.9%
Equ 1Rx	20.7%	35.0%	23.3%	38.0%
Equ 2Rx	41.1%	48.0%	3.9%	8.9%

PF is slightly larger in Pedestrian A than in Vehicular A. Furthermore, even a higher benefit of PF is seen with 10 codes as the achieved throughput increases considerably when the probability to use higher CQI's is increased. Also the throughput offered by the medium range CQIs is improved as can be seen from Figure 50, which shows the relationship between transport block size and CQI with different number of HS-PDSCH codes. Equalizer gains more from the increased number of available codes than Rake, since the equalizer provides better E_s/N_0's especially in high end as seen from Figure 45 resulting similarly higher CQI's on average.

Another aspect to increase system performance besides the scheduler is a number of supported HS-DSCH codes. Enhancing the system with RR scheduler from 5 to 10 codes gives a gain varying from 19 % to 41 % depending on the receiver scheme. Increasing the code capability of the system increases the throughput dynamics of CQI and this is especially beneficial for receive diversity schemes as they have a higher E_s/N_0's on average than 1Rx schemes as shown in Figures 44 and 45. The benefit from increased code capability is larger in the Pedestrian A channel due to the higher achieved E_s/N_0's.

As the PF scheduler accounts for the individual users' channel conditions in scheduling, highest benefit from PF is achievable when channel variations are high, but not too fast to be able to be traced with CQI reporting messages. Figure 51 presents the standard deviation of HS-DSCH E_s/N_0 in Vehicular A channel with RR and PF schedulers. Without any code limitations it would be predictable that the benefit of PF would be directly proportional to the standard deviation of E_s/N_0 gathered from RR simulations. Except the 2Rx equalizer this is actually the case when using of 10 codes, as can be seen from Table 7, but with 5 codes, equalizer gains are the same magnitude as the gains of Rake with/without receive diversity. This indicates that equalizer performance is limited by the CQI table dynamics, as seen in Figure 47. Higher relative gains could be seen for e.g. increasing CQI table dynamics to 15 codes or lowering transmit power allocation of HSDPA.

A combined benefit from PF and 10 codes is from 50 % to 100 % for each receiver scheme. In Vehicular A the benefit is between 50 % to 66 % for all schemes where as in Pedestrian A, the benefit is nearly 70 % for the receive

diversity schemes and around 100 % for the 1Rx receivers. The improvement is larger for 1Rx schemes as Pedestrian A channel lacks the multipath diversity causing a large E_s/N_0 variation. As the PF scheduler tries to account for the user condition is scheduling the impact of the low Es/N_0 tail is reduced, thereby benefiting more the 1Rx schemes.

TABLE 8 Average cell throughput gains of 10 codes and Proportional fair scheduler in Pedestrian A.

Throughput gain [%]	Throughput gain of 10 codes		Throughput gain of PF	
	RR	PF	5 codes	10 codes
	5 ⇒ 10	5 ⇒ 10	RR ⇒ PF	RR ⇒ PF
Rake 1Rx	30.8%	42.0%	39.7%	51.6%
Rake 2Rx	42.3%	52.9%	9.9%	18.0%
Equ 1Rx	26.4%	43.0%	42.0%	60.7%
Equ 2Rx	44.5%	56.4%	8.0%	17.0%

5.5.4 Relative cell throughput gains

The cell throughputs with full penetration of the advanced receivers are compared to the Rake 1Rx results with RR scheduler and 5 codes and achieved cell throughput gains are presented in Figures 54 and 55. As can be seen from those, using advanced receivers in the network without enhancing the system capabilities (RR and 5 codes) otherwise, the cell throughput can be improved by 25 % with 1Rx equalizer, 65 % with 2Rx Rake and 120 % with 2Rx equalizer. PF gives a clear gain with single antenna receivers when using 5 codes, but with two antenna receivers the gains are only marginal due to the limited dynamic range of CQI. By increasing the number of supported codes from 5 codes to 10 in both Node B and UE with 1Rx receivers, the offered gain in cell throughput (from 20 % to 50 %) is similar as by improving the scheduler in Node B alone. For receive diversity schemes the improvement from increased code capability is larger, giving 120 % to 210 % additional gain compared to the baseline. On the other hand, introducing 10 codes in the system with single antenna receivers, better scheduling is needed to get the most out of the system improvement. With receive diversity the PF scheduler does not give much gain either with 10 codes when compared to the RR. However, when compared to a reference case, Rake 2Rx and equalizer 2Rx with 10 codes and PF scheduler gives remarkable gains in cell throughput. Enhancing Node B with PF scheduler improves the gains offered by advanced receivers with 10 codes to 108 %, 150 % and 243 % for 1Rx equalizer, 2Rx Rake and 2Rx equalizer, respectively. Introducing larger amount of codes and PF scheduler improves the cell throughput offered by 1Rx Rake also by 59 %.

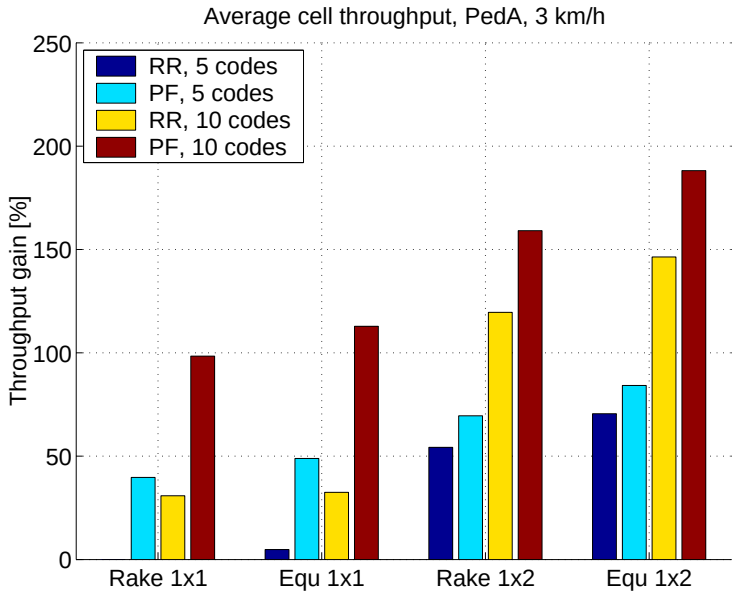

FIGURE 54 Cell throughput gain of different schemes as compared to Rake 1Rx with Round robin in Pedestrian A channel.

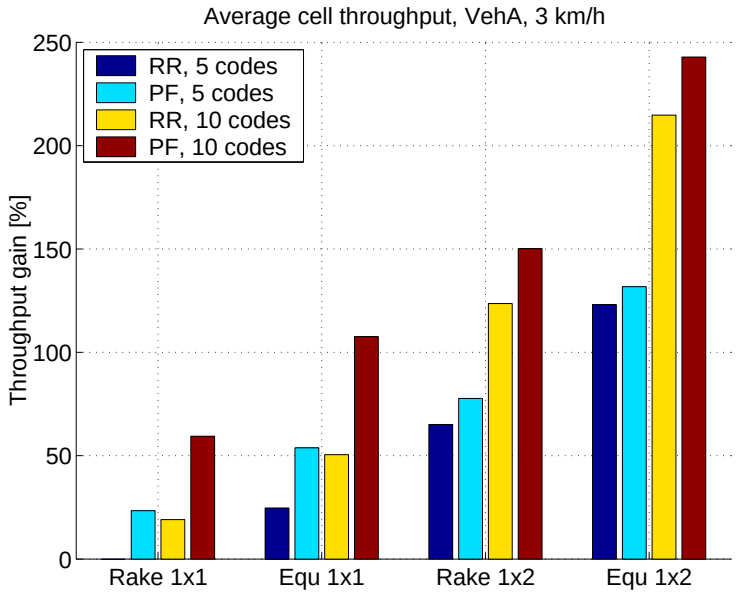

FIGURE 55 Cell throughput gain of different schemes as compared to Rake 1Rx with Round robin in Vehicular A channel.

5.5.5 User throughputs

This section covers the effect of different receiver schemes to user throughput. Different from cell throughput, which is calculated at each TTI, user throughput statistics are gathered when a call is ended. The resulted user throughput is the average bit rate of the ended call i.e. correctly received bits divided by the duration of the call.

User throughput gains of advanced receivers as compared to Rake 1Rx are presented in the Figure 56 from Pedestrian A and in the Figure 57 from Vehicular A channel simulations. As in cell throughput results, receive diversity offers the most benefit for user throughput with RR and 10 codes and again 2Rx equalizer is able to more than double the benefit as compared to Rake 2Rx in Vehicular A. With 1Rx equalizer the average user throughputs are now closer to the throughput offered by 2Rx Rake. It should be noted that the number of users in a scheduling queue affects the user bit rate results. With long queues users are scheduled less frequently, which means that the achieved bit rates are lower than in the case of a shorter queue. The number of users in the queue depends on the performance of the scheduler and the receiver, as can be seen in the Figures 58 and 59. The better the performance of the receiver and scheduler is, the faster the scheduling queue empties and the higher the user bit rates are.

In Pedestrian A channel equalizer gains are much lower compared to Vehicular A as expected due to reduced multipath interference. Especially the gains are lower with a PF scheduler than with RR. As the PF scheduler accounts for the individual users' channel conditions in scheduling, the performance of the Rake 1Rx has already increased, thus the gains of advanced receivers are lower. On the other hand CQI table dynamics starts to limit achievable throughput in Pedestrian A channel as was discussed earlier (see Figure 46) and that way the gains of the different advanced receivers with PF scheduler are clearly lower than with RR.

User throughputs of different receivers in Vehicular A and Pedestrian A channels are also presented in the form of CDF in Figures 60 and 61. It can be seen that a PF scheduler offers higher user bit rates than RR with all receivers and especially it provides clear improvement for the users with low bit rates, thus it can be seen that it improves the fairness of the system. Receive diversity provides protection against fading and power gain, thus there is a lower number of users with low bit rates as compared to 1Rx schemes. However receive diversity schemes are able to provide almost constant improvement for all users. In Vehicular A channel 2Rx Rake provides higher average bit rate and also better coverage as compared to 1Rx equalizer, but 1Rx equalizer is able to provide higher peak data rates.

5.6 Simulations with different receiver penetrations

In reality it would not be the case that all the UE will be employed with the same kind of receiver, thus it would be beneficial to see how cell throughput

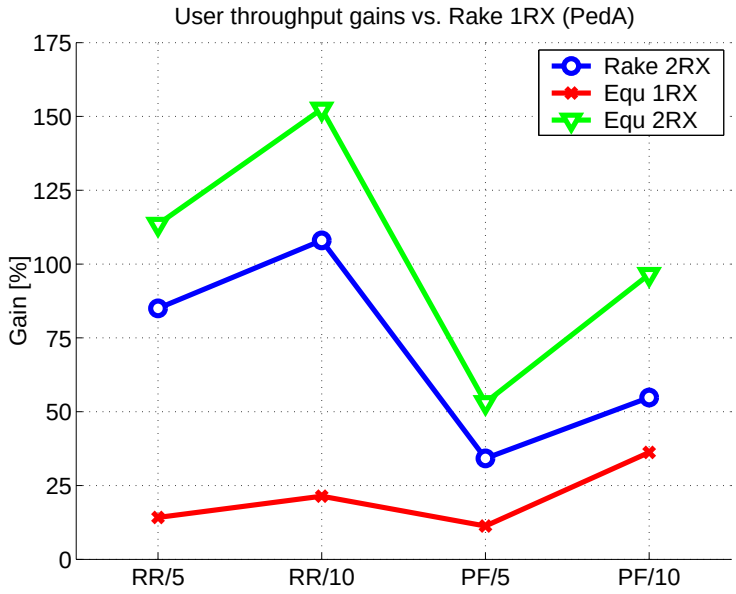

FIGURE 56 User throughput gain of advanced receivers in Pedestrian A channel.

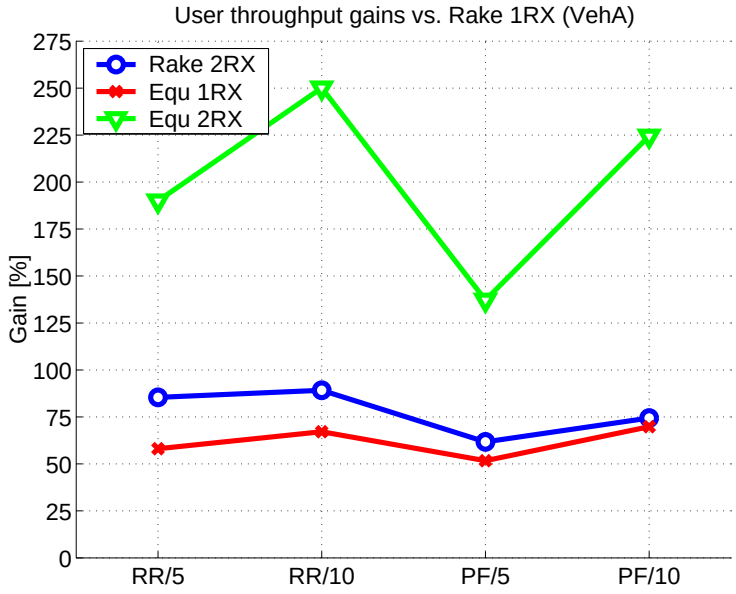

FIGURE 57 User throughput gain of advanced receivers in Vehicular A channel.

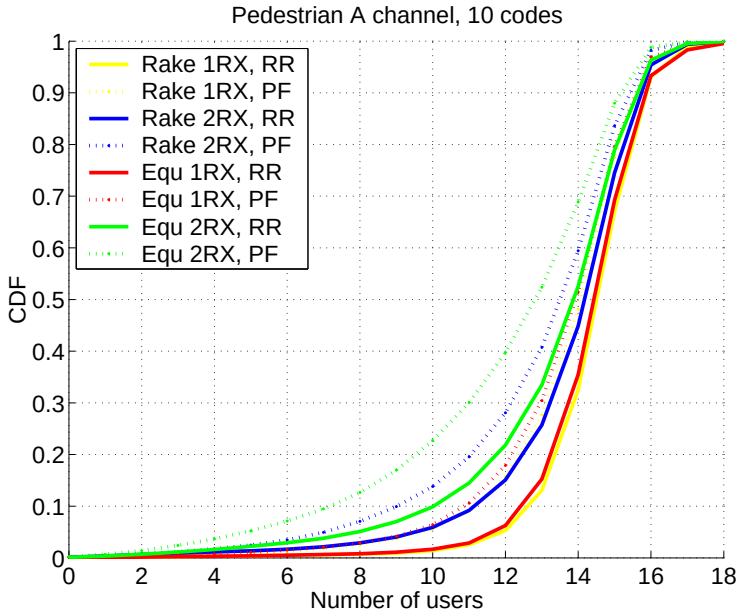

FIGURE 58 Number of HSDPA users per cell in Pedestrian A channel.

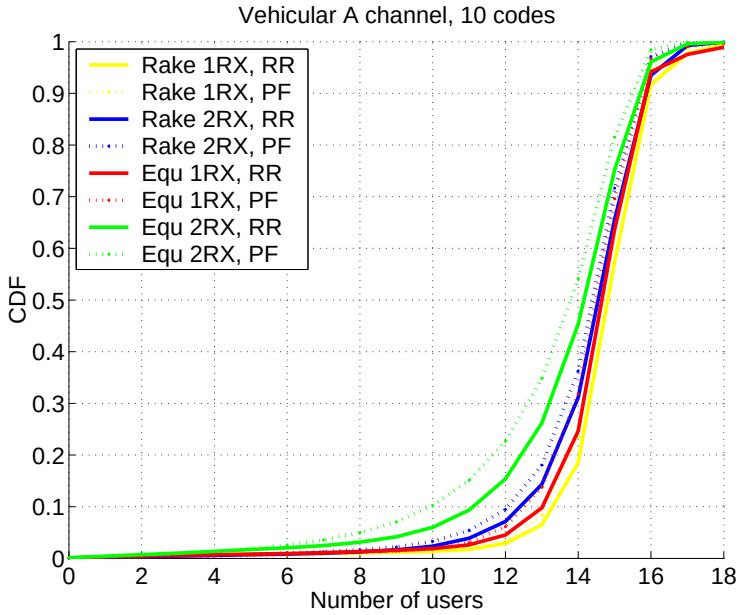

FIGURE 59 Number of HSDPA users per cell in Vehicular A channel.

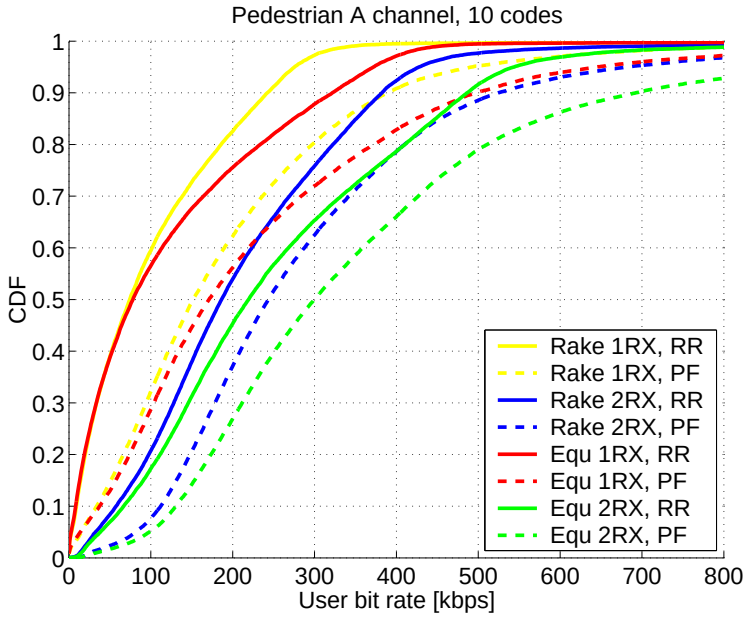

FIGURE 60 User bit rate of different receivers in Pedestrian A channel.

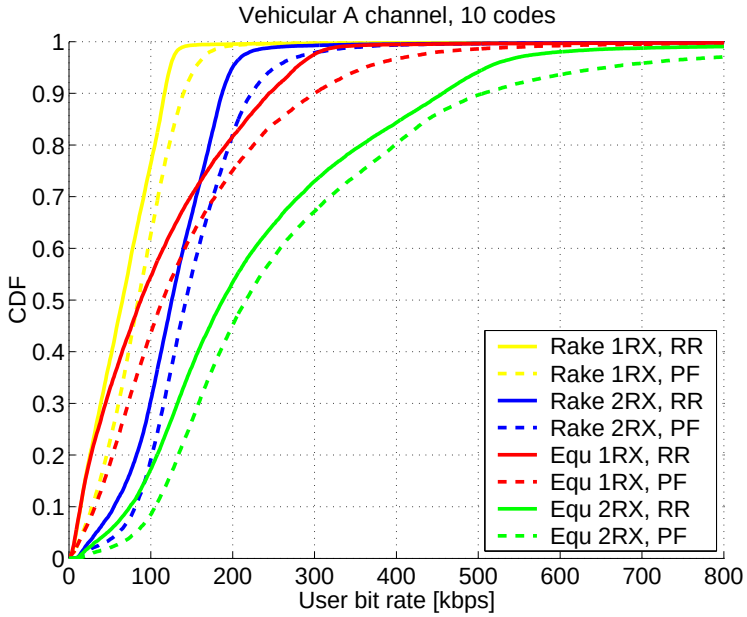

FIGURE 61 User bit rate of different receivers in Vehicular A channel.

behaves when advanced receivers are gradually added to the system with Rake 1Rx receivers and how the fairness of the system with different receivers can be maintained. In this section the effect of different receiver penetrations are studied and simulations are performed with RR and PF schedulers in Vehicular A channel with 3 km/h. Advanced receivers with penetrations of 0%, 30%, 50%, 70% and 100% are compared to Rake 1Rx receiver.

5.6.1 Cell throughput

Figure 62 shows the cell throughputs as a function of a percentage of advanced receivers subscribers and Table 9 shows the gain in cell throughput of different advanced receiver percentages compared to 100% Rake 1Rx penetration. The throughput increases quite linearly as a function of the increasing advanced receiver penetration, already showing enhancement at low advanced receiver penetrations. As can be seen in Table 9 in order to obtain for example a 20% improvement in system performance in terms of cell throughput, the percentage of 2Rx receivers needs to be around 30% of all subscribers. Correspondingly, the initial percentage of 1Rx equalizers has to be at least 70% to achieve a similar gain.

TABLE 9 Average cell throughput gain of advanced receivers over 100% Rake 1Rx penetration.

Initial AR subs. [%]	Round robin			Proportional fair		
	Rake 2Rx	Equ 1Rx	Equ 2Rx	Rake 2Rx	Equ 1Rx	Equ 2Rx
30%	29.7%	6.9%	35.5%	16.5%	8.9%	21.4%
50%	46.0%	10.3%	63.8%	27.8%	14.7%	44.1%
70%	63.1%	21.5%	100.0%	40.0%	20.1%	68.2%
100%	87.7%	26.3%	164.3%	57.0%	30.3%	115.2%

5.6.2 Realized percentage of advanced receiver subscribers

In Figure 64 the actual percentage of advanced receiver users of all HSDPA users admitted to the system are shown as a function of the initial percentage of subscribers using advanced receivers. It can be observed that the realized distribution of advanced receivers in active users is quite close to the distribution among all users, which explains why the improvement in cell throughput behaves coherently over the advanced receiver penetration. The highest difference between initial and realized percentages of advanced receiver users is seen with 2Rx equalizer, which was found to provide the highest throughput in full penetration simulation. Higher throughput will decrease the length of the calls, thus that is the reason for a slight reduction of realized percentages of advanced receivers as compared to the initial percentage.

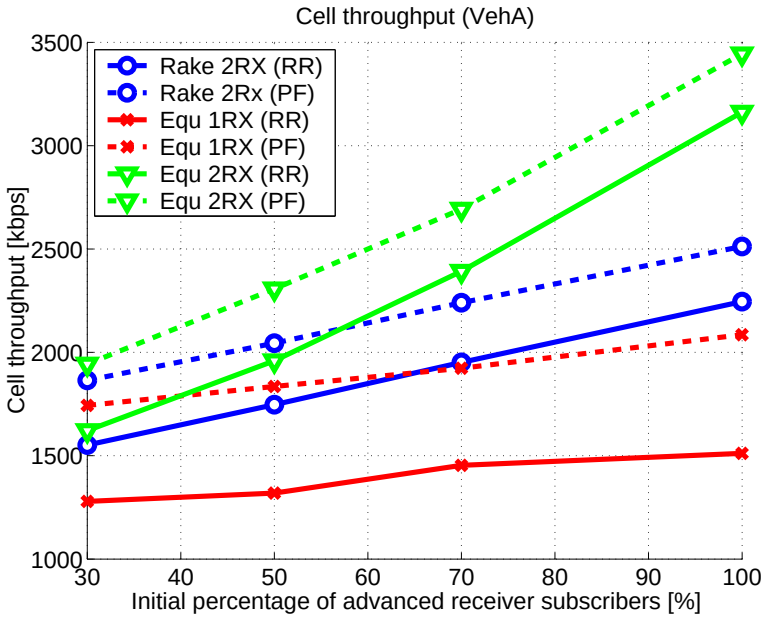

FIGURE 62 Average cell throughput with different advanced receiver user penetrations in Vehicular A channel.

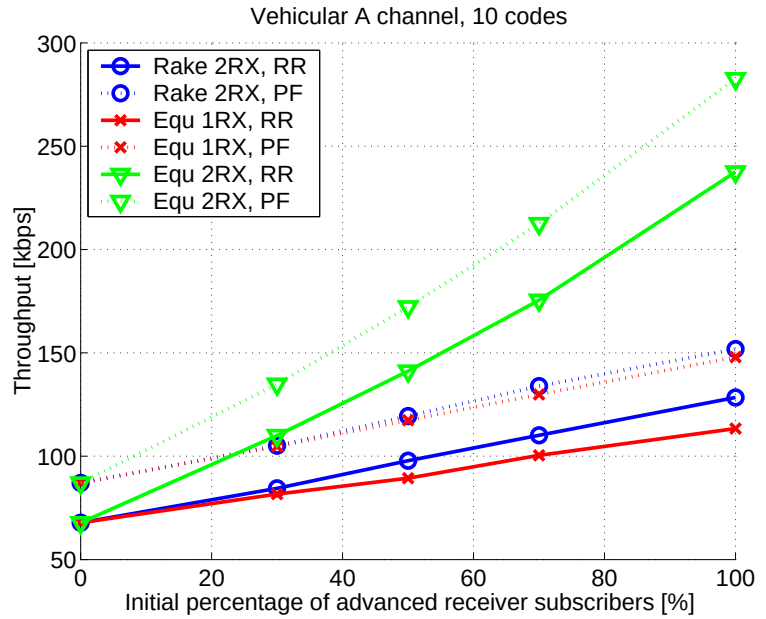

FIGURE 63 Average user throughput with different advanced receiver user penetrations in Vehicular A channels.

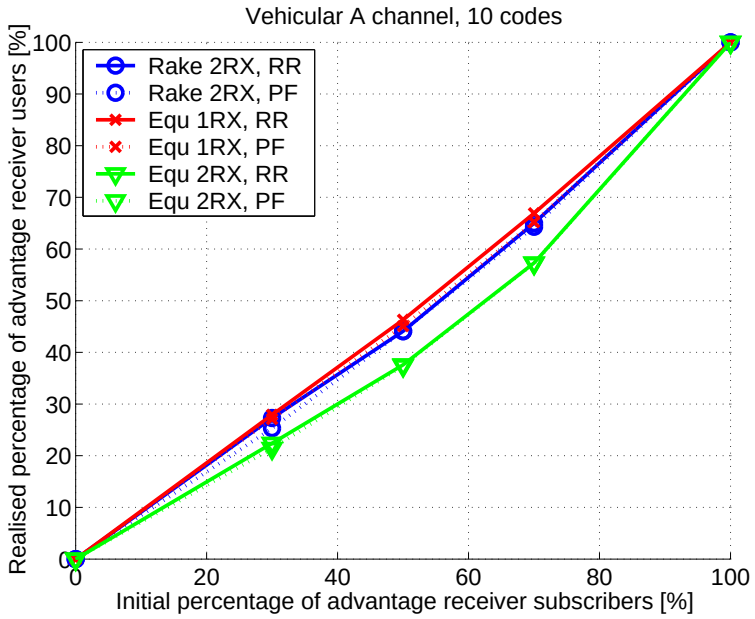

FIGURE 64 Realized percentage of advanced receiver users as a function of initial percentage of advanced receiver subscribers in Vehicular A channel.

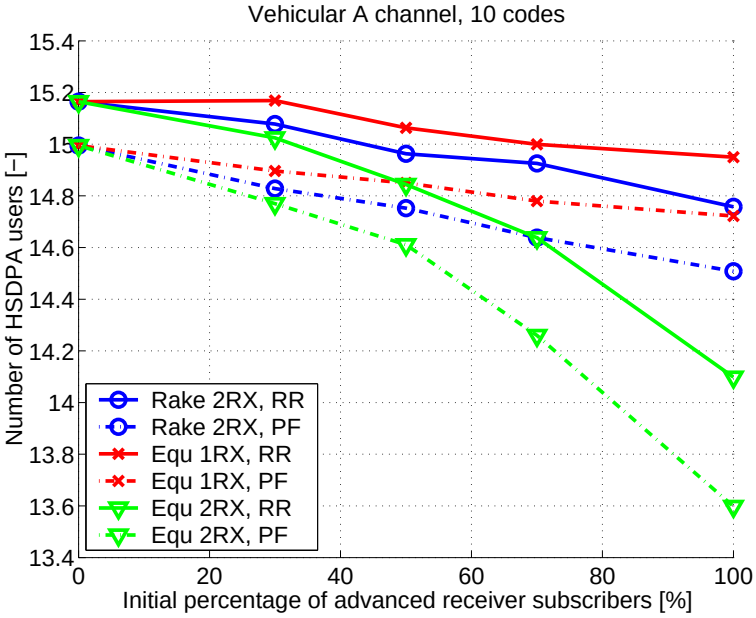

FIGURE 65 Number of users with different advanced receiver penetrations in Vehicular A channel.

5.6.3 User throughput

In Figure 63 average user bit rates of all users are shown including Rake 1Rx users and advanced receiver users. Basically an almost linear increase of user bit rates is seen similarly as in the case of cell throughput when advanced receiver users are gradually added to the system. However, in cell throughput results Figure 62 Rake 2Rx was able to provide clearly higher throughputs that 1Rx equalizers, whereas in user bit rates in Figure 63 Rake 2Rx provides only a minor gain as compared to 1Rx equalizer. As 1Rx equalizer provides improvement especially at the high end of the E_s/N_0 distribution as presented in 45, users close to the base station will experience much higher bit rates than Rake 2Rx users. The user bit rate is saved at the end of each call, thus the bit rate of short calls will dominate in the distribution. Short call are basically the calls with high bit rates, thus as seen in 61 1Rx equalizer clearly provides higher bit rates for e.g. 10 % of the users, but the average is about the same as Rake 2Rx. On the other hand cell throughput is collected in every TTI, thus Rake 2Rx clearly provides higher throughputs than 1Rx equalizer.

Figure 66 presents the average user bit rates for advanced receivers and Figure 67 for Rake receiver respectively. It can be seen that the user throughputs of different penetrations (excluding 0% for each scheme) are quite constant. Especially for PF this indicates that there is good fairness for different users. What is notable is that as the penetration of receive diversity schemes reaches the 70% point, even the average user throughput of Rake users is improved. With high penetration of advanced receiver subscribers the average queue length is slightly decreased (see Figure 65), thus the scheduling frequency of individual users is increased. In addition the scheduling frequency of Rake 1Rx users will be increased with PF scheduler, since to guarantee the fairness of the system the scheduling frequency of the advanced receiver users can be decreased due to the usage of higher transport block sizes.

5.7 Achieved results

In this section the performance of Rake and LMMSE chip-level linear equalizer with/without UE receiver (Rx) diversity was analysed with dynamic network simulations when High Speed Downlink Packet Access (HSDPA) is used. Both HSDPA simulations with single receiver type and with different receiver penetrations were studied in Pedestrian A and Vehicular A channel models. The aim of these simulations was to identify the effect of receive diversity and advanced receivers with different schedulers (Round robin, Proportional fair) on HSDPA system performance. The selected parameters for the system simulations were set to facilitate the comparison i.e. to maintain the activity in a system near to its maximum.

When studied the improvement provided by different receiver schemes with 5 and 10 code capabilities and RR and PF schedulers to cell throughput it was found that receive diversity provides the largest gains with all the used scheduler

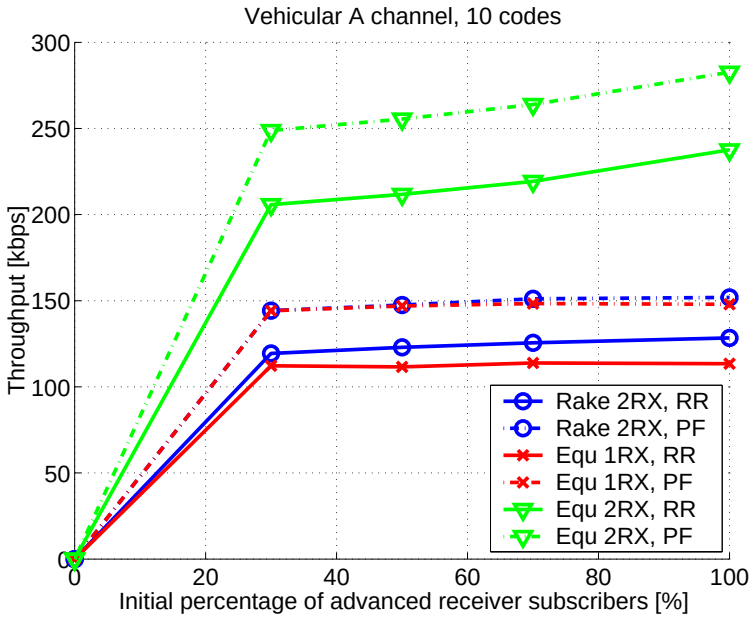

FIGURE 66 Average user throughput of advanced receivers with different advanced receiver user penetrations in Vehicular A channel.

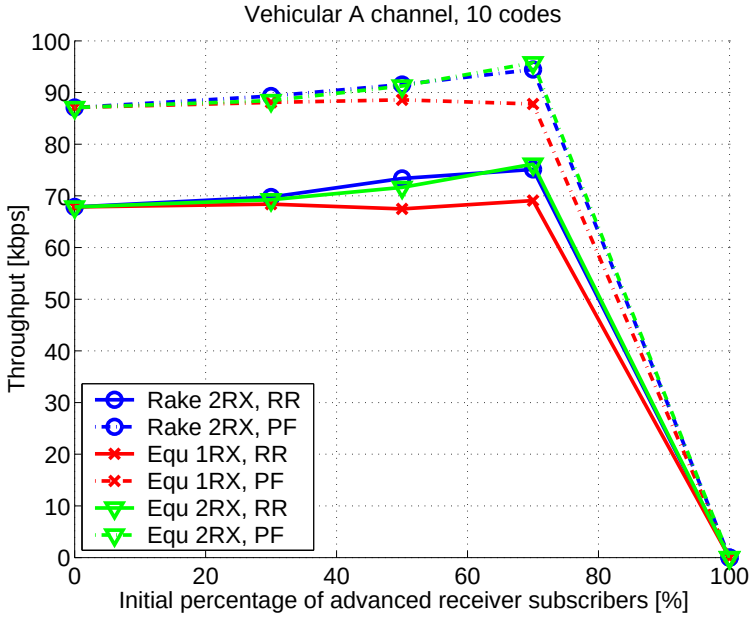

FIGURE 67 Average user throughput of Rake 1Rx with different advanced receiver user penetrations in Vehicular A channel.

or code resource combinations in both channel models. In Vehicular A channel 2Rx Rake provides from 50 % to 90 % gain as compared to 1Rx Rake, which is then doubled by the 2Rx equalizer. 1Rx equalizer provides 25-30 % gain compared to 1Rx Rake in system level throughput regardless of the used scheduler and number of codes. In Pedestrian A channel the gain of 1Rx equalizer towards Rake 1Rx diminishes along the reduced amount of multipath interference with all schedulers and used code resources. Similarly 2Rx equalizer gains over the 2Rx Rake are halved compared to the gains in Vehicular A channel. The absolute cell throughputs in the Pedesrian A channel have increased from Vehicular A channel simulations due to an improved average E_s/N_0's.

The gain achieved through different system improvements was analysed separately for each receiver scheme. By replacing the blind RR scheduling with PF gives in each scheme gain varying from 4 % to 23 % with 5 codes. The 1Rx schemes benefit more than 2Rx schemes as the standard deviation of their E_s/N_0 (CQI) distribution is larger and similarly the benefit from PF is slightly larger in Pedestrian A than in Vehicular A. Furthermore, even a higher benefit of PF is seen with 10 codes as the achieved throughput increases considerably when the probability to use higher CQI's is increased. Also the throughput offered by the medium range CQIs is improved. Equalizer gains more from the increased number of available codes than Rake, since the equalizer provides better E_s/N_0's especially in high end resulting similarly higher CQI's in average.

Other aspects to increase system performance besides the scheduler is the number of supported HS-DSCH codes. Enhancing the system with RR scheduler from 5 to 10 codes gives a gain varying from 19 % to 41 % depending on the receiver scheme. Increasing the code capability of the system increases the throughput dynamics of CQI and this is especially beneficial for receive diversity schemes as they have higher E_s/N_0's in average than 1Rx schemes. The benefit from increased code capability is larger in the Pedestrian A channel due to the fact that the achieved E_s/N_0's are higher.

The combined benefit from PF and 10 codes is from 50 % to 100 % for each receiver scheme. In Vehicular A the benefit is between 50 % to 66 % for all schemes where as in Pedestrian A, benefit is nearly 70 % for the receive diversity schemes and around 100 % for the 1Rx receivers. The improvement is larger for 1Rx schemes as Pedestrian A channel lacks the multipath diversity causing a large E_s/N_0 variation. As PF scheduler tries to account for the user condition is scheduling the impact of the low Es/N_0 tail is reduced, thereby 1Rx schemes benefit from PF scheduler more than 2Rx schemes.

Similarly as in cell throughput results user throughput gains of advanced receivers as compared to Rake 1Rx showed that receive diversity offers the most benefit for user throughput with RR and 10 codes and again 2Rx equalizer is able to more than double the benefit as compared to Rake 2Rx in Vehicular A. With 1Rx equalizer the average user throughputs are now closer to the throughput offered by 2Rx Rake. In Pedestrian A channel equalizer gains are much lower compared to Vehicular A as expected due to reduced multipath interference.

User throughputs of different receivers in Vehicular A and Pedestrian A

channels were also analysed in the form of CDF and it was seen that a PF scheduler offers higher user bit rates than RR with all receivers and especially it provides clear improvement for the users with low bit rates, thus it can be seen that it improves the fairness of the system. Receive diversity provides protection against fading and the power gain, thus there is a lower number of users with low bit rates as compared to 1Rx schemes. However receive diversity schemes are able to provide almost constant improvement for all users. In Vehicular A channel 2Rx Rake provides a higher average bit rate and also better coverage as compared to 1Rx equalizer, but 1Rx equalizer is able to provide higher peak data rates.

When different penetrations of advanced receivers were evaluated it was observed that the benefit in cell throughput increased as a function of the advanced receiver penetration almost linearly. Hence introducing even a small portion of receivers with better performance to the system is beneficial. In order to obtain for example a 20% improvement in system performance in terms of cell throughput, the percentage of 2Rx receivers needs to be around 30% of all subscribers. Correspondingly, the initial percentage of 1Rx equalizers has to be at least 70% to achieve a similar gain.

Based on these studies it can be said that UE receive diversity and equalizer complement each other as these both improve the system performance through two different means. The equalizer provides higher bit rates near the cell centre where the own cell interference can be cancelled, whereas receive diversity improves the throughput at cell border where additional signal energy is required. On the gains attainable through advanced receivers schemes the receive diversity seems to be most prominent. 1x2 equalizer offers the best performance in all cases. As impact of different parameters was evaluated, the amount of superiority of 2Rx Rake over 1Rx equalizer depends on the selected set up.

6 CONCLUSIONS

The main contributions of this thesis are (i) the modeling of dynamic TD-CDMA and WCDMA system level simulator, (ii) TD-CDMA system level performance evaluation, (iii) WCDMA network performance analysis with transmit diversity in dedicated channels and with HSDPA, and (iv) HSDPA network performance with advanced UE receivers. The main findings are summarized in the following.

The performance of TD-CDMA and WCDMA networks and radio resource management algorithms were analysed by the means of dynamic system level simulations. In Chapter 2 implementation and modelling issues related to dynamic TD-CDMA system simulator was discussed and modelling for the TD-CDMA interference, synchronization, handover, power control and dynamic channel allocation were presented. Interface between link and system level tools and the modeled operation environment for TD-CDMA were presented. With the developed system simulator behaviour and performance of TD-CDMA system can be studied in a detailed way.

Concerning the TD-CDMA evaluation different radio resource management algorithms were studied in Chapter 3. TD-CDMA uplink power control is based on several UE made measurements, thus the effect of accuracy of the different measurement was evaluated as well as the convergence of uplink power control in the presence of realistic errors. Up to 500 % gain was seen from the uplink power control in ideal conditions and usage of relative measurements were proposed to improve measurement accuracy. In addition to the uplink studies, downlink power control was also analysed. Downlink power control is based on the similar closed loop power control as WCDMA, but feedback rate is reduced from 1500 Hz to 100 Hz. Different methods were proposed and evaluated to improve downlink power control performance. By using variable step sizes downlink performance was improved up to 52 %. Along with the power control studies evaluation of the usage of the WCDMA type of handover for the TD-CDMA was carried out. The effect of different handover parameters was thoroughly analysed.

Dynamic channel allocation is TDD specific algorithm that has been widely

studied with the theoretical models. In this thesis a slot segregation method was evaluated for the uplink and downlink in the presence of signalling delays and measurement errors. It was found that the need for measurements can be minimized by limiting the inter-cell interference and good system performance can be achieved regardless of signalling delay.

Chapter 4 concentrated on the WCDMA network performance evaluation. Closed Loop Mode 1 and STTD transmit diversity schemes were presented and firstly their performance was analysed on dedicated channels. Closed Loop Mode 1 was found to double the downlink capacity with speech users in low mobility scenario. As the closed loop signalling is not able to follow channel variations with higher speeds Closed Loop Mode 1 performance degrade below 1Tx and STTD already at moderate UE speeds. On the other hand 1Tx provides a rather constant performance with different velocities, since the degradation of the performance of fast power control is compensated with the interleaving gain with high UE speeds. STTD was found to provide slightly better performance than 1Tx.

In the 3GPP Release 5 *High Speed Downlink Packet Access (HSDPA)* was introduced to provide higher peak data rates and improved spectral efficiency. HSDPA concept is introduced in Chapter 4.1 and transmit diversity schemes are analysed with HSDPA. These simulation results clearly indicate that CL Mode 1 has good performance especially in low mobility environments as compared to STTD and 1Tx. With low mobile speed CL Mode 1 is not sensitive to feedback command delay and also a 10 percent feedback error rate has only a minor impact on the overall system performance.

Relative throughput gain of about 30 % was achieved with CL Mode 1 in Pedestrian A channel with Round robin scheduler as compared to 1Tx, while the relative throughput gain is reduced to 26 % when UE speed is increased to 50 km/h. In a multipath environment (Vehicular A) the relative throughput gain is reduced to 18 % and 4 % with 3 and 50 km/h UE speed. Naturally CL Mode 1 performance decreases in moderate and high mobile environments due to fast channel variations.

In Chapter 5 the performance of Rake and LMMSE chip-level linear equalizer with/without UE receive (Rx) diversity was analysed with a dynamic network simulations when HSDPA is used. HSDPA simulations with single receiver type and with different advanced receiver penetrations were studied. The aim of these simulations was to identify the system impact of receive diversity and advanced receivers with different schedulers (Round robin, Proportional fair).

Based on these studies it can be said that UE receive diversity and equalizer complement each other as these both improve the system performance through two different means. The equalizer provides higher bit rates near the cell centre where own cell interference can be cancelled, whereas receive diversity improves the throughput at the cell border where additional signal energy is required. On the gains attainable through advanced receiver schemes the receive diversity seems to be the most prominent. 1x2 equalizer offers the best performance in all cases. As the impact of different parameters was evaluated, the amount of

superiority of 2Rx Rake over 1Rx equalizer depends on the selected set up.

When different penetrations of advanced receivers were evaluated it was observed that the benefit in cell throughput increased as a function of the advanced receiver penetration nearly linearly. Hence introducing even a small portion of receivers with better performance to the system is beneficial. In order to obtain for example a 20% improvement in system performance in terms of cell throughput, the percentage of 2Rx receivers needs to be around 30% of all subscribers. Correspondingly, the initial percentage of 1Rx equalizers has to be at least 70% to achieve a similar gain.

Further research topics include system level performance evaluation of advanced receivers with higher UE speeds, with transmit diversity and with spatial interference reduction (e.g. interference rejection combining). Furthermore more realistic load and traffic models could be considered (e.g. joint simulations of HSDPA and DCH or HSDPA simulations with web browsing and delay sensitive traffic such as VoIP (Voice over IP)).

APPENDIX 1: STATISTICAL CONFIDENCE OF SIMULATION RESULTS

The used dynamic system simulator has been an important tool for the WCDMA system level studies in recent years. In [46] it has been verified and presented on a very detailed level. The statistical confidence of these simulation results are evaluated in this section by using one example test case. Main simulation parameters are presented in Table 6. In this test case Rake 1x1 receiver is used in modified ITU Vehicular A channel. A maximum number of HS-PDSCH codes is 10 and Proportional fair scheduler is used.

For each simulation a seed is given as a parameter to a random number generator. Based on the seed a random starting position and direction of movement is generated for each UE. Also start times of calls and their duration will change when changing the seed. In addition to this there are several random numbers used in the simulation (e.g. measurement error for CQI) which will change if the seed is changed. All the simulation results depend on different random processes during the simulation run and the results are reproducible with a certain accuracy for a specified level of confidence.

An interval estimation can be used to define a confidence interval, which means that the sample, ϕ, is within a defined interval with a certain probability i.e.

$$P(a \leq \phi \leq b) = 1 - \alpha, \tag{.1}$$

where the interval $[a, b]$ is a $(1-\alpha) \cdot 100\%$ confidental interval of ϕ. A probability that the ϕ is not within the interval is α. When the number of samples $n \geq 30$ the standardized normal distribution $N(0, 1)$ can be used to define a confidential interval, which is

$$(\bar{x} - z_{\alpha/2} \cdot \frac{s}{\sqrt{n}}, \bar{x} + z_{\alpha/2} \cdot \frac{s}{\sqrt{n}}), \tag{.2}$$

where $\bar{x}$ is the average value, $z_{\alpha/2}$ is critical value taken from the standardized normal distribution $N(0, 1)$, s is standard deviation and n is number of samples i.e. number of simulations.

The confidence interval can be used to evaluate the statistical confidence of the simulation results and in this analysis average cell throughput, HS-DSCH E_s/N_0 and user bit rate are taken into account. Average cell throughput is collected from all the sectors in simulation area during the whole simulation time. Average HS-DSCH E_s/N_0 is collected from all the mobiles during the whole simulation time. Average user bit rate is calculated at the end of each call i.e it is the number of transmitted bits divided by the users active time which is running whenever a user data buffer is not empty.

The simulation results from $n = 35$ simulation runs with the different random generator seeds are presented in Table 10.

TABLE 10 Simulation results from 35 simulations with different seeds.

Cell throughput [kbps]	HS-DSCH E_s/N_0 [dB]	User bit rate [kbps]
1719.937459	12.10689557	219.1948777
1734.096951	12.13662105	221.7476474
1735.700184	12.14683535	218.5812453
1728.460725	12.12786459	218.4653544
1703.069397	12.05371926	219.747321
1709.580855	12.09004347	221.6856656
1746.418434	12.19140943	217.8321447
1721.658673	12.11302598	220.0363123
1698.94725	12.04222502	219.6214137
1696.816757	12.04973254	221.9957756
1702.628338	12.05278651	220.9146819
1734.261251	12.16600891	220.077911
1717.968636	12.11362091	219.5328917
1722.537591	12.12131865	218.29857
1715.20638	12.08396587	219.6474874
1735.463172	12.16647244	219.9561996
1697.248821	12.04769501	218.3409553
1682.129065	11.99838109	222.270825
1698.419881	12.05546932	219.7015051
1747.59777	12.18683866	221.510384
1733.179603	12.16673703	222.9163185
1722.711415	12.12707489	220.6494865
1728.36639	12.1245529	217.45105
1756.376728	12.22471803	218.9333912
1716.79052	12.06999428	222.4741683
1740.727275	12.18058765	220.4404591
1738.256125	12.17787311	224.3152147
1742.831374	12.16308634	220.0754995
1711.037396	12.08309655	220.0759938
1733.408844	12.16849011	218.021073
1721.655412	12.13423358	217.3590205
1749.171802	12.1939739	220.0624443
1710.225075	12.0792357	217.6435098
1678.730244	11.9805757	223.9951824
1693.250493	12.03434518	219.5472933

Confidence intervals of 90 %, 95 % and 99 % are presented in Table 11 and concerning the cell throughputs they are ± 0.32 %, ± 0.38 % and ± 0.50 % respectively.

TABLE 11 Statistical confidence interval.

Variable	90 %	95 %	99 %
Cell throughput	± 0.32 %	± 0.38 %	± 0.50 %
HS-DSCH E_s/N_0	± 0.14 %	± 0.16 %	± 0.22 %
User bit rate	± 0.23 %	± 0.27 %	± 0.35 %

APPENDIX 2: SIMULATION PARAMETERS

DPCH simulations

TABLE 12 Common simulation parameters for DPCH simulations.

Parameter	Value
Cellular layout	Hexagonal cell grid
Cell radius	933 m
UE speed	3, 50 and 120 km/h
Antenna pattern	Horizontal iid pattern similar to [113]
CPICH power	33 dBm
Std. deviation of slow fading	8 dB
Carrier frequency	2000 MHz
Minimum coupling loss	70 dB
BS antenna gain	14 dB
UE antenna gain	0 dB
Noise power for DL	-100.1 dB
BS Tx power per link	33 dBm
BS total Tx power	43 dBm
Dynamic range	30 dB
Maximum active set size	3
Candidate set size	8
Window add	1 dB
Window drop	3 dB
Window replace	2 dB
HO measurement window length	20 samples i.e. 200 ms
Frame length	10 ms i.e 15 slots
Interleaving period	20 ms
BLER target	0.01
Call arrival rate	0.001389 calls/second/terminal
Minimum call length	1 s
Average call length	120 s
Service	Speech service (12.2 kbps)
Channel models	Mod. ITU Vehicular A and Pedestrian A, where delay between paths equals at least 1 chip-time
CL Mode 1 feedback bit error rate	4% and 10%
CL Mode 1 feedback delay	1 slots
CL Mode 1 antenna verification	Ideal

Advanced receiver simulations

Table 13 Parameters for HSDPA simulations with advanced receivers.

Parameter	Value
Cellular layout	Hexagonal cell grid, 7 Node B's and 21 sectors, wrap-around
Cell radius	933 m, BS-to-BS distance 2 800 m.
UE speed	3 km/h
CPICH power	33 dBm
Std. deviation of slow fading	8 dB
Correlation between sectors	1.0
Correlation between BSs	0.5
Correlation distance of slow fading	50 m
Carrier frequency	2000 MHz
Minimum path loss	70 dB
Antenna pattern	Horizontal iid pattern similar to [113]
BS antenna gain	18 dB
Antenna front to back ratio	-20 dB
UE number of RAKE fingers	8 for 1 Rx and 16 for 2 Rx
UE DPCH receiver	RAKE
UE HS-SCCH receiver	Always decoded
UE HS-DSCH receiver	RAKE and LMMSE
Noise power for DL	-100.1 dB
Noise power for UL	-103.1 dB
BS Tx power per link	33 dBm
BS total Tx power	43 dBm
UE Tx power max	21 dBm
P Tx Target	40 dBm
P Tx Threshold	15 W
P Rx Target	-97.1 dBm
P Rx Threshold	-96.1 dBm
Dynamic range	30 dB
Max active set size	3
Window add	1.5 dB
Window drop	2.5 dB
Window replace	2 dB
Add timer	100 ms
Drop timer	640 ms
Replace timer	100 ms
Frame length	10 ms i.e 15 slots
HSDPA sub-frame	2 ms i.e. 3 slots
Power resource for HS-DSCH	14 W
Code resource for HS-DSCH	5 and 10 with SF = 16
Max number of HSDPA users	16 users/cell

HSDPA RLC PDU size	480 bits
Packet scheduling algorithm	Round robin in time, Proportional fair and Max C/I
Initial throughput value for PF	64 bits/TTI, corresponds to 32 kbps i.e. 32 kbit/s / 500 TTI/s = 64 bits/TTI
Forgetting factor for PF	0.005
Initial Scheduling Delay	10 TTI's
Number of HS-SCCH per cell	1
PC method for HS-SCCH	Fixed power used for all HS-SCCH
Outer-loop PC for HS-SCCH	Not used
CQI in One-Way SHO	2 TTI's
CQI in SHO	2 TTI's
CQI Averaging Window	1 TTI
CQI Error Std	1.5 dB
CQI Delay	1 TTI
Error probability for CQI	0
Used Redundancy Version	Chase combining
Max number of retransmissions	4
Ack/Nack signaling delay	8 slots
Minimum Inter TTI Interval	1 TTI
Number Of SAW channels	6
Number of subscribers	28000 i.e offered load of 6 Mbps
Simulation time	6 minutes i.e. 540 000 slots
Service	Modified version of web traffic model from [128] (No reading time)
Admission control	Based on UL/DL power targets and thresholds.
Channel models	Mod. ITU Vehicular A and Pedestrian A, where delay between paths equals at least 1 chip-time
Pedestrian A tap gains	[-0.2; -13.0]
Vehicular A tap gains	[-3.1; -5.0; -10.4; -13.4; -13.9; -20.4]

APPENDIX 3: TFRC TABLES

TABLE 14 Throughput optimized CQI TFRC table for 5 codes

CQI No.	Transport block size [bits]	Codes	Modulation	Power offset
1	137	1	QPSK	0
2	173	1	QPSK	0
3	233	1	QPSK	0
4	325	1	QPSK	0
5	396	1	QPSK	0
6	466	2	QPSK	0
7	650	2	QPSK	0
8	792	2	QPSK	0
9	975	3	QPSK	0
10	1300	4	QPSK	0
11	1625	5	QPSK	0
12	1980	5	QPSK	0
13	2327	5	QPSK	0
14	2849	5	QPSK	0
15	3319	5	QPSK	0
16	3565	5	16QAM	0
17	4189	5	16QAM	0
18	4664	5	16QAM	0
19	5287	5	16QAM	0
20	5887	5	16QAM	0
21	6554	5	16QAM	0
22	7168	5	16QAM	0
23	7251	5	16QAM	0
24	8074	5	16QAM	0
25	8519	5	16QAM	0
26	8519	5	16QAM	-1
27	8519	5	16QAM	-2
28	8519	5	16QAM	-3
29	8519	5	16QAM	-4
30	8519	5	16QAM	-5

TABLE 15 Throughput optimized CQI TFRC table for 10 codes

CQI No.	Transport block size [bits]	Codes	Modulation	Power offset
1	137	1	QPSK	0
2	173	1	QPSK	0
3	233	1	QPSK	0
4	325	1	QPSK	0
5	396	1	QPSK	0
6	466	2	QPSK	0
7	650	2	QPSK	0
8	792	2	QPSK	0
9	975	3	QPSK	0
10	1300	4	QPSK	0
11	1625	5	QPSK	0
12	1980	5	QPSK	0
13	2600	8	QPSK	0
14	3250	10	QPSK	0
15	4207	10	QPSK	0
16	4655	10	QPSK	0
17	5697	10	QPSK	0
18	5974	9	QPSK	0
19	7130	10	16QAM	0
20	8378	10	16QAM	0
21	9328	10	16QAM	0
22	9517	9	16QAM	0
23	10597	9	16QAM	0
24	13108	10	16QAM	0
25	14411	10	16QAM	0
26	14503	10	16QAM	0
27	16148	10	16QAM	0
28	17039	10	16QAM	0
29	17039	10	16QAM	-1
30	17039	10	16QAM	-2

YHTEENVETO (FINNISH SUMMARY)

Tämän tutkimuksen tavoitteena on analysoida UMTS:n radioverkon suorityskykyä. UMTS:n radioverkon TDD-tekniikka perustuu yhdistettyyn aika- ja koodijakoiseen monikäyttöön, josta käytetään yleisesti lyhennettä TD-CDMA. UMTS radioverkon FDD-tekniikka perustuun laajakaistaiseen koodijakoiseen monikäyttöön ja siitä käytetään lyhennettä WCDMA.

TDD-tekniikan analyysi keskittyy kolmeen tärkeään radioresurssien hallinta-algoritmiin: tehonsäätö, solun vaihto ja dynaaminen kanavan varaus. Tehonsäädön toimintaa tutkitaan sekä tukiasemalta matkapuhelimelle että matkapuhelimelta tukiasemalle tapahtuvalle tiedonsiirrolle.

WCDMA-tekniikkaan kehitetty solunvaihtoalgoritmi sovitetaan tässä tutkimuksessa TD-CDMA käyttöön ja sen suorituskykyä tutkitaan erilaisilla parametreillä sisätilaympäristössä.

Dynaaminen kanavanvaihtoalgoritmi on erityinen TDD tekniikkaan tarvittava algoritmi, joka voidaan jakaa hitaaseen (S-DCA) ja nopeaan (F-DCA) kanavanvaihtoon. Hitaalla kanavanvaihtoalgoritmilla jaetaan resursseja tukiasemien käyttöön ja vastaavasti nopealla kanavanvaihtoalgoritmilla jaetaan resursseja eri puheluille. Tässä tutkimuksessa keskitytään nopean kanavanvaihtoalgoritmin toimintaan erilaisilla hitaan kanavanvaihtoalgoritmin asetuksilla.

FDD-tekniikan tutkimukset jakautuvat kahteen osaan: kahden antennin lähetysdiversiteetti ja kehittyneet vastaanottimet. Lähetysdiversiteettitekniikoiden suorityskykyä tutkitaan ensin käyttäjäkohtaisilla kanavilla ja sen lisäksi jaetulla kanavalla, kun käytetään suuria bittinopeuksia HSDPA-tekniikan avulla. Tutkimukset keskittyvät tila-aika koodiin perustuvaan avoimen silmukan lähetysdiversiteettiin ja suljetun silmukan lähetysdiversiteettitekniikkaan, jossa matkapuhelin raportoi jatkuvasti kanavatilanteen tukiasemalle. Lähetysdiversiteettitekniikoiden suorityskykyä verrataan yhden antennin lähetykseen.

Kehittyneistä vastaanottimista tässä tutkimuksessa keskitytään lineaariseen MMSE korjaimeen ja vastaanottodiversiteettiin. Niitä verrataan perinteiseen Rake vastaanottimeen, kun käytössä on HSDPA tekniikan mahdollistamat suuret bittinopeudet. Tutkimukset perustuvat dynaamisiin systeemisimulointeihin ja ensin tutkitaan tilannetta, jossa kaikka vastaanottimet ovat samanlaisia. Sen jälkeen tutkimus etenee realistisempaan suuntaan, kun kehittyneiden vastaanottimien osuutta verkossa vaihdellaan.

REFERENCES

[1] http://www.3gpp.org.

[2] http://www.3gpp2.org.

[3] Siavash M. Alamouti. A simple transmit diversity technique for wireless communications. *IEEE Journal on selected areas in communications*, 16(8):1451–1458, October 1998.

[4] Pablo Ameigeiras, Jeroen Wigard, and Preben Mogensen. Performance of packet scheduling methods with different degree of fairness in HSDPA. In *IEEE Vehicular Technology Conference (VTC'04 - Fall)*, Los Angeles, USA, September 2004.

[5] A. Assalini, M. Borgo, and S. Pupolin. Dynamic channel allocation optimization using a closed loop power control in CDMA TDD systems. In *The 5th International Symposium on Wireless Personal Multimedia Communications*, pages 946–950, October 2002.

[6] Kevin L. Baum, Teresa A. Kostas, Philippe J. Sartori, and Brian K. Classon. Performance characteristics of cellular systems with different link adaptation strategies. *IEEE Transactions on Vehicular Technology*, 52(6):1497 – 1507, November 2003.

[7] E Biglieri, J Proakis, and S Shamai. Fading channels; information-theoretic and communications aspects. *IEEE Transactions on Information Theory*, 44(6):2619–2692, October 1998.

[8] Bjørn A. Bjerke, Zoran Zvonar, and John G. Proakis. Antenna diversity combining schemes for WCDMA systems in fading multipath channels. *IEEE Transactions on Wireless Communications*, 3(1):97 – 106, January 2004.

[9] M. Canales, A. Valdovinos, J.R. Gallego, and F. Gutierrez. Performance analysis of downlink transmit diversity system applied to the UTRA FDD mode. In *IEEE 7th International Symposium on Spread-Spectrum Technologies & Applications (ISSSTA)*, Prague, Czech Republic, September 2002.

[10] Américo Correia, Ari Hottinen, and Risto Wichman. Space-time transmitter diversity schemes for wideband CDMA. In *IEEE Vehicular Technology Conference (VTC'00 - Fall)*, pages 313–317, Boston, USA, September 2000.

[11] Anand G. Dabak, Srinath Hosur, Tim Schmidl, and Chaitali Sengupta. A comparison of the open loop transmit diversity schemes for third generation wireless systems. In *IEEE Wireless Communications and Networking Conference (WCNC)*, pages 437–442, Chicago, USA, September 2000.

[12] E. Damosso and L. M. Correia (editors). Digital mobile radio towards future generation systems. Technical report, COST231 Final report, 1999.

[13] Arnab Das, Krishna Balachandran, Farooq Khan, Ashwin Sampath, and Hsuan-Jung Su. Network controlled cell selection for the high speed downlink packet access in UMTS. In *IEEE Wireless Communications and Networking Conference (WCNC 2004)*, pages 1975 – 1979, Atlanta, USA, March 2004.

[14] Arnab Das, Farooq Khan, Ashwin Sampath, and Hsuan-Jung Su. Design and performance of downlink shared control channel for HSDPA. In *IEEE International Symposium on Personal, Indoor and Mobile Radio Communications (PIMRC)*, pages 1088 – 1091, Lisbon, Portugal, September 2002.

[15] Martin Döttling, Bernhard Raaf, and Jürgen Michel. Efficient channel quality feedback schemes for adaptive modulation and coding of packet data. In *IEEE Vehicular Technology Conference (VTC'04 - Fall)*, Los Angeles, USA, September 2004.

[16] Eva Englund, Ke Wanz Helmersson, Magnus Persson, Maria Samuelsson, and Stefan Parkvall. Impacts of higher order modulation on HS-DSCH system performance. In *Proc. IEEE Vehicular Technology Conference (VTC'03-Spring)*, pages 2172 – 2176, Jeju, South Korea, April 2003.

[17] Riaz Esmailzadeh, Masao Nakagawa, and Essam A. Sourour. Time-division duplex CDMA communications. *IEEE Personal Communications*, 4(2):51–56, April 1997.

[18] Frank Frederiksen and Troels Emil Kolding. Performance and modeling of WCDMA/HSDPA transmission/H-ARQ schemes. In *IEEE Vehicular Technology Conference (VTC) 2002 Fall*, pages 472–476, Vancouver, Canada, September 2002.

[19] Pål Frenger, Stefan Parkvall, and Erik Dahlman. Performance comparison of HARQ with chase combining and incremental redundancy for HSDPA. In *IEEE Vehicular Technology Conference (VTC) 2001 Fall*, pages 1829–1833, Atlantic City, USA, September 2001.

[20] Noriyuki Fukui. Study of channel quality feedback in UMTS HSDPA. In *IEEE International Symposium on Personal, Indoor and Mobile Radio Communications (PIMRC)*, pages 336 – 340, Beijing, China, September 2004.

[21] Amitava Ghosh, Rupeeput Ratusirk, Colin Frank, Robert Love, Ken Stewart, and Eoin Buckley. Control channel design for high speed downlink shared channel for 3GPP W-CDMA, rel-5. In *Proc. IEEE Vehicular Technology Conference (VTC'03 - Spring)*, pages 2085 – 2089, Jeju, South Korea, April 2003.

[22] M. Gudmundson. Correlation model for shadow fading in mobile radio systems. *IEEE Electronics Letters*, 27(23):2145–2146, November 1991.

[23] Yile Guo and Hemant Chaskar. Class-based quality of service over air interface in 4G mobile networks. *IEEE Communications Magazine*, pages 132 – 137, March 2002.

[24] Martin Haardt, Anja Klein, R Koehn, S Oestreich, M Purat, V Sommer, and T Ulrich. The TD-CDMA based UTRA TDD mode. *IEEE Journal on Selected Areas in Communications*, 18(8):1375–1385, August 2000.

[25] H. Haas, B. Wegmann, and S. Flanz. Interference diversity through random time slot opporing (ROT) in a cellular TDD system. In *IEEE International Symposium on Personal, indoor, and mobile radio communications*, pages 1384–1388, Beijing, China, September 2002.

[26] Harald Haas, , B. Wegmann, and S. Flanz. Interference diversity through random time slot opposing (RTO) in a cellular TDD system. In *IEEE Vehicular Technology Conference 2002 Fall (VTC 2002 Fall)*, volume 3, pages 1384–1388, Vancouver, Canada, September 2002.

[27] Harald Haas, P.K. Jain, and B. Wegmann. Capacity improvement through random timeslot opposing (RTO) algorithm in cellular TDD systems with asymmetric channel utilisation. In *IEEE Symposium of Personal, Indoor and Mobile Radio Communications (PIMRC 2003)*, volume 2, pages 1790–1794, Beijing, China, September 2003.

[28] Harald Haas, Steve Laughlin, and Gordon. J. R. Povey. A novel interference resolving algorithm for the TDD TD-CDMA mode in UMTS. In *IEEE International Symposium on Personal, indoor and mobile radio communications (PIMRC 2000)*, volume 2, pages 1231–1235, London, UK, September 2000.

[29] Harald Haas and Steven Laughlin. A novel channel assignment approach in TDMA/CDMA-TDD systems. In *IEEE International Symposium on Personal, Indoor and Mobile Radio Communications (PIMRC)*, volume 2, pages E–142–E–146, San Diego, USA, October 2001.

[30] Harald Haas and Steven Laughlin. A novel decentralised DCA concept for a TDD network applicable for UMTS. In *IEEE Vehicular Technology Conference 2001 Spring (VTC 2001 Spring)*, volume 2, pages 881–885, Rhodes, Greece, September 2001.

[31] Harald Haas, Steven Laughlin, and Gordon J. R. Povey. The effects of inter-system interference in UMTS at 1920 MHz. In *IEE International Conference on 3G Mobile Communication Technologies*, pages 103–107, London, UK, March 2000.

[32] Harald Haas, Steven Laughlin, and Gordon J. R. Povey. The effects of interference between the TDD and FDD mode in UMTS at the boundary of 1920 MHz. In *IEEE Sixth International Symposium on Spread Spectrum Techniques and Applications*, volume 2, pages 486–490, New Jersey, USA, September 2000.

[33] Harald Haas, Steven Laughlin, and Gordon J. R. Povey. An investigation on capacity versus guard-bands in the TDD mode of UMTS. In *IEEE Vehicular Technology Conference 2000 Fall(VTC 2000 Fall)*, volume 4, pages 1820 – 1824, Boston, USA, September 2000.

[34] Harald Haas, Steven Laughlin, and Gordon J. R. Povey. Capacity-coverage analysis of TDD and FDD mode in UMTS at 1920 MHz. *IEE Proceedings - Communications*, 149(1):51–57, February 2002.

[35] Harald Haas and Stephen McLaughlin. A dynamic channel assignment algorithm for a hybrid TDMA/CDMA-TDD interface using the novel TS-opposing technique. *IEEE Journal on selected areas in communications*, 19(10):1831–1846, October 2001.

[36] Harald Haas and Gordon. J. R. Povey. Outage probability of CDMA-TDD micro cells in a CDMA-FDD environment. In *IEEE International Symposium on Personal, Indoor and Mobile Radio Communications (PIMRC)*, volume 1, pages 94–98, Boston, USA, September 1998.

[37] Harald Haas and Gordon J. R. Povey. The effect of adjacent channel interference on capacity in a hybrid TDMA/CDMA-TDD system using UTRA-TDD parameters. In *IEEE Vehicular Technology Conference (VTC'99- Spring)*, volume 2, pages 1086–1090, Houston, USA, May 1999.

[38] Seppo Hämäläinen, Harri Holma, and Kari Sipilä. Advanced WCDMA radio network simulator. In *IEEE International Symposium on Personal, Indoor and Mobile Radio Communications (PIMRC)*, pages 951–955, Osaka, Japan, September 1999.

[39] Seppo Hämäläinen, P. Slanina, M. Hartman, Antti Lappeteläinen, Harri Holma, and Oscar Salonaho. A novel interface between link and system level simulations. In *Proc. ACTS Summit 1997*, pages 599–604, Aalborg, Denmark, October 1997.

[40] M. Hata. Empirical formula for propagation loss in land mobile radio services. *IEEE Trans. on Vehicular Technology*, 29:317–325, 1980.

[41] Kari Heiska. *On the Modeling of WCDMA System Performance with Propagation Data*. PhD thesis, Helsinki University of Technology, 2004.

[42] Ke Wang Helmersson and Gunnar Bark. Performance of downlink shared channels in WCDMA radio network. In *Proc. IEEE Vehicular Technology Conference (VTC'01 - Spring)*, pages 2690 – 2694, Rhodes, Greece, May 2001.

[43] Jyri Hämäläinen and Risto Wichman. Closed-loop transmit diversity for FDD WCDMA systems. In *Asilomar Conference on Signals and systems and Computers*, Asilomar, USA, October 2000.

[44] Jyri Hämäläinen and Risto Wichman. The effect of feedback delay to the closed-loop transmit diversity in FDD WCDMA. In *IEEE Personal Indoor and Mobile Radio Communications (PIMRC)*, pages D–27–D–31, San Diego, USA, September 2001.

[45] Jyri Hämäläinen and Risto Wichman. Feedback schemes for FDD WCDMA systems in multipath environments. In *IEEE Vehicular Technology Conference (VTC'01 - Spring)*, pages 238–242, Rhodes, Greece, May 2001.

[46] Seppo Hämäläinen. *WCDMA Radio Network Performance*. PhD thesis, University of Jyväskylä, 2003.

[47] Harri Holma. *A Study of UMTS Terrestrial Radio Access Performance*. PhD thesis, Helsinki University of Technology, 2003.

[48] Harri Holma, Otto Lehtinen, and Sanna Heikkinen. Interference between uplink and downlink in UTRA TDD. *IEEE Journal on Selected Areas in Communications*, 18(8):1386–1393, August 2000.

[49] Harri Holma and Antti Toskala, editors. *WCDMA for UMTS*. John Wiley & Sons Ltd, 2nd edition, 2002.

[50] Kari Hooli. *Equalization in WCDMA terminals*. PhD thesis, University of Oulu, 2003.

[51] Ari Hottinen, Olav Tirkkonen, and Risto Wichman. Closed-loop transmit diversity techniques for multi-element transceivers. In *IEEE Vehicular Technology Conference (VTC'00 - Fall)*, pages 70–73, Boston, USA, September 2000.

[52] Ari Hottinen, Olav Tirkkonen, and Risto Wichman. *Multi-antenna Tranceiver Techniques for 3G and beyond*. John Wiley & Sons Ltd, 1st edition, 2003.

[53] Ari Hottinen, Jussi Vesma, Olav Tirkkonen, and Nikolai Nefedov. High bit rates for 3G and beyond using MIMO channels. In *IEEE International Symposium on Personal, Indoor and Mobile Radio Communications (PIMRC)*, pages 854 – 858, Lisbon, Portugal, September 2002.

[54] Ari Hottinen and Risto Wichman. Transmit diversity by antenna selection in CDMA downlink. In *IEEE International Symposium on Spread Spectrum Techniques and Applications (ISSSTA)*, pages 767–770, Sun City, South Africa, September 1998.

[55] Ari Hottinen and Risto Wichman. Transmit diversity using filtered feedback weights in the FDD/WCDMA system. In *International Zurich Seminar on Broadband Communications*, pages 15–21, Zurich, Switcherland, February 2000.

[56] Nasreddine J. and Lagrange X. Power control and slot allocation in a TD-CDMA system. In *IEEE 55th Vehicular Technology Conference (VTC 2002 Spring*, pages 880–884, Birmingham, USA, May 2002.

[57] W. Jakes. *Microwave mobile communications*. John Wiley & Sons Ltd, 1974.

[58] Ann-Louise Johansson, Klas Johansson, and David Astély. Transmit diversity for high data rates in WCDMA indoor system. In *IEEE Vehicular Technology Conference (VTC'01 - Spring)*, pages 2650–2654, Rhodes, Greece, May 2001.

[59] M. Juntti. *Multiuser Demodulation for DS-CDMA Systems in Fading Channels*. Acta Universitatis Ouluensis C 106. University of Oulu Press, Oulu, Finland, 1997.

[60] Marcos Katz, Esa Tiirola, and Juha Ylitalo. Combining space-time block coding with diversity antenna selection for improved downlink performance. In *IEEE Vehicular Technology Conference (VTC'01 - Fall)*, pages 178–182, September, Atlantic City, USA 2001.

[61] I. Katzela and M. Naghshineh. Channel assignment schemes for cellular mobile telecommunication systems: a comprehensive surveys. *IEEE Personal communications*, 3(3):10–31, June 1996.

[62] Troels Emil Kolding. Link and system performance aspects of proportional fair scheduling in WCDMA/HSDPA. In *IEEE Vehicular Technology Conference 2003 Fall*, pages 1717–1722, Orlando, Florida, USA, October 2003.

[63] Troels Emil Kolding, Klaus Ingemann Pedersen, Jeroen Wigard, Frank Frederiksen, and Preben Elgaard Mogensen. High speed downlink packet access: WCDMA evolution. *IEEE Vehicular Technology Society (VTS) News*, 50(1):4–10, February 2003.

[64] Petri Komulainen. Space-time equalization for interference suppression in CDMA terminals. In *Finnnish Wireless Communications Workshop (FWCW)*, 2000.

[65] Chang-Soo Koo, Sung-Hyuk Shin, Robert A DiFazio, Donald Grieco, and Ariela Zeira. Outer loop power control using channel adaptive processing for 3G WCDMA. In *IEEE Vehicular Technology Conference 2003 Spring*, pages 490–494, Jeju, South Korea, April 2003.

[66] Thomas P. Krauss and Michael D. Zoltowski. Oversampling diversity versus dual antenna diversity for chip-level equalization on CDMA downlink. In *IEEE Sensor Array and Multichannel Signal Processing Workshop*, pages 47–51, Cambridge, USA, March 2000.

[67] Thomas P. Krauss, Michael D. Zoltowski, and Geert Leus. Simple MMSE equalizer for CDMA downlink to restore chip sequence: comparison to

zero-forcing and rake. In *IEEE International Conference on Acoustics, Speech, and Signal Processing (ICASSP)*, pages 2865–2868, Istanbul, Turkey, June 2000.

[68] Janne Kurjenniemi. *Method, device and system for power control step size selection based on received signal quality*. US Patent, 3760598, 2004.

[69] Janne Kurjenniemi, Seppo Hämäläinen, and Tapani Ristaniemi. System simulator for UTRA TDD. In *Proc. 5th CDMA International Conference and Exhibition (CIC'00)*, volume 1, pages 370–374, Seoul, Korea, November 2000.

[70] Janne Kurjenniemi, Seppo Hämäläinen, and Tapani Ristaniemi. Handover and uplink power control performance in the 3.84 Mcps TDD mode of UTRA network. *Wireless Personal Communications*, 27(4):337–351, December 2003.

[71] R. Kwan, P. Chong, and M. Rinne. Analysis of the adaptive modulation and coding algorithm with the multicode transmission. In *Proc. IEEE Vehicular Technology Conference (VTC'02 - Fall)*, pages 2007 – 2011, Vancouver, Canada, September 2002.

[72] R. Kwan, P.H.J. Chong, E. Poutiainen, and M. Rinne. The effect of code-multiplexing on the high speed downlink packet access (HSDPA) in a WCDMA network. In *Proc. IEEE Wireless Communications and Networking Conference (WCNC'03)*, pages 1728 – 1732, New Orleans, USA, March 2003.

[73] Jaana Laiho, Achim Wacker, and Thomas Novosad, editors. *Radio network planning and optimisation for UMTS*. John Wiley & Sons Ltd, 1st edition, 2002.

[74] Robert Love, Brian Classon, Amitava Ghosh, and Mark Cudak. Incremental redundancy for evolutions of 3g CDMA systems. In *Proc. IEEE Vehicular Technology Conference (VTC'02 - Spring)*, pages 454 – 458, Birmingham, USA, May 2002.

[75] Robert Love, Amitava Ghosh, Robert Nikides, Louay Jalloul, Mark Cudak, and Brian Classon. High speed downlink packet access performance. In *Proc. IEEE Vehicular Technology Conference (VTC'01 - Spring)*, pages 2234 – 2238, Rhodes, Greece, May 2001.

[76] Robert Love, Amitava Ghosh, Weimin Xiao, and Rapeepat Ratasuk. Performance of 3GPP high speed downlink packet access (HSDPA). In *IEEE Vehicular Technology Conference (VTC'04 - Fall)*, Los Angeles, USA, September 2004.

[77] Robert Love, Kenneth Stewart, Raja Bachu, and Amitava Ghosh. MMSE equalization for UMTS HSDPA. In *Proc. IEEE Vehicular Technology Conference (VTC'03 - Fall)*, pages 2416 – 2420, Orlando, USA, October 2003.

[78] SINR computation in system simulations with multipath channels and arbitrary linear FIR space-time receivers. 3GPP-3GPP2 spatial channel modelling ad hoc SCM-AHG SCM-105, January 2003.

[79] Magnus Lundevall, Birgitta Olin adn Jonas Olsson, Niclas Wiberg, Stefan Wänstedt, Jonas Eriksson, and Frida Eng. Streaming applications over HSDPA in mixed service scenarios. In *IEEE Vehicular Technology Conference (VTC'04 - Fall)*, Los Angeles, USA, September 2004.

[80] C. Mihailescu, X. Lagrange, and P. Godlewski. Locally centralized dynamic resource allocation algorithm for the UMTS in manhattan environment. In *IEEE Personal, Indoor and Mobile Radio Communications (PIMRC)*, pages 420–423, Boston, USA, September 1998.

[81] C. Mihailescu, X. Lagrange, and P. Godlewski. Radio resource management for packet transmission in UMTS WCDMA system. In *IEEE Vehicular Technology Conference 1999 Fall (VTC'99 - Fall)*, pages 573–577, Amsterdam, The Netherlands, September 1999.

[82] C. Mihailescu, X. Lagrange, and P. Godlewski. Performance evaluation of a dynamic resource allocation algorithm for UMTS-TDD systems. In *IEEE Vehicular Technology Conference 2000 Sping (VTC'00 - Spring)*, pages 2339–2343, Tokyo, Japan, May 2000.

[83] C. Mihailescu, X. Lagrange, P. Godlewski, and A.G.C. Acx. Dynamic resource allocation in locally centralized cellular systems. In *IEEE Vehicular Technology Conference (VTC'98)*, pages 1695–1699, Ottawa, Canada, May 1998.

[84] Michiharu Nakamura, Yassin Awad, and Sunil Vadgama. Adaptive control of link adaption for high speed downlink packet access (HSDPA) in WCDMA. In *The 5th International Symposium on Wireless Personal Multimedia Communications (WPMC)*, pages 382–386, Honolulu, Hawaii, October 2002.

[85] Dejan M. Novakovic, Markku J. Juntti, and Miroslav L. Dukic. The influence of the channel estimation error on the closed loop transmit diversity algorithms performance. In *IEEE Symposium on Personal, Indoor and Mobile Radio Commmunications (PIMRC)*, pages 1427–1431, Lisbon, Portugal, September 2002.

[86] Y. Okumura, E. Ohmori, T. Kawano, and K. Fukuda. Field strength and its variability in vhf and uhf land-mobile service. *Review of the Electrical Communication Laboratory*, 16(9-10):825–873, 1968.

[87] Eko N. Onggosanusi, Alan Gatherer, Anand G. Dabak, and Srinath Hosur. Performance analysis of closed-loop transmit diversity in the presence of feedback delay. *IEEE Transactions on communications*, 49(9):1618–1630, September 2001.

[88] S. Parkvall, M. Karlsson, M. Samuelsson, L. Hedlund, and B. Göransson. Transmit diversity in WCDMA: link and system level results. In *Proc. IEEE Vehicular Technology Conference (VTC'00 - Spring)*, pages 864–868, Tokyo, Japan, May 2000.

[89] Stefan Parkvall, Erik Dahlman, Pål Frenger, Per Beming, and Magnus Persson. The evolution of WCDMA towards higher speed downlink packet data access. In *IEEE Vehicular Technology Conference (VTC) 2001 Spring*, pages 2287–2291, Rhodes, Greece, May 2001.

[90] A. Paulraj and C. Papadias. Space-time processing for wireless communications. *IEEE Signal Processing Magazine*, 14(6):49 – 83, 1997.

[91] Klaus I. Pedersen, Tako F. Lootsma, Michael Stottrup, Frank Frederiksen, Troels E. Kolding, and Preben E. Mogensen. Network performance of mixed traffic on high speed downlink packet access and dedicated channels in WCDMA. In *IEEE Vehicular Technology Conference (VTC'04 - Fall)*, Los Angeles, USA, September 2004.

[92] Klaus I. Pedersen, Antti Toskala, and Preben E. Mogensen. Mobility management and capacity analysis for high speed downlink packet access in WCDMA. In *IEEE Vehicular Technology Conference (VTC'04 - Fall)*, Los Angeles, USA, September 2004.

[93] Mugen Peng, Jinwen Zhang, Chunjing Hu, and Wenbo Wang. Handover performance analysis in TDD-CDMA cellular network. In *IEEE Wireless Communications and Networking (WCNC 2003)*, pages 806–811, March 2003.

[94] R. Price and P. E. Jr. Green. A communication technique for multipath channels. In *Proceedings of the IRE*, pages 555 – 570, March 1958.

[95] J. G. Proakis. *Digital Communications*. McGraw-Hill, Inc., New York, NY, USA, 3 edition, 1995.

[96] 3^{rd} Generation Partnership Project. Technical specification group, radio access network, working group 2. *Radio Resource Management Strategies*, TS25.922(v0.5.0), September 1999.

[97] 3^{rd} Generation Partnership Project. Technical specification group, radio access network, working group 2. *Radio Resource Management Strategies*, TR25.922(v0.5.0), September 1999.

[98] 3^{rd} Generation Partnership Project. Technical specification group, radio access network, working group 4. *Evaluation of up- and downlink adjacent channel performance*, TSGR4#2(99) 048, February 1999.

[99] 3^{rd} Generation Partnership Project. Technical specification group, radio access network. *UE Radio Access capabilities (Release 5)*, TS25.306(v5.9.0), December 2000.

[100] 3rd Generation Partnership Project. Technical specification group, radio access network, working group 1. *Physical Channels and mapping of transport channels onto physical channels (TDD)*, TS25.221(v3.3.0), June 2000.

[101] 3rd Generation Partnership Project. Technical specification group, radio access network, working group 1. *Multiplexing and channel coding (TDD)*, TS25.222(v3.3.0), June 2000.

[102] 3rd Generation Partnership Project. Technical specification group, radio access network, working group 1. *Spreading and modulation (TDD)*, TS25.223(v3.3.0), June 2000.

[103] 3rd Generation Partnership Project. Technical specification group, radio access network, working group 1. *Physical Layer procedures (TDD)*, TS25.224(v3.3.0), June 2000.

[104] 3rd Generation Partnership Project. Technical specification group, radio access network, working group 1. *Physical Layer - Measurements*, TS25.225(v3.3.0), June 2000.

[105] 3rd Generation Partnership Project. Technical specification group, radio access network, working group 4. *UTRA (UE) TDD; Radio Transmission and Reception*, TS25.102(v3.3.0), June 2000.

[106] 3rd Generation Partnership Project. Technical specification group, radio access network, working group 4. *UTRA (BS) TDD; Radio Transmission and Reception*, TS25.105(v3.3.0), June 2000.

[107] 3rd Generation Partnership Project. Technical specification group, radio access network, working group 4. *Requirements for Support of Radio Resource Management*, TS25.123(v3.3.0), June 2000.

[108] 3rd Generation Partnership Project. Technical specification group, radio access network, working group 2. *TDD base station classification*, TS25.952(v4.0.0), September 2001.

[109] 3rd Generation Partnership Project. Technical specification group, radio access network, working group 4. *Physical layer aspects of UTRA High Speed Downlink Packet Access*, TS25.848(v4.0.0), March 2001.

[110] 3rd Generation Partnership Project. Technical specification group, radio access network, working group 2. *UTRAN Iub Interface NBAP Signalling*, TS25.433(v4.0.0), September 2002.

[111] 3rd Generation Partnership Project. Technical specification group, radio access network, working group 4. *Physical layer Procedures (FDD)*, TS25.214(v5.6.0), September 2003.

[112] 3^{rd} Generation Partnership Project. Technical specification group, radio access network, working group 4. *Physical channels and mapping of transport channels onto physical channels (FDD) release 5P*, TS25.211(v5.5.0), September 2003.

[113] 3^{rd} Generation Partnership Project. Technical specification group, radio access network, working group 4. *Feasibility Study for Enhanced Uplink for UTRA FDD (Release 6)*, TR25.896(v6.0.0), March 2004.

[114] Balaji Raghothaman, Giridhar Mandyam, and R. Thomas Derryberry. Performance of closed loop transmit diversity with feedback delay. In *The Thirty-Fourth Asilomar Conference on Signals, Systems and Computers*, pages 102–105, Asilomar, USA, November 2000.

[115] Mika Raitola, Ari Hottinen, and Risto Wichman. Transmission diversity in wideband CDMA. In *IEEE Vehicular Technology Conference (VTC'99 - Spring)*, pages 1545–1549, Houston, USA, May 1999.

[116] Juan Ramiro-Moreno, Klaus I. Pedersen, and Preben E. Mogensen. Radio resource management for WCDMA networks supporting dual antenna terminals. In *IEEE Vehicular Technology Conference (VTC) 2002 Spring*, pages 694–698, Birmingham, USA, May 2002.

[117] Juan Ramiro-Moreno, Klaus I. Pedersen, and Preben E. Mogensen. Network performance of transmit and receive antenna diversity in hsdpa under different packet scheduling strategies. In *IEEE Vehicular Technology Conference (VTC) 2003 Spring*, pages 1454–1458, Jeju, Korea, April 2003.

[118] ITU-R Recommendation. M.1645. *Framework and overall objectives of the future development of IMT-2000 and systems beyond IMT-2000*, ITU-R M.1645 1, 2003.

[119] Kari Rikkinen and Soni Koul. TDD/FDD system coexistence at 1920 MHz frequency border. In *3G Wireless '01*, San Fransisco, California, USA, June 2001.

[120] Kamyar Rohani, Mark Harrison, and Kiran Kuchi. A comparison of base station transmit diversity methods for third generation cellular standards. In *IEEE Vehicular Technology Conference (VTC'99 - Spring)*, pages 351–355, Houston, USA, May 1999.

[121] A. Sampath, P. Kumar, and J. Holzman. On setting reverse link target SIR in a CDMA system. In *IEEE Vehicular Technology Conference (VTC'97)*, pages 929–933, Arizona, USA, May 1997.

[122] M. Sandell. Analytical analysis of transmit diversity in WCDMA on fading multipath channels. In *Proc. IEEE Symposium on Personal, Indoor and Mobile Radio Communications (PIMRC'99)*, September 1999.

[123] Sung-Hyuk Shin, Chang-Soo Koo, Donald Grieco, and Ariela Zeira. Pathloss-aided closed loop transmit power control for 3G UTRA TDD. In *IEEE Vehicular Technology Conference 2003 Spring*, pages 2226–2230, Jeju, South Korea, April 2003.

[124] Stüber. *Principles of mobile communication*. Kluwer Academic Publishers, 1st edition, 1996.

[125] S. M. Sussman. A matched filter communication system for multipath channels. *IEEE Transactions on Information Theory*, 6(3):367 – 373, June 1960.

[126] G. L. Turin. Introduction to spread-spectrum antimultipath techniques and their applications to urban digital radio. *Proceedings of the IEEE*, 68(3):328 – 353, March 1980.

[127] Universal Mobile Telecommunications System (UMTS). UMTS 21.01. *Requirements for the UMTS Terrestrial Radio Access System (UTRA)*, TR 101.111(v3.0.1), November 1997.

[128] Universal Mobile Telecommunications System (UMTS). UMTS 30.03. *Selection procedures for the choice of radio transmission technologies of the UMTS*, TR 101.112(v3.1.0), November 1997.

[129] Mika Ventola, Esa Tuomaala, and Pekka A. Ranta. Performance of dual antenna diversity reception in WCDMA terminals. In *IEEE Vehicular Technology Conference (VTC) 2003 Spring*, pages 1035–1040, Jeju, Korea, April 2003.

[130] S. Verdú. *Multiuser Detection*. Cambridge University Press, Cambridge, UK, 1998.

[131] Y.-P. Eric Wang, Jung-Fu Cheng, and Eva Englund. The benefits of advanced receivers for high speed data communications in WCDMA. In *IEEE Vehicular Technology Conference 2002 Fall*, pages 132–136, Vancouver, Canada, September 2002.

[132] Jack H. Winters. Optimum combining in digital mobile radio with cochannel interference. *IEEE Journal on Selected Areas in Communications*, 2(4):528 – 539, 1984.